

The Cu_A Site in Cytochrome c Oxidase:
Its Role in Coupling Electron Transport to Proton Pumping

Thesis by
Jeff Gelles

In Partial Fulfillment of the Requirements
for the Degree of
Doctor of Philosophy

California Institute of Technology
Pasadena, California

1986

(Submitted June 4, 1986)

"We are in the position of a man who lives in a town with no Chinese restaurants and has to make his own Moo Goo Gai Ding. It's almost impossible to make right, he doesn't have a recipe, the Super Valu doesn't stock the right herbs and spices, but every so often he pulls off a Ding that brings back memories of Dings he used to know. For a man in the wrong place at the wrong time, that's as good as it gets."

Garrison Keillor (1980)

ACKNOWLEDGEMENT

I have been privileged to spend the last five years working in an environment which has been both extremely intellectually stimulating and personally supportive.

Sunney Chan made innumerable contributions to this work by proposing experiments, suggesting interpretations of data, sharing insights into relevant aspects of chemistry, biology, and physics, and providing general moral support, but his most important contributions are simultaneously more subtle and more profound. Sunney's general philosophy of doing science, his strategies of experimental design, and a large number of his ideas about biophysical chemistry in general and about the structure and function of cytochrome oxidase in particular form a pervasive foundation upon which the specific projects described in this thesis rest. It has been a pleasure to work for someone who cares at least as much about people as he does about science.

Several of the projects described in this thesis have been conducted in partnership with other people in the lab. I am grateful to Dave Blair, Darrin Takemoto, Mark Li, and Thomas Nilsson for their contributions of ideas, enthusiasm, and the many hours of hard labor they devoted to bringing this work to fruition. It has been a pleasure to collaborate with such talented and dedicated people.

Nearly everybody who has been part of the Chan group while I have worked here has at one time or another helped me with ideas and suggestions about the conduct of this research. I would particularly like to thank Joe Falke, Dave Blair, and Joel Morgan for the thought-provoking discussions in which many of the ideas presented here were elaborated and a far greater number were discarded. I also want to thank Craig Martin for sharing his knowledge of EPR spectroscopy, particularly that provided in the highly distilled form of the computer program used to produce the simulated EPR spectra in Chapter II. Prof. Walter Schroeder and Roger Shelton gave unstintingly of their time while introducing me to some of the fine points of protein chemistry and generously allowed me free run of the equipment in their laboratory.

The research described in this thesis was funded by grants to Sunney Chan from the National Institute of General Medical Sciences and the Biomedical Research Support Grant Program of the National Institutes of Health. I am grateful to the National Science Foundation for supporting me during the first part of this work with a predoctoral fellowship. I would also like to thank Prof. Elias Lazarides for providing me with financial support and valuable educational experiences during the early part of my stay at Caltech.

Science isn't an abstract intellectual endeavor, it is

something that human beings do. For making sure I remained human, I want to thank the many people, my housemates and labmates in particular, whose friendship has made living in a city with Perfect Days so enjoyable. I especially want to thank Connie, the alumni of the Siskind Friday Lunch Table, and all the scratchers for many good times and healthy doses of sanity.

I dedicate this thesis to my parents, who have nourished me with their love and understanding.

ABSTRACT

Cytochrome c oxidase contains a copper-ion electron transfer site, Cu_A, which has previously been found to be unreactive with externally added reagents under conditions in which the protein remains structurally intact. We have studied the reaction of cytochrome oxidase with sodium p-hydroxymercuribenzoate (pHMB) and found that the reaction proceeds, under appropriate conditions, to give an excellent yield of a particular derivative of the Cu_A center which has electron paramagnetic resonance and near-infrared absorption spectroscopic properties which are distinctly different from those of the unmodified center. Spectroscopic and chemical characterization of the other metal-ion sites of the enzyme reveals little or no effect of the pHMB modification on the structures of and reactions at those sites. Of particular interest is the observation that the modified enzyme still displays a substantial fraction of the native steady-state activity of electron transfer from ferrocytochrome c to O₂. Although the modified copper center retains the ability to receive electrons from the powerful reductant Na₂S₂O₄ and to transfer electrons to O₂, it is not significantly reduced when the enzyme is treated with milder (higher potential) reductants such as NADH/phenazine methosulfate or the physiological substrate ferrocytochrome c.

Cu_A exhibits many spectroscopic and chemical properties which make it highly atypical of cuproprotein active sites; the singular nature of this site has prompted speculation about the importance of the structural peculiarities of this metal-ion center in the catalytic cycle of the enzyme. In this work, we demonstrate that the unusual features of this site are not prerequisites for competent catalysis of electron transfer and O₂ reduction by the enzyme. These observations suggest that a secondary electron transfer pathway not involving Cu_A exists between the cytochrome c and oxygen binding sites which can function at a rate at least 20% of the total turnover rate of the native enzyme.

Cytochrome c oxidase converts free energy released in respiratory electron transport into a metabolically useful form by contributing to the potential gradient across the mitochondrial inner membrane. Both a process involving electron transfer linked proton pumping and a process involving electron transfer from ferrocyanochrome c to O₁ contribute to the potential gradient. Taken together with those from other recent studies, the results of the experiments support a model for electron transfer in cytochrome oxidase in which Cu_A and Fe_a are parts of separate, parallel electron transport pathways between cytochrome c and the cytochrome oxidase O₂ reduction site.

This model has important implications for the role of Cu_A in respiratory energy transduction by cytochrome oxidase. It suggests that Cu_A is the best candidate among the four metal center sites in cytochrome oxidase to be the site of redox-linked proton pumping.

In order to explore more fully the mechanistic aspects of energy transduction in cytochrome oxidase, we propose a complete chemical mechanism for the enzyme's proton pump. The mechanism achieves pumping with chemical reaction steps localized at a single redox site within the enzyme; no indirect coupling through protein conformational changes is required. The proposed mechanism is based on a novel redox-linked transition metal ligand substitution reaction. The use of this reaction leads in a straightforward manner to explicit mechanisms for achieving all of the processes determined by Blair, et al. (D.F. Blair, J. Gelles, and S.I. Chan, Biophys. J., in press) to be needed to accomplish redox-linked proton pumping. These processes include: 1) modulation of the energetics of protonation/deprotonation reactions and modulation of the energetics of redox reactions by the structural state of the pumping site; 2) control of the rates of the pump's redox reactions with its electron transfer partners during the turnover cycle (gating of electrons); and 3) regulation of the rates of the

protonation/deprotonation reactions between the pumping site and the aqueous phases on the two sides of the membrane during the reaction cycle (gating of protons). The model is the first proposed for the cytochrome oxidase proton pump which is mechanistically complete and specific enough that a realistic assessment can be made of how well the model pump would function as a redox-linked energy transducer. This assessment is accomplished via analyses of the thermodynamic properties and steady-state kinetics expected of the model. These analyses demonstrate that the behavior of a pump based on the model would be very similar to that observed of cytochrome oxidase both in the mitochondrion and purified preparations. Specifically, calculation of the properties of the model pump at equilibrium demonstrates that the behavior expected of the model pump in an electrochemical titration is the same as that observed for the Cu_A center: a nearly pH-independent midpoint potential of approximately 290 mV. An analysis of the performance of the pump during steady-state turnover demonstrates that the model pump is expected to function efficiently and with good power output under physiological conditions, and that its properties under conditions of varying load are similar to those observed in experiments on respiring mitochondria and on purified cytochrome oxidase reconstituted into artificial lipid vesicles.

Although the analysis presented here concerns only a single model of a redox-linked proton pump, it leads to some important general conclusions regarding the mechanistic features of such pumps. The first is that a workable proton pump mechanism does not require large protein conformational changes. Another conclusion is that a redox-linked proton pump need not display a pH-dependent midpoint potential as has frequently been assumed. A final conclusion is that mechanisms for redox-linked proton pumps that involve transition metal ligand exchange reactions are quite attractive because such reactions readily lend themselves to the linked gating processes necessary for proton pumping.

Several of the results of this research form the basis of a new approach to studying the role of Cu_A in energy transduction by cytochrome oxidase. I describe several continuing experimental programs based on this method, and summarize the goals, experimental design, and progress of these studies. I conclude by considering the physiological significance of the new conceptions about the role of Cu_A in energy transduction by cytochrome oxidase arising from this research.

TABLE OF CONTENTS

Acknowledgement	iii
Abstract	vi
List of Figures and Tables	xiii
I. Introduction	1
Footnotes	10
References	11
II. Chemical Modification of the Cu _A Center in Cytochrome <u>c</u> Oxidase by Sodium p-Hydroxy- mercuribenzoate	12
Materials and Methods	18
Results	24
Discussion	50
Footnotes	62
References	63
III. The Proton Pumping Site of Cytochrome <u>c</u> Oxidase: A Model of Its Structure and Mechanism	68
The Environment, Structure, and Function of the Cytochrome Oxidase Proton Pump	75
Constraints on Kinetics and Thermodynamics in a Redox-linked Proton Pump Mechanism	84
A Model of the Cytochrome Oxidase Proton Pump	88
The Gating of Electron and Proton Flows in the Model Pump Mechanism	100
Quantitative Evaluation of the Behavior of the Proton Pump Model at Equilibrium	117
Quantitative Evaluation of the Behavior of the Model Proton Pump During Steady-State Turnover	127

Structural Requirements of the Proton Pump Model	151
Summary	156
Appendix I: State Populations of the Model Pump at Equilibrium	158
Appendix II: The Turnover Rate and Efficiency of the Model Pump at Steady State	163
Footnotes	170
References	172
IV. Cu_A and Energy Transduction in Cytochrome <u>c</u> Oxidase	177
Summary: Results Leading to a Reevaluation of the Role of Cu_A in Cytochrome Oxidase Energy Transduction	179
The Further Study of the Role of Cu_A in Energy Transduction by Cytochrome Oxidase	
A. A Methodological Foundation	189
B. Research in Progress	191
Biochemical and Physiological Implications	209
Summary	216
Footnotes	217
References	218

LIST OF FIGURES AND TABLES

Chapter II

Figure 1.	EPR signal from the Cu_A^{2+} site after treatment of cytochrome oxidase with thiol modification reagents	25
Figure 2.	Comparison of the near-infrared and visible spectra of native and pHMB-modified cytochrome oxidase	29
Figure 3.	Comparison of the low-temperature EPR spectra of native and pHMB-modified cytochrome oxidase	32
Table I.	Catalytic activity of pHMB-modified and unmodified samples of cytochrome <u>c</u> oxidase	37
Figure 4.	Redox behavior of Fe_a and the EPR-visible copper center in pHMB-modified cytochrome oxidase: reduction by sodium dithionite and reoxidation by O_2	39
Figure 5.	Reduction of the hemes of pHMB-modified cytochrome oxidase with NADH and PMS	42
Figure 6.	Reduction of the EPR-visible copper centers in native and PHMB-modified cytochrome oxidase by NADH and PMS.	46

Chapter III

Figure 1.	The environment of a localized proton pump in an enzyme in the mitochondrial inner membrane	77
Figure 2.	Chemical mechanism of the proton pump model	89
Figure 3.	Comparison of "coupling" and "uncoupling" reactions of the model pump	101
Figure 4.	Calculated behavior of the model pump in electrochemical titrations at different pH values	125
Figure 5.	Reaction scheme for the steady-state calculations	129

Table I.	Parameters used in the steady-state analysis of the pump model	132
Figure 6.	Energy transduction efficiency and electron transfer rate in the steady-state reaction scheme	139
Figure 7.	Fractional population of the states of the model pump	144
Figure 8.	Free energy transduction efficiency and electron transfer rate of the model pump	148
Figure 9.	States of the model pump considered in the equilibrium concentrations calculation.	159

Chapter IV

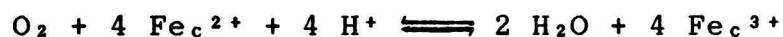
Figure 1.	Two models of the intramolecular electron transfer pathways in a cytochrome <u>c</u> -cytochrome oxidase complex	180
Figure 2.	An experiment to measure the proton pumping activity of cytochrome oxidase	197
Figure 3.	Effect of improperly reconstituted enzyme on a measurement of proton pumping activity	201
Table I.	Respiratory control ratios of vesicle-reconstituted cytochrome oxidase preparations	204

Chapter I

Introduction

Cytochrome c oxidase is the terminal enzyme in the respiratory chain of mitochondria. The respiratory chain is a metabolic pathway which transfers electrons from food-derived organic substrates with low standard reduction potentials [e.g., fumaric acid/succinic acid; $E^{\circ'} = 30 \text{ mV}$] to O_2 [$\text{O}_2/\text{H}_2\text{O}$; $E^{\circ'} = 816 \text{ mV}$] (1). A fraction of the large amounts of free energy released under physiological conditions by these electron transfer processes is not dissipated as heat but is stored by the respiratory chain as a proton electrochemical potential gradient ($\Delta\tilde{\mu}_{\text{H}^+}$)¹ across the inner membrane of the mitochondrion (2). This stored energy is used by other enzymes to fuel a variety of metabolic processes (3).

Cytochrome oxidase catalyzes the transfer of electrons from cytochrome c to O_2 by the reaction



where Fe_c^{2+} and Fe_c^{3+} represent ferro- and ferricytochrome c, respectively. In this reaction, the electrons transferred from cytochrome c originate on the outside of the mitochondrial inner membrane (c-side) and the protons originate in the mitochondrial matrix (m-side). The reaction therefore contributes to $\Delta\tilde{\mu}_{\text{H}^+}$ by creating both an

electrostatic potential across the membrane and a difference in proton chemical potential (i.e., a difference in pH) between the two sides.

Over the last decade, there has been a great stimulation of interest in energy transduction by cytochrome oxidase. In the "redox loop" model of the respiratory chain, which Mitchell proposed as a mechanistic implementation of his chemiosmotic hypothesis, oxidase functions as a passive conductor which accepts electrons from ferrocytochrome c and uses them to reduce O_2 (2). Thanks largely to the pioneering work of Wikström and colleagues [reviewed in (4)], we now know that this picture is incomplete: Cytochrome oxidase makes an additional contribution to $\Delta\tilde{\mu}_H^+$ by functioning as a redox-linked proton pump. Electron transfer through the enzyme causes translocation of protons from the m-side to the c-side (5). Experiments with purified oxidase show that the number of protons pumped per electron transferred to O_2 can approach 1 under certain (non-physiological) conditions (6).

The fact that oxidase is a proton pump places it in the same class with other chemically-driven ion active transport systems such as the (Na,K)-ATPase, and the H^+ -ATPases of mitochondria, bacteria, and chloroplasts. The detailed

functioning of these enzymes remains a fundamental unsolved problem of mechanistic enzymology. For this reason, and because of their great physiological importance, these ion pumps are currently one of the most intensively studied classes of membrane proteins.

Cytochrome oxidase has been isolated and studied in pure form for more than twenty-five years (7, 8). The enzyme is a complex structure which contains some 14 different polypeptides (9), two copper ions, two heme a cofactors, and a poorly characterized phospholipid component. One heme and one copper, referred to as Fe_a , and Cu_B , are closely apposed in the enzyme structure and together make up the site at which O_2 is bound to the enzyme and reduced to H_2O (10). This site binds classical respiratory inhibitors (e.g., CN^- , CO), and its chemical and spectroscopic properties have been extensively studied [reviewed in (10)].

The other heme and copper in the enzyme, called Fe_a and Cu_A , are isolated metal center sites which are separated by more than 10 Å from each other and from the oxygen binding site. These centers are probably buried in the interior of the protein, and unlike the heme and copper at the oxygen binding site, do not bind solutes which are added to the enzyme solution. Fe_a^{3+} and Cu_A^{2+} are reduced more rapidly

than $\text{Fe}_{a_3}^{3+}$ or Cu_B^{2+} when ferrocytochrome c is added to an anaerobic enzyme solution and are reoxidized more rapidly than ferrocytochrome c when oxygen is subsequently added. For this reason, they are thought to play a role in transferring electrons from cytochrome c to the oxygen binding site. There is a widely held belief among workers in the field that one of these two sites is the locus of proton pumping by the enzyme. It is fair to state, however, that our knowledge about the role of these sites in the catalytic mechanism of the enzyme is still at a rather primitive stage, despite the great amount of work which has been devoted to their study [reviewed in (7)].

Cu_A in particular has been something of an enigma to biochemists studying cytochrome oxidase. Research on the enzyme had its genesis in Germany during the years between the two world wars. During this period, Warburg, Keilin, Hartree, and others first became aware of the enzyme by studying the strong optical absorptions of its heme co-factors. It was not until after 1958 that Beinert, Wharton, and their co-workers provided evidence for involvement of copper in catalysis by the enzyme.

The spectroscopic properties of the Cu_A site [reviewed in (10, 11)] are in several respects unique among those of

copper proteins and even those of small-molecule copper complexes (12). These features have stimulated a great interest in the structure of the site and speculation about its functional significance. Chan and co-workers have provided the most detailed information about the structure of the site by demonstrating that the copper ion has two nitrogenous ligands, one of which is a histidine, and one or two cysteine ligands. This group proposed that the unusual spectroscopic features of the site arise from a ligation geometry which allows partial delocalization of the unpaired electron of Cu_A^{2+} onto cysteine ligand(s). Chan et al. proposed eight years ago that Cu_A is the site of redox-linked proton pumping in cytochrome oxidase (13); however, most workers in the field regard Fe_a as a more likely candidate [e.g., (7)].

This thesis describes a series of related investigations which use our knowledge about the structure of the Cu_A site as a starting point to study its role in energy transduction by cytochrome c oxidase. The first section consists of a series of experimental studies which use a chemically-modified protein derivative to probe the function of the site. We use the thiol-modification reagent sodium p-hydroxymercuribenzoate (pHMB) to modify the structure of the Cu_A center and show that it has spectroscopic properties

which are distinctly different from those of the unmodified center. Spectroscopic and chemical characterization of the other metal-ion sites of the enzyme reveals little or no effect of the pHMB modification on the structures of and reactions at those sites. Of particular interest is the observation that the modified enzyme still displays a substantial fraction of the native steady-state activity of electron transfer from ferrocytochrome c to O_2 . Further studies demonstrate that the modified copper center probably does not undergo oxidoreduction under the conditions in which the enzyme turnover is demonstrated.

The results presented here demonstrate that oxidoreduction of Cu_A is not a prerequisite for competent catalysis of electron transfer and O_2 reduction by the enzyme. The observations suggest that a secondary electron transfer pathway not involving Cu_A exists between the cytochrome c and oxygen binding sites which can function at a rate at least 20% of that in the native enzyme. This interpretation supports a model for electron transfer in cytochrome oxidase in which Cu_A and Fe_a are parts of separate, parallel electron transport pathways between cytochrome c and the cytochrome oxidase O_2 reduction site. This model has important implications for the role of Cu_A in respiratory energy transduction, and suggests that Cu_A is

the best candidate among the four metal centers in cytochrome oxidase to be the site of redox-linked proton pumping.

In order to more fully explore the mechanistic aspects of energy transduction in cytochrome oxidase, we propose a complete model and chemical mechanism for the enzyme's proton pump based around the structure of Cu_A. A central feature of the proposed mechanism is a novel redox-linked transition metal ligand substitution reaction. The use of this reaction leads in a straightforward manner to explicit mechanisms for all of the processes (14) needed to accomplish redox-linked proton pumping. The model is the first proposed for the cytochrome oxidase proton pump which is sufficiently complete and specific that a realistic assessment can be made of how well the model pump would function as a redox-linked energy transducer. This assessment is accomplished via quantitative analyses of the behavior expected of the model at equilibrium and under steady-state turnover conditions. These analyses demonstrate that the properties of the model pump are very similar to those observed for cytochrome oxidase in the mitochondrion and in purified preparations, and demonstrate that the proposed mechanism is a feasible way for a proton pump to operate.

The analysis of the proton pump model leads to some important general conclusions regarding the mechanistic features of such pumps. The first is that a workable proton pump mechanism does not require large protein conformational changes. A second conclusion is that a redox-linked proton pump need not display a pH-dependent midpoint potential as has previously been assumed. A final conclusion is that mechanisms for redox-linked proton pumps that involve transition metal ligand exchange reactions are quite attractive because such reactions readily lend themselves to the linked gating processes necessary for proton pumping.

Several of the results of this research form the basis of a new approach to studying the role of Cu_A in energy transduction by cytochrome oxidase. We have several continuing experimental programs based on this approach, and I summarize the goals, experimental design, and progress of these studies. I conclude this thesis by considering the biochemical and physiological significance of the new conceptions about the role of Cu_A in energy transduction by cytochrome oxidase which have arisen from this research.

FOOTNOTES

¹Abbreviations and symbols used in this chapter: $\Delta\tilde{\mu}_H^+$, difference in hydrogen ion electrochemical potential between the aqueous phases separated by the mitochondrial inner membrane; pHMB, sodium *p*-hydroxymercuribenzoic acid; m-side, side of the mitochondrial inner membrane facing the matrix of the mitochondrion; c-side, side of the mitochondrial inner membrane facing the outer membrane.

REFERENCES

1. Wikström, M., Saraste, M. (1984) in Bioenergetics (Ernster, Ed.) pp. 49-94, Elsevier, Amsterdam.
2. Mitchell, P. (1976) Biochem. Soc. Trans. 4, 399-430.
3. Mitchell, P. (1979) Eur. J. Biochem. 95, 1-20.
4. Wikström, M., Krab, K. (1979) Biochim. Biophys. Acta 549, 177-222.
5. Wikström, M., Krab, K., Saraste, M. (1981) Annu. Rev. Biochem. 50, 623-655.
6. Thelen, M., O'Shea, P.S., Azzi, A. (1985) Biochem. J. 227, 163-167.
7. Wikström, M., Krab, K., Saraste, M. (1981) Cytochrome Oxidase: A Synthesis, Academic Press, London.
8. Lemberg, M.R. (1969) Physiol. Rev. 49, 48-121.
9. Buse, G., Meinecke, L., Bruch, B. (1985) J. Inorg. Biochem. 23, 149-153.
10. Blair, D.F., Martin, C.T., Gelles, J., Wang, H., Brudvig, G.W., Stevens, T.H., Chan, S.I. (1983) Chemica Scripta 21, 43-53.
11. Gelles, J., Blair, D.F., Martin, C.T., Wang, H., Chan, S.I. (1983) in Frontiers in Biochemical and Biophysical Studies of Proteins and Membranes (Liu, T-Y. et al., Eds.) pp. 259-277, Elsevier, New York.
12. Toftlund, H., Becher, J., Olesen, P.H., Pedersen, J.Z. (1985) Isr. J. Chem. 25, 56-65.
13. Chan, S.I., Bocian, D.F., Brudvig, G.W., Morse, R.H., Stevens, T.H. (1979) in Cytochrome Oxidase (King, T.E., et al., Eds.) pp. 177-188, Elsevier/North-Holland Biomedical Press, Amsterdam.
14. Blair, D.F., Gelles, J., Chan, S.I. (1986) Biophys. J. in press.

Chapter II

Chemical Modification of the Cu_A Center
in Cytochrome c Oxidase by Sodium p-Hydroxymercuribenzoate

Cytochrome c oxidase catalyzes the final step of the mitochondrial electron transport chain in which electrons derived from the oxidation of ferrocytochrome c are consumed in the reduction of oxygen to water. Each molecule of the enzyme contains two copper ions and two hemes. Three of these four metal centers are known to play critical roles in the catalytic cycle: one of the hemes (referred to as Fe_a)¹ is thought to be the primary electron acceptor from cytochrome c and its location within the enzyme is presumed to be near that of the cytochrome c binding site (1) [although for an alternative view see (2)]; the other heme (Fe_a) and one of the copper ions (Cu_B) together make up the binuclear site which binds O_2 and O_2 -derived intermediates while they undergo a complex sequence of chemical conversions that ultimately result in the synthesis of two H_2O molecules. The O_2 binding site is thought to reside in a hydrophobic environment inside the protein (3, 4), and is located a substantial distance (approximately 20 Å) away from Fe_a (5). The enzyme must therefore contain an electron transfer pathway which connects the two sites and facilitates the rapid movement of electrons during turnover.

The role played by the fourth metal center, the low-potential copper-ion site (Cu_A), is less well

understood. Pioneering studies of the reduction and oxidation kinetics of this site during the reaction of the enzyme with ferrocyclochrome c or with O_2 by Gibson and Greenwood (6, using optical spectroscopy) and by Beinert and Palmer (7, using electron paramagnetic resonance [EPR] spectroscopy) revealed rapid reaction rates similar to those observed for Fe_a . The results of these and more recent kinetic studies have in general been interpreted in terms of a catalytic mechanism in which Cu_A is located between Fe_a and the O_2 binding site in the electron transfer pathway within the enzyme and serves as a redox mediator facilitating electron transfer from the former to the latter (6). It should be noted, however, that more elaborate (8) or completely different (9) mechanisms have also been proposed. Since it is difficult to distinguish between these alternative mechanisms on the basis of kinetic data alone, other types of studies are required to provide additional insight.

An approach which has proven to be particularly valuable in elucidating the functional role of individual metal centers in multi-site metalloproteins is the preparation of enzyme derivatives in which the structure of an individual metal center is perturbed by chemical modification. Chemical, spectroscopic, and kinetic analyses of these

derivatives can yield information about the involvement of that center in particular parts of the catalytic cycle. Studies on Polyporus laccase, for example, have shown that fluoride ions bind specifically to the type 2 copper of this enzyme. This structural change decreases the reduction potential of the copper center and inhibits enzyme turnover (10, 11).

The oxygen binding site of cytochrome oxidase also reacts readily with certain externally added reagents, and these reactions have been used extensively as structural probes of the chemical structure and reactivity of this site (12, (13). Cu_A , in contrast, appears to be inaccessible to added reagents; although chemical modification of this site has been reported, this has only been accomplished under conditions which cause denaturation and/or complete inhibition of the enzyme (14, 15, 16). Even though no reagents are known which produce chemical changes at the Cu_A site in the intact enzyme (except for the reversible, one-electron redox transformations associated with electron transfer through the enzyme), a great deal of information about Cu_A has been obtained through extensive study of the spectroscopic properties of this center. A number of these features are unique among the copper proteins and undoubtedly reflect an unusual ligation structure at the

site. Some of the amino acid side chains which serve as ligands to Cu_A were recently identified by Chan and co-workers (17), who used a variety of magnetic resonance techniques to study yeast cytochrome c oxidase which had been metabolically labelled with isotopically substituted amino acids. These studies demonstrated the presence of at least one histidine and at least one cysteine ligand at the site. Data from subsequent experiments suggest that a second cysteine is also associated with the Cu_A site (18, 19).

It has long been suspected that one or more thiol groups play important roles in the catalytic turnover of cytochrome oxidase. The effect on the enzyme's structure and activity of chemical modification with thiol-reactive compounds, particularly mercury compounds, has been extensively investigated (14, 20, 21, 22, 16, 23, 24, 25, 26). It has been suggested that the non-polar mercurial reagents HgCl₂, CH₃HgCl, and CH₃CH₂HgCl, which at low concentrations cause partial inhibition of oxidase turnover, do so by chemically modifying cysteine ligand(s) to an (unspecified) copper center in the enzyme (25); however, no evidence of such a modification was detected in EPR studies of CH₃CH₂HgCl-treated cytochrome oxidase (24). In this work, we report conditions under which the thiol chemical

modification reagent sodium p-hydroxymercuribenzoate (pHMB) can be used to prepare a derivative of cytochrome c oxidase in which Cu_A has been converted from its native structure into a new, spectroscopically distinctive form. Characterization of the spectroscopic properties of the enzyme derivative and of its reactions with cytochrome oxidase substrates and inhibitors reveals little or no change in the structural and chemical properties of Fe_a and the oxygen binding site; the observed changes which accompany the modification reaction are confined to Cu_A. We further show that the modification of Cu_A is accompanied by only a partial loss of the overall cytochrome c-to-O₂ electron transfer activity. The residual activity is unlikely to involve electron transfer through Cu_A since there is no detectable reduction of Cu_A²⁺ by substrate under the conditions employed. As these results suggest that Cu_A is not required for simple electron transfer turnover of the enzyme, we discuss the possible roles which this center may play in catalysis by the enzyme.

MATERIALS AND METHODS

pHMB, p-chloromercuribenzoic acid (pCMB), phenazine methosulfate (PMS), NADH, Tween 20, and Tween 80 were purchased from Sigma; mercuric chloride was from Mallinckrodt and methylmercuric chloride and ethylmercuric chloride were from Alfa. All anaerobic work was performed under 1 atm of argon gas which had been scrubbed of residual oxygen by bubbling the gas through a solution of 0.1 M vanadium(II) in 2N HCl. Nitric oxide (Matheson) was passed through a cold trap before use (27); research grade carbon monoxide (99.99%, Matheson) was used without further purification.

Cytochrome c oxidase was purified from beef heart mitochondria by the method of Hartzell and Beinert (28) and was stored frozen at -80° until used. The enzyme preparation used in these studies had a specific activity of 9.0 nmol O₂ min⁻¹ (μg protein)⁻¹, and contained 8.0 nmol heme a (mg protein)⁻¹.

Protein concentration measurements. Protein concentrations were assessed by a modification of the Lowry procedure which includes 1% sodium dodecyl sulfate to solubilize integral membrane proteins (29). This technique

eliminates interference from non-ionic detergents (30). A bovine serum albumin standard was used routinely to check the linearity of the assay; however, except for the measurements of the specific activity and the heme-to-protein ratio reported above, only determinations of the relative concentrations of cytochrome oxidase protein are used in this work.

Preparation of pHMB-modified cytochrome oxidase. 10 ml of 22 μ M cytochrome c oxidase in 50 mM Tris-Cl, pH 7.7, 50 mM NaCl, 0.5% Tween 20 was saturated with pHMB by incubation with 18 mg of this compound with periodic stirring at 20° C. The reaction time was 25 hr unless otherwise specified. The mixture was then cooled to 4° C and centrifuged at 15,000 rpm in a Sorvall SS-34 rotor for 10 min to remove undissolved pHMB. In order to remove unreacted pHMB from solution, the supernatant was transferred to a stirred pressure ultrafiltration apparatus (Amicon 8010 cell with an XM300 membrane) at 4° C and subjected to three cycles of concentration to 1 ml under 10 psig N₂ gas followed by redilution to 10 ml with fresh buffer. Separate control experiments demonstrated that essentially all of the cytochrome oxidase but only a small fraction of the Tween 20 is retained by the ultrafiltration membrane under these conditions. After a final concentration step, the enzyme

solution was frozen in liquid nitrogen and stored at -80°C for future use. Samples identified as "unmodified control" were prepared exactly as described above except that pHMB was not included in the reaction mixture.

No precipitation or turbidity was observed in samples prepared by the above procedure; however, excessive light scattering was observed in samples from preliminary experiments in which the reaction with pHMB was conducted at a concentration of enzyme approximately 10-fold larger than that described above.

Reaction with reductants and with oxygen. For the single-turnover reaction studies, enzyme samples were placed in stopcock-equipped spectrometer cells and were made anaerobic by repeated cycles of evacuation, filling with purified argon, and agitation. Additions of NADH/PMS or sodium ascorbate were accomplished by anaerobic syringe techniques. Additions of sodium dithionite were conducted by the method of Beinert and co-workers (31, 32), except that the reductant capillary was placed unsealed in the sample cell sidearm and the entire apparatus was evacuated as a unit. Samples reduced by any of these techniques were reacted with oxygen by replacing the atmosphere over the enzyme solution with 1 atm air and agitating the cell.

For the EPR spectroscopic studies at -20° of enzyme samples reduced by cytochrome c/ascorbate, the reaction mixture contained 110 μM cytochrome oxidase, 120 μM cytochrome c, and 520 μM sodium ascorbate; the reaction was conducted at 0°C for 70 min. Conditions for all other reactions with reductants are specified in the figure legends.

Enzyme activity measurements. Cytochrome c oxidase activity was assayed by observing the rate of O_2 consumption with a YSI Model 53 polarographic oxygen sensor. The measurements were made at 30.0° in 3 ml of 50 mM potassium phosphate buffer, pH 7.4, containing 0.5% Tween 80, 15 mM sodium ascorbate, 51 μM cytochrome c, and less than 0.1 μM cytochrome c oxidase. Neither the native nor the pHMB-modified enzyme preparations displayed any detectable ascorbate oxidase activity when assayed in the absence of added cytochrome c.

EPR Spectroscopy. Samples for EPR spectroscopy were equilibrated with 1 atm argon immediately before freezing to eliminate signals from O_2 . EPR spectra were recorded using a Varian E-line Century Series X-band spectrometer, the output signal of which was digitized by a 12-bit

analog-to-digital converter interfaced to a minicomputer. Samples were maintained at -20°C with a nitrogen gas flow system (Varian V4540), at 77 K by immersion in liquid nitrogen, or at 10 K with a helium gas flow system (Air Products Heli-Tran). All combinations of sample temperature and microwave power employed in this study were checked to ensure that they did not cause saturation of the Cu^{2+} EPR signal being observed. Spectra were recorded at the lowest instrument time constant consistent with efficient data sampling; additional post-acquisition filtering was applied to some spectra (33, 34). All spectra were corrected for instrument response by subtracting the spectrum of an equal volume of water.

EPR Integration and Simulation. EPR powder spectra were simulated by summing a large number (greater than 8000) of gaussian envelopes computed for various powder angles. Line positions were calculated assuming coincident A and g tensors (35), and line intensities were scaled by $1/g$ (36).

EPR signal intensities were measured by numerical integration of all or a portion of the signal as described by Aasa and Vänngård (36). In cases where the second integral of the entire signal was calculated, the position of the integration baseline was determined by requiring the

first integral to be zero. For the integration of the high-spin ferric heme signals, the above method could not be used because of the presence of interfering Cu^{2+} and low-spin heme signals in the $g=2$ region. In this case, the line shape of the $g=6$ region of the signal was simulated (with g_z assumed to be 2.0) and the simulated spectrum was used as a standard for the partial double integration of the experimental spectrum as described by van Gelder and Beinert (37).

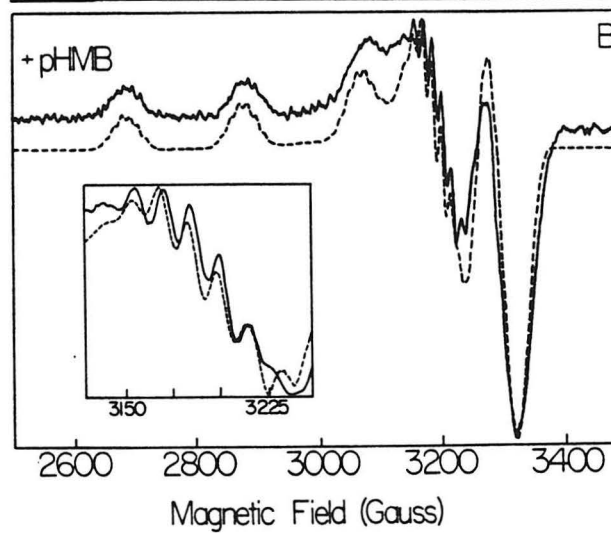
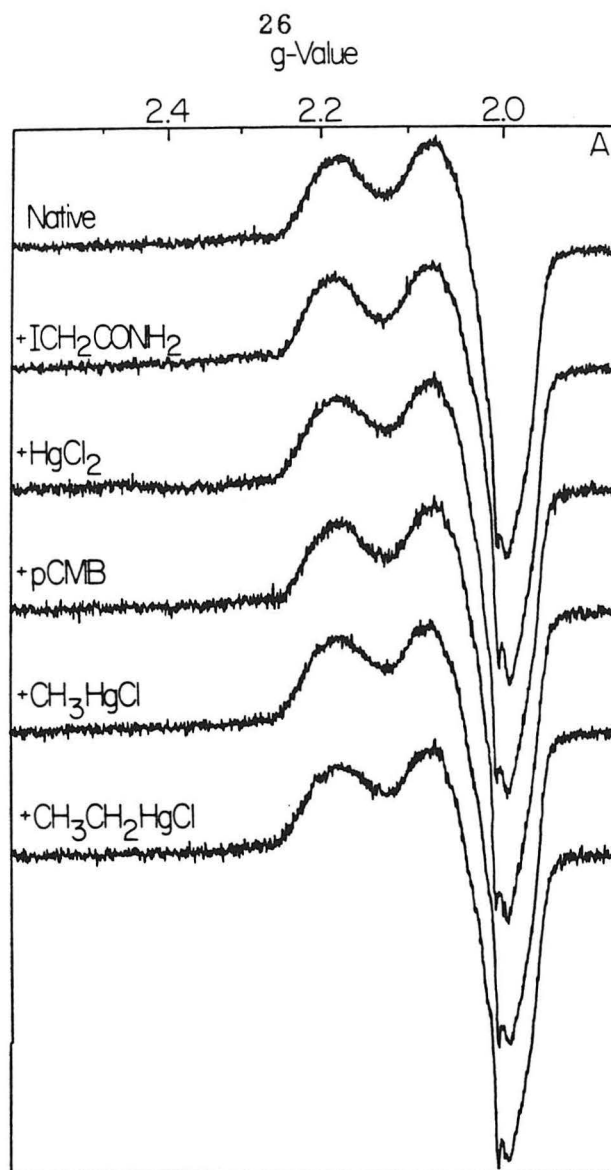
Optical Spectroscopy. Optical absorption spectra were measured at 4° or 20° in a Beckman Acta CIII spectrophotometer and were recorded on a Spex Industries SCAMP SC-31 data processor. Spectra were corrected for instrument response by subtracting the spectrum of an equal volume of water.

RESULTS

Effects of thiol-modification reagents on the spectroscopic properties of Cu_A. The EPR spectra of native cytochrome c oxidase and a number of its previously characterized sulfhydryl reagent derivatives are shown in Fig. 1A. Under the spectrometer conditions used, the observed EPR spectrum arises almost exclusively from the oxidized Cu_A center, and it is rather atypical of Cu²⁺ EPR spectra, particularly in that it does not display resolved Cu hyperfine splittings (38, 39, 17). The shape of the EPR signal is unchanged by treatment of the enzyme with CH₃CH₂HgCl [as was reported by Mann and Auer (24)], with CH₃HgCl or with HgCl₂. Cu²⁺ EPR spectra are quite sensitive to changes in the ligands or ligation geometry of the metal center (40); this observation therefore argues strongly that the reactions of cytochrome oxidase with these reagents do not involve chemical modification of any ligands to Cu_A. The spectrum is also unchanged by treatment of the enzyme with pCMB under conditions shown by Tsudzuki, et al. (20) to label all but one or two of the approximately 14 thiol groups present in one molecule of the beef heart enzyme. If, in contrast, the enzyme is reacted with a high concentration of pHMB² for a much longer period of time (see Experimental Section), a derivative which has a distinctly

Figure 1

EPR signal from the Cu_A^{2+} site after treatment of cytochrome oxidase with thiol modification reagents. A: Reactions with reagents previously reported to modify cytochrome oxidase cysteine residues. Treatment with the indicated reagent was conducted under the conditions described in the specified reference, with the exception of the detergent used, which was 0.5% Tween 20 in all cases. Trace 1: untreated cytochrome c oxidase. Trace 2: treated with iodoacetamide (25). Trace 3: treated with HgCl_2 (25). Trace 4: treated with pCMB (20). Trace 5: treated with methylmercuric chloride (26). Trace 6: treated with ethylmercuric chloride (24). B: Solid trace: Reaction with pHMB under conditions described in this work (see experimental section). Dashed trace: Simulated EPR powder spectrum calculated for an $S=1/2$ spin system ($g_x=2.046$, $g_y=2.084$, $g_z=2.226$) with hyperfine coupling to a natural abundance mixture of ^{63}Cu and ^{65}Cu ($I = 3/2$) nuclei and superhyperfine coupling to three equivalent ^{14}N ($I = 1$) nuclei (Cu: $A_x=A_y=0$, $A_z(^{63}\text{Cu})=555$ MHz, $A_z(^{65}\text{Cu})=595$ MHz; N: $A_x=24.0$ MHz, $A_y=43.7$ MHz, $A_z=40.0$ MHz). Inset: Magnified view of the spectral region exhibiting the ^{14}N superhyperfine splittings. Spectrum acquisition conditions: sample temperature, 77 K; power, 4 mW; frequency, 9.28 GHz; modulation amplitude, 10 G.



different EPR spectrum is formed (Fig. 1B). This spectrum, which resembles those of the type 2 copper proteins (41) is well fitted by a computer-simulated Cu^{2+} EPR powder spectrum which includes a strong ($A_z \approx 590$ MHz) hyperfine coupling to the copper nucleus as well as superhyperfine interactions with three ^{14}N nuclei. Like the EPR signal from Cu_A in the native enzyme, this signal is not modified by treatment with a low ($33 \mu\text{M}$) concentration of EDTA, and the species from which it originates cannot be removed from the enzyme by dialysis. We have compared the integrated intensity of the Cu^{2+} EPR absorption spectrum (measured under the same conditions as those in Fig. 1) of the pHMB-modified enzyme with that of an unmodified control sample. If the signal from the unmodified enzyme is taken to represent 0.8 mol Cu_A^{2+} per mol enzyme (28), then the intensity of the signal after treatment with pHMB corresponds to 1.1 mol Cu^{2+} per mol enzyme. The observed spectroscopic change is therefore more consistent with the conversion of the Cu_A site to a structurally different form than it is with the development of an additional signal from the normally EPR-undetectable Cu_B site.

Comparison of the optical absorption spectra of the native and pHMB-modified enzyme samples provides further evidence of a chemical change at the Cu_A center. Native

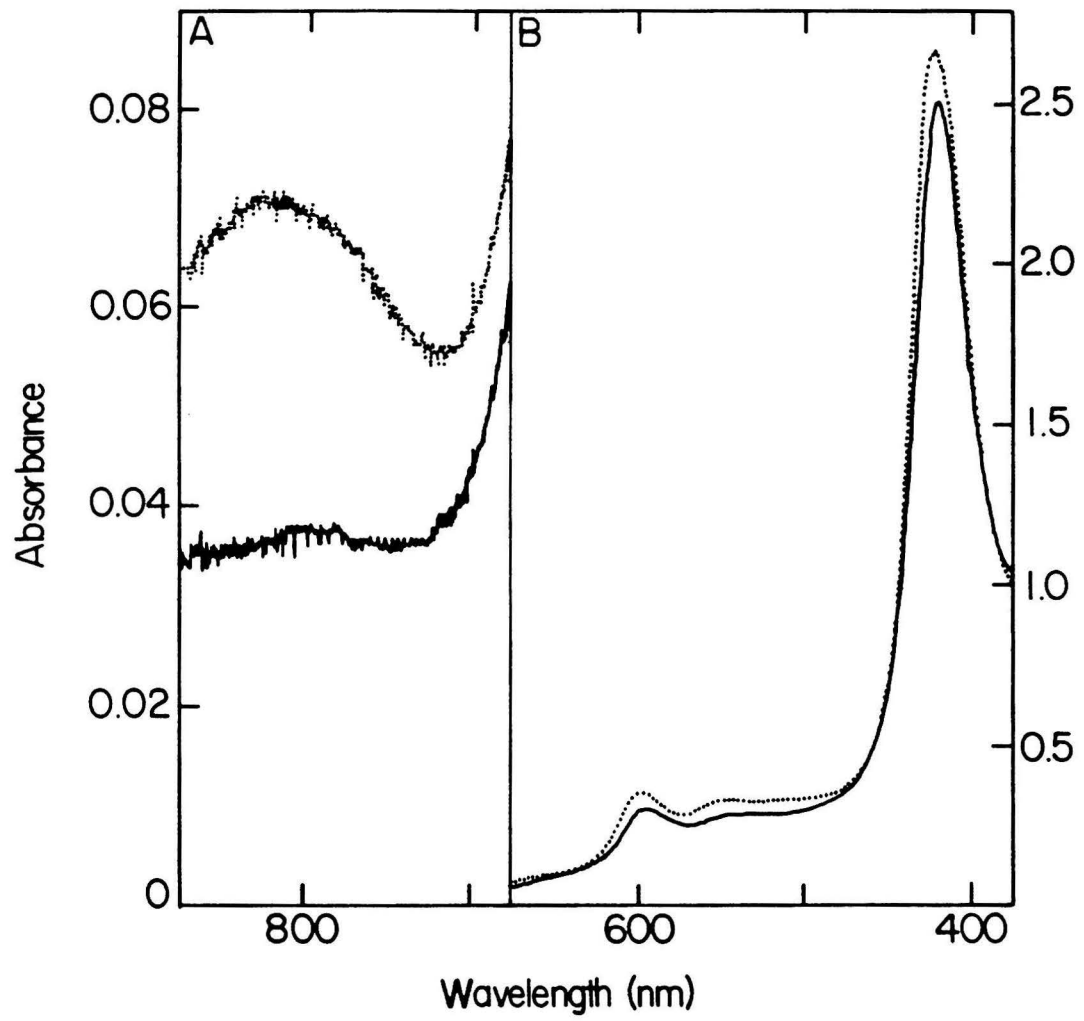
cytochrome oxidase shows a broad absorption band in the near-infrared region, centered at 830 nm. The band arises from the Cu_A^{2+} site and has been assigned to a charge-transfer transition between the cupric ion and a cysteine ligand (42, 13). This absorption is completely abolished when the enzyme is reacted with pHMB (Fig. 2A). In contrast, only small intensity changes are observed in the visible region, the spectral features of which are largely due to the two heme chromophores of the enzyme (Fig. 2B).

Fe_a and the oxygen binding site in the pHMB-modified enzyme. The foregoing observations show that, under appropriate conditions, the treatment of cytochrome oxidase with pHMB causes a structural alteration of the Cu_A site; however, they do not clearly indicate whether the other two electron-transfer sites are also affected by this treatment or whether the changes in the heme spectra are merely indicative of a minor perturbation in the environments of these chromophores. Moreover, it is important to ascertain whether the modified protein is still largely in its native conformation or whether it has been partially or completely unfolded.

In order to more thoroughly characterize the states of

Figure 2

Comparison of the near-infrared and visible spectra of native and pHMB-modified cytochrome oxidase. Absorption spectra of a sample of cytochrome oxidase taken before (dotted trace) and after (solid trace) reaction with pHMB under the conditions described in the Experimental section.

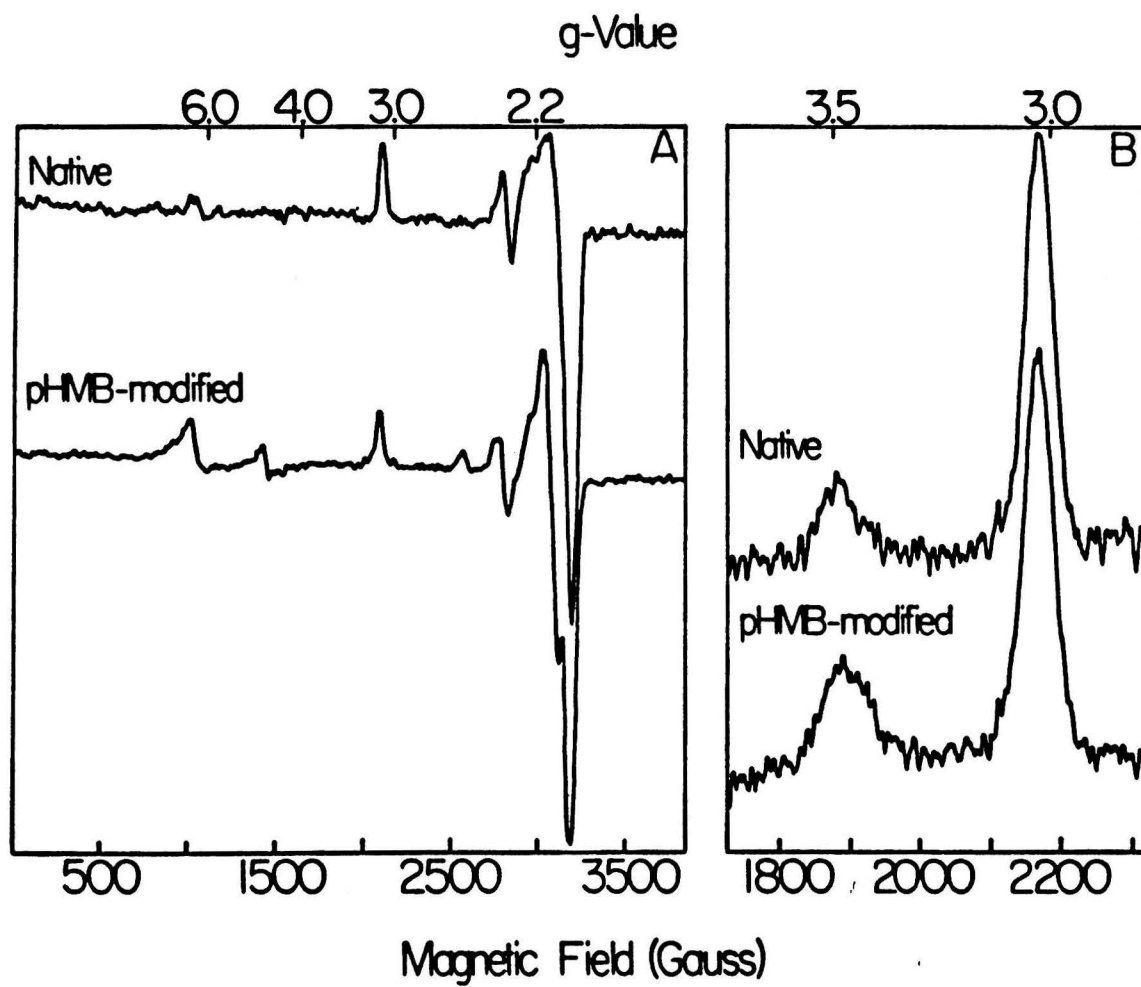


the iron centers Fe_a and Fe_a , in the pHMB-modified enzyme, we examined the EPR signals from these centers at low temperature (10 K). The g -values of ferric heme complexes are very sensitive to changes in the identity of the axial ligands to the iron (43). The native enzyme contains a signal due to Fe_a^{3+} at $g_z=3.0$; an identical peak is observed in the spectrum of the modified enzyme (Fig. 3A). Both spectra also contain an Fe_a^{3+} peak at $g_y=2.2$, although in the case of the pHMB-modified enzyme this is partially obscured by the $M_I=1/2$ parallel hyperfine component of the signal from the modified Cu_A center. Integration of the $g=3.0$ signals from two similar enzyme preparations revealed that the modified enzyme retains 87% (after adjusting for the relative protein concentrations of the two samples) of the Fe_a signal intensity in the native enzyme.

Fig. 3A shows that the modification reaction is accompanied by the appearance of EPR signals in the $g=4$ and $g=6$ regions. Signals at $g=4$ are frequently seen in cytochrome oxidase preparations and are thought to arise from low concentrations of contaminants containing non-heme Fe^{3+} ions (37). The larger signal in the $g=6$ region is of some concern since axial or rhombic epr signals with $g_x \approx g_y \approx 6$ and $g_z \approx 2$ are characteristic of high-spin ferric hemes (44). For the bottom spectrum in Fig. 3A, however, the integrated

Figure 3

Comparison of the low-temperature EPR spectra of native and pHMB-modified cytochrome oxidase. Top traces: cytochrome oxidase (unmodified control). Bottom traces: pHMB-modified cytochrome oxidase. Conditions: sample temperature, 10 K; power, 0.2 mW; frequency, 9.18 GHz. A: Samples equilibrated with 1 atm argon. Modulation amplitude: 10 G. B: Samples containing 3 mM KCN equilibrated with 1 atm nitric oxide. Modulation amplitude: 20 G.



intensity in the $g=6$ signal corresponds to only 2% of the number of Fe^{3+} centers that give rise to the $g=3$ signal in the same spectrum. This signal may originate in a minor contaminant in the enzyme preparation, or may arise from denaturation of a small fraction of the cytochrome oxidase present, but it clearly does not represent a structural alteration at a significant fraction of the oxidase heme sites.

Under ordinary conditions, the Fe_a and Cu_b centers in native cytochrome c oxidase do not exhibit EPR signals (as would ordinarily be expected from Fe^{3+} and Cu^{2+} centers) because they are closely apposed at the oxygen binding site in such a way that a strong exchange interaction exists between the unpaired electrons of the two metal ions (37, (45)). The fact that the reaction of the enzyme with pHMB induces only an insubstantial signal at $g=6$ and no other new EPR signals that could be assigned to ferric hemes is therefore consistent with the presence of an intact O_2 binding site in the modified enzyme.

More direct information about the structure of the oxygen binding site is provided by the EPR spectra of native cytochrome oxidase and the pHMB derivative after incubation with nitric oxide and KCN (Fig. 3B). Fe_a^{3+} readily binds

CN⁻ ions, and when NO is also present, the latter binds to Cu_B and breaks the ferromagnetic coupling (46) between this center and Fe_{a₃}-CN, thereby rendering the Fe_{a₃}³⁺-CN center EPR-visible (47, 48). The peak position observed for this g=3.5 cyanochrome a₃ signal and its intensity relative to the amount of protein in the sample are identical in the native and the pHMB-modified samples (g-values: native, 3.49; modified, 3.47; intensity ratio modified:native = 1.1:1). The above data, taken together, constitute evidence that both Fe_{a₃} and Fe_a are not significantly affected by pHMB treatment under the same conditions in which this reagent completely converts Cu_A into a new, spectroscopically distinctive form.

Catalytic turnover of the PHMB-modified enzyme. We have assessed the catalytic competence of the enzyme containing the modified Cu_A center by measuring its specific activity of cytochrome c-driven O₂ reduction under pseudo-steady state conditions. Table I shows that the reaction with pHMB is accompanied by an approximately five-fold decrease in the activity. As judged by spectroscopic criteria, the pHMB-modified oxidase preparation is virtually free of enzyme molecules containing an unmodified Cu_A site. By comparing the peak height of the near-infrared absorptions (A₈₃₀-A₉₀₀ from the data of Fig. 2) in the control and

pHMB-modified samples, we conclude that the modified enzyme contains less than 4% of the original amount of intact Cu_A chromophore. A similar analysis of the EPR spectra of Fig. 1 reveals no detectable intensity above the baseline from the Cu_A²⁺ g_z=2.18 signal in the region of 2975 G. The bulk of the specific activity remaining after pHMB-modification (approximately 20% that of the native enzyme) must therefore be attributed to enzyme molecules containing the modified Cu_A center; the specific activity of the modified oxidase preparation is too large to be accounted for by the small amount of native oxidase which might still be present. The observation of residual activity thus implies that the modified enzyme sample contains a substantial number of molecules which possess functionally intact cytochrome c binding and O₂ reduction sites and that these sites are connected by an electron transfer pathway which is at least one-fifth as effective as that in the unmodified control enzyme.

Reduction of the pHMB-modified enzyme by sodium dithionite and reoxidation by O₂. It is unclear from the measurements of turnover kinetics whether the modified Cu_A center participates in the electron transfer process or whether the reactions occur independently of it. However, the effect of reductants and oxidants on the EPR spectrum of

Table I: Catalytic Activity of pHMB-Modified and Unmodified Samples of Cytochrome *c* Oxidase

sample no.	sample type	incubation time (h) ^a	relative protein concn	activity (nmol of O ₂ min ⁻¹) (mean \pm SD) ^b	relative specific activity
1	pHMB modified	24	29.7	22.7 \pm 1.6	0.76 \pm 0.05
2	pHMB modified	36	24.5	11.9 \pm 2.4	0.48 \pm 0.10
3	unmodified control	0	16.7	55.2 \pm 0.4	3.30 \pm 0.02
4	unmodified control	36	25.9	82.2 \pm 1.7	3.17 \pm 0.06

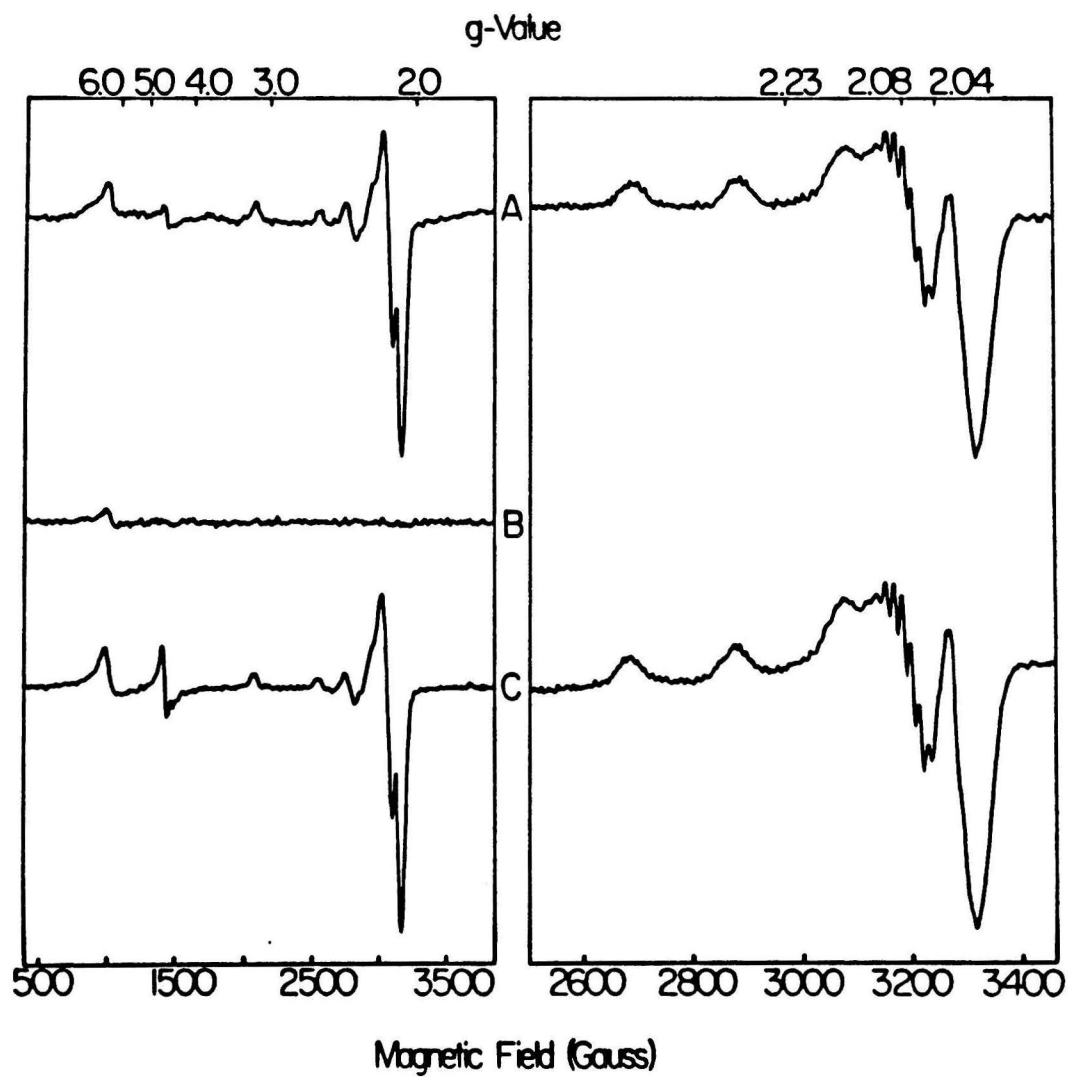
^a Incubation time at 20 °C; see Materials and Methods. ^b Mean of three determinations.

the modified enzyme provides some clues about the role that the modified Cu_A center plays in the redox behavior of this species. When an anaerobic sample of native cytochrome c oxidase is treated with the powerful reductant sodium dithionite (Na₂S₂O₄), all four of its metal centers are reduced and the EPR signals from Fe_a³⁺ and Cu_A²⁺ are consequently eliminated. The corresponding EPR signals from the pHMB-modified enzyme (Fig. 4A) are also removed by Na₂S₂O₄ treatment (Fig. 4B). As would be expected, the optical spectra of such samples are consistent with complete reduction of both hemes (data not shown). It should be noted that the reduction of the modified copper is reversible: re-exposure of a dithionite-reduced sample of the modified enzyme to air results in the reappearance of Fe_a³⁺ and modified copper EPR signals identical to the original oxidized signals (Fig. 4C). These results provide strong evidence for the existence of a competent electron transfer pathway in the pHMB-modified enzyme which directly or indirectly connects both the EPR-visible copper and the Fe_a centers to the oxygen binding site.

Reduction of the pHMB-modified enzyme by ascorbate/ cytochrome c or NADH/PMS and reoxidation by O₂. Sodium dithionite is thought to reduce cytochrome oxidase by transferring electrons into the enzyme primarily through the

Figure 4

Redox behavior of Fe_a and the EPR-visible copper center in pHMB-modified cytochrome oxidase: reduction by sodium dithionite and reoxidation by O₂. A: Oxidized pHMB-modified cytochrome oxidase (approximately 140 μ M). B: Same sample after anaerobic reduction for 10 min with 1.1 mM Na₂S₂O₄. C: Same sample after subsequent reoxidation with air. Left side spectra conditions: same as Fig. 3A; temperature, 9-10 K. Right side spectra conditions: temperature, 77 K; power, 4.0 mW; frequency, 9.26 GHz; modulation amplitude 10 G.

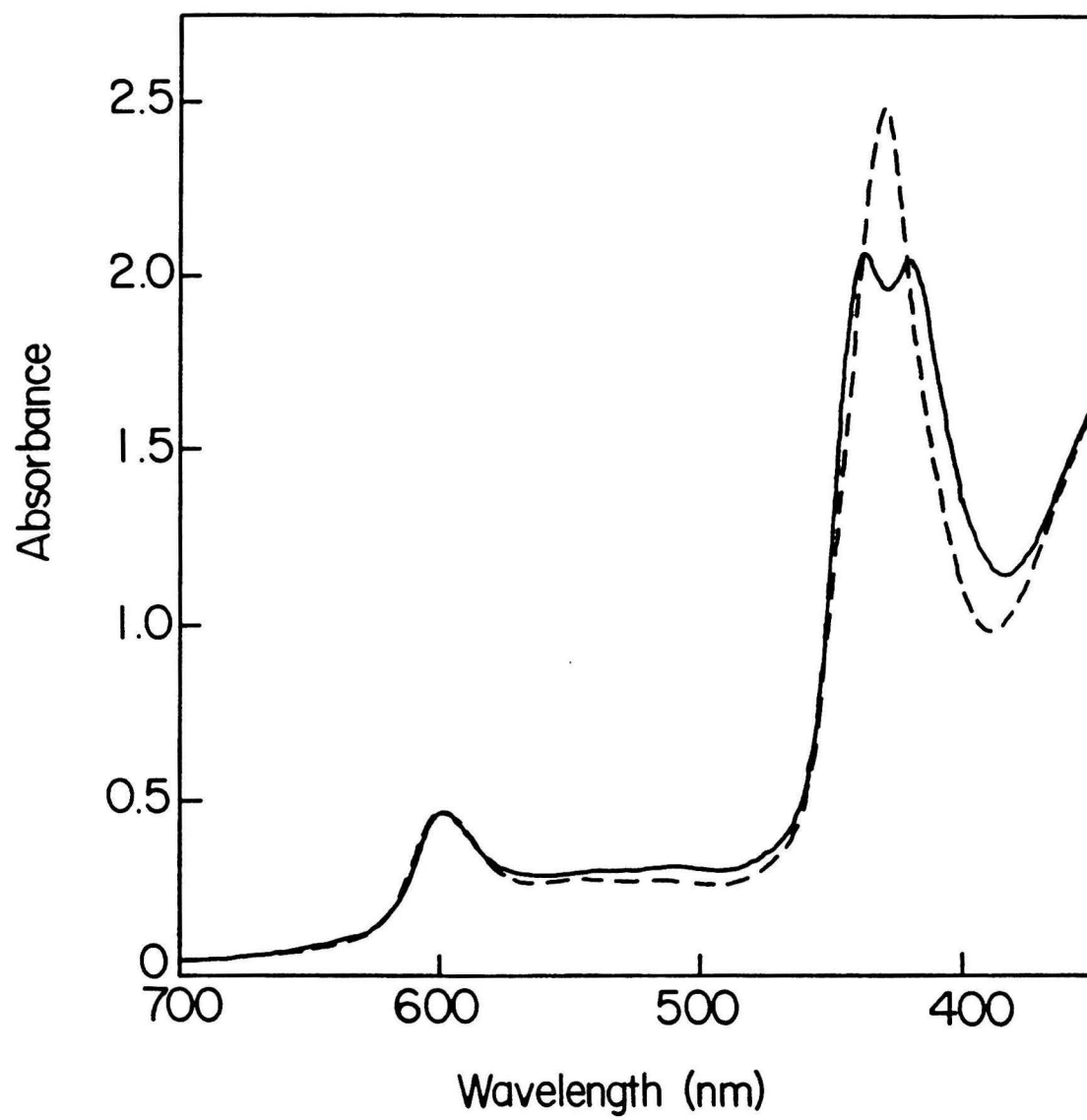


oxygen binding site rather than through the physiologically-relevant reduction pathway involving the cytochrome c binding site (49). In contrast, cytochrome c (reduced by sodium ascorbate, which does not reduce cytochrome oxidase directly) and phenazine methosulfate (reduced by NADH, which does not reduce cytochrome oxidase directly) are both known to react with the enzyme via the cytochrome c binding site (50, 49). These reductants can therefore be used in experiments to examine the functioning of this electron-transfer pathway. Under steady-state aerobic conditions, electron transfer to all of the metal centers in native cytochrome oxidase is rather rapid (turnover $> 10^2 \text{ sec}^{-1}$). When cytochrome oxidase is treated with NADH/PMS or ferrocytochrome c in the absence of O_2 , however, Fe_a^{3+} is still reduced rapidly but Fe_a^{3+} reacts at a much slower rate (50).

The hemes in the pHMB-modified enzyme exhibit similar behavior to those in the native enzyme when the modified protein is treated with reductants that act at the cytochrome c binding site. After reduction with NADH/PMS for 75 min, the optical spectrum (Fig. 5) of the enzyme shows two Soret peaks (438 and 421 nm), one of which displays the shift to longer wavelengths expected from reduction of a heme chromophore. EPR spectra of this sample

Figure 5

Reduction of the hemes of pHMB-modified cytochrome oxidase with NADH and PMS. Optical spectra of an anaerobic solution of pHMB-modified cytochrome oxidase. Enzyme concentration approximately 110 μM . Solid trace: after reduction with 430 μM NADH and 0.93 μM PMS at 0° C for 75 min. Dashed trace: same sample after reduction for 90 min and equilibration with 1 atm CO.



revealed no detectable Fe_a^{3+} signal at $g=3.0$, confirming the reduction of this center to Fe_a^{2+} . Incubation of the sample for longer times resulted in a progressive intensity increase of the longer wavelength optical band and concomitant diminution of the shorter wavelength band, as is expected if the initial reduction of Fe_a is followed by the slower reduction of Fe_a ; this process is somewhat slower in the modified enzyme than in the unmodified control. [It should be noted, however, that the rates of electron transfer to the oxygen binding site under anaerobic conditions are not necessarily relevant to kinetics under turnover (i.e. aerobic) conditions. It is thought that the effective reduction potential of this site is greatly increased in the presence of O_2 ; this change in reduction potential is associated with a dramatic increase in the rate of electron transfer to the oxygen binding site from Fe_a^{2+} and Cu_A^{1+} (50).] Finally, addition of CO to a sample which had been reduced with PMS/NADH for 90 min immediately gave rise to the dashed spectrum in Fig. 5; identical spectra were obtained even when the CO was added after an extremely long (c. 50 h) incubation with NADH/PMS (data not shown). Since CO binds only to the reduced Fe_a heme, the CO-induced spectral change must involve production of a species containing an Fe_a^{2+} -CO complex. In fact, the observed spectrum ($\lambda_{\text{max}}=429.5$) is almost identical to that of the

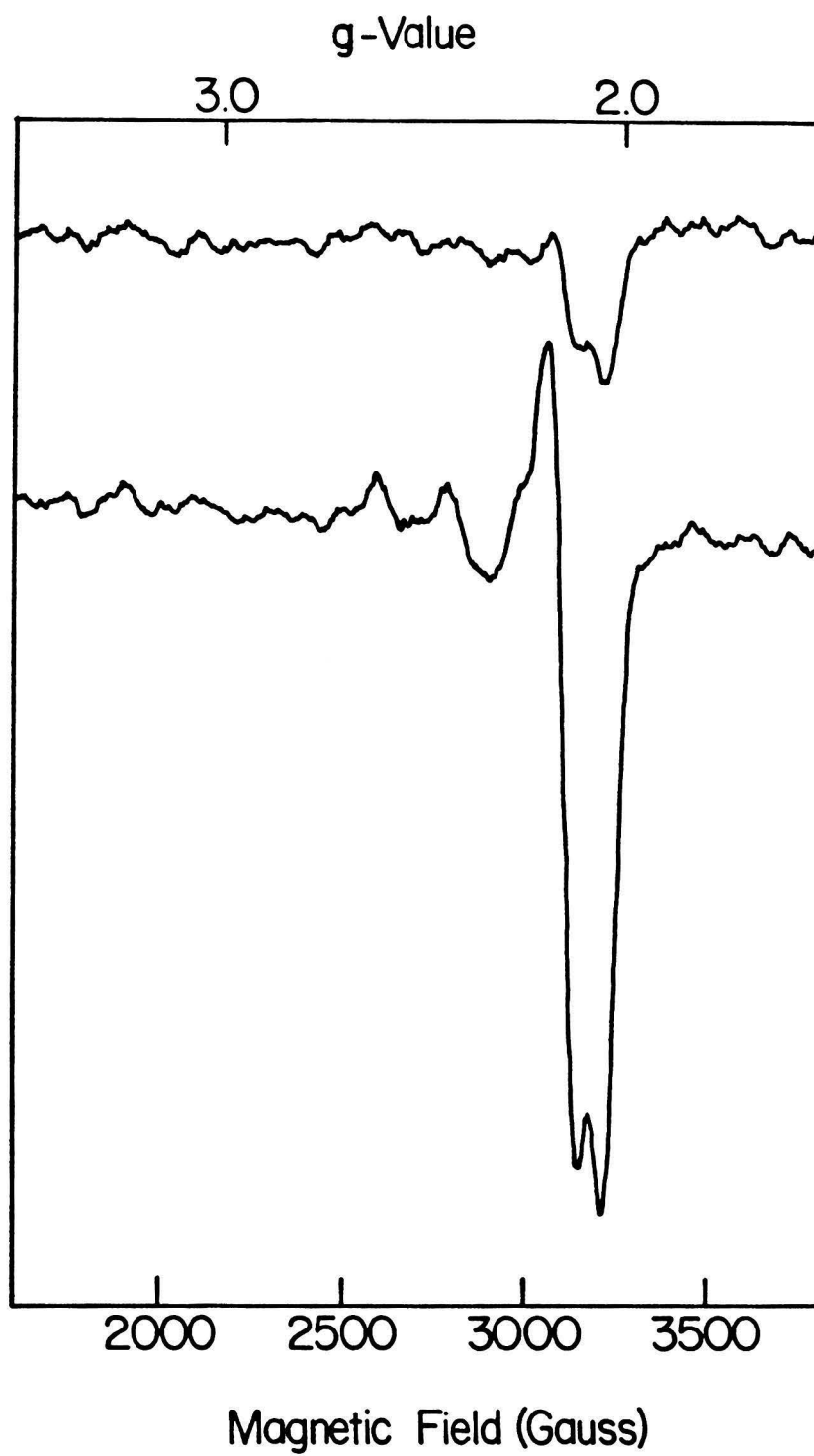
fully reduced-CO complex of native cytochrome oxidase ($\lambda_{\text{max}}=430.0$), and EPR spectroscopy at 10 K confirms that Fe_a is reduced in this species.

Similar results were obtained when an ascorbate/cytochrome c mixture was employed as the reductant. When O_2 was introduced to the reduced or partially-reduced enzyme samples, reoxidation of both the cytochrome oxidase and the excess ferrocytochrome c reductant was observed, again demonstrating that the modified oxidase has the ability to catalyze the oxidation of cytochrome c by O_2 . The optical absorbance change at 442 nm associated with the reoxidation of both the modified and unmodified control samples is completed on a time scale faster than that observable by manual mixing methods (c. 10 s). Taken together, the results of the single-turnover experiments indicate that the iron centers of the modified enzyme retain the electron transfer functions of those in the native enzyme.

In contrast to the redox behavior of the heme irons, the response of the EPR-visible copper to the milder reductants is inhibited after reaction of the enzyme with pHMB. The top spectrum in Fig. 6 demonstrates that, in the native enzyme, both Fe_a and Cu_A are largely reduced by treatment with NADH and PMS under anaerobic conditions. When the

Figure 6

Reduction of the EPR-visible copper centers in native and PHMB-modified cytochrome oxidase by NADH and PMS. EPR spectra of anaerobic enzyme samples incubated with NADH and PMS under the conditions of Fig. 5A. Top trace: cytochrome oxidase (unmodified control). Bottom trace: PHMB-modified cytochrome oxidase. Conditions for EPR spectroscopy same as Fig. 3A.



pHMB-modified enzyme is incubated under identical conditions, Fe_a is again reduced, but the EPR signal from the modified copper center is still present, indicating that this site remains in its cupric oxidation state. Even when a sample of the modified enzyme is treated with NADH/PMS for as long as 50 h, a decrease in the intensity of the modified Cu^{2+} EPR signal is not observed. The optical spectrum of this sample is consistent with complete reduction of both hemes (data not shown). Since the EPR spectra in Fig. 6 are taken at cryogenic temperatures, the positions of the redox equilibria between the Cu^{2+} and potential reductants studied under these conditions are not necessarily the same as those at physiological temperatures. We have therefore examined the redox properties of the modified copper center by exposing it to the physiological reductant, cytochrome c (reduced by the addition of excess sodium ascorbate), and recording the copper EPR signal intensity at a substantially higher temperature (-20°). Comparison of the mean relative intensity of the modified Cu^{2+} signals in the samples after the addition of reductant with that before reduction and after reoxidation with air (6.6 ± 1.4 and 6.0 ± 1.0 , respectively) reveals no reduction of the modified copper under these conditions. Thus, the pHMB modified copper center is not substantially reduced under conditions of applied reduction potential similar to those under which the

substantial steady-state turnover activities were measured.

DISCUSSION

It is unlikely that the chemical modification of cytochrome c oxidase by pHMB described in this chapter is a specific chemical modification of cysteine ligand(s) of Cu_A. Tsudzuki et al. (20) treated cytochrome oxidase with pCMB and demonstrated that approximately all but 1 or 2 of the thiol groups present in a molecule of the beef heart enzyme were modified. Since we have employed both a much higher concentration (of pHMB) and a much longer reaction time for the preparation of the pHMB-modified enzyme, we expect that this reagent has also reacted with a majority of (or possibly with all of) the thiol groups present. It is therefore perhaps somewhat surprising that the reaction with pHMB does not cause more global changes in the structural and functional properties of the metal center active sites of the enzyme. The spectroscopic studies of the pHMB-modified enzyme do nonetheless demonstrate that, despite the major changes to the EPR and optical signatures of Cu_A, the EPR signals arising from the other oxidase metal centers are identical to the corresponding signals from the native enzyme. It is important to note that the EPR g-values and hyperfine coupling constants of a transition metal ion depend in a sensitive way on the electronic structure of the ion and are therefore responsive to

relatively minor changes in ligation. In the cases of ferric heme (40) and of Cu^{2+} (43) sites with ligands of the types found in metalloproteins, changes in the identity of ligands will almost invariably cause large, easily observable changes in the X-band EPR spectrum.

The optical absorption features of the cytochrome c oxidase hemes are also essentially unchanged by the modification; this observation is also consistent with the absence of major structural changes at these sites. In the absence of changes in the EPR spectra, the observed slight shifts in the peak positions of the heme optical bands most likely arise from small changes in the environment of the porphyrin macrocycle rather than from changes in the coordination environment of the iron. Even a change in the hydrogen bonding of a substituent on the periphery of the heme a ring can cause the type of perturbation of the optical spectrum noted here (51).

Structure of the modified copper center. Comparison of the spectroscopic properties of the native and pHMB-modified enzyme preparations shows clearly that treatment of the enzyme with pHMB induces a structural change at the Cu_A site; however, there is insufficient information to unambiguously determine the structure of the modified copper

center and the nature of the chemical transformations which produce it. The most straightforward mechanistic interpretation of the data is that the pHMB reacts with one or more cysteinate ligand(s) of Cu_A , thereby weakening or eliminating entirely the association of said ligand(s) with the copper ion and thus causing the changes in the electronic structure of the site which manifest themselves in the EPR and optical spectra. The assignment of the hyperfine structure in the g_y region of the EPR spectrum of the modified copper center to couplings with three equivalent ^{14}N nuclei is consistent with at least one ligand substitution at the site, since there are thought to be no more than two nitrogenous ligands to Cu_A in the native enzyme (17, 18, 19). It is also possible, however, that the reaction with pHMB of cysteine residues more distant from the Cu_A site induces conformational changes in the protein. If this is the case, these reactions might indirectly cause an alteration of the ligation structure at the Cu_A site, thereby inducing the spectroscopic changes.

Although the available data do not allow an unambiguous determination of the chemical nature of the modified copper center, several of the experiments demonstrate that the modified enzyme molecules retain their full complement of structurally intact Cu_B sites. The modified copper center

must therefore be derived from Cu_A only. Observations which support this conclusion are: 1) The total intensity of the Cu^{2+} EPR signal from the modified enzyme corresponds to one mole of Cu^{2+} per mole of enzyme. This observation is inconsistent with the production of an EPR-visible species from the (normally EPR-invisible) Cu_B center. 2) Production of an EPR-visible species from Cu_B^{2+} would require the elimination of the strong exchange coupling of this site with $\text{Fe}_{a_3}^{3+}$ and the latter center would then also be expected to exhibit an EPR signal; however, no substantial amounts of new signals that could be attributed to Fe_{a_3} -derived species are observed in the EPR spectrum of the pHMB-treated enzyme (Fig. 3A). 3) The production of the cytochrome a_3 EPR signal requires that CN^- and NO bind in a specific arrangement to both $\text{Fe}_{a_3}^{3+}$ and Cu_B^{2+} (52, 48). The observation that essentially all of the modified enzyme molecules can be converted into this form (Fig. 3B) is strong evidence that they contain functionally intact oxygen binding sites in which both metal centers display the same chemical properties as their analogs in the native enzyme. 4) The rapid four-electron reduction of oxygen by cytochrome oxidase is thought to involve ligation of both Fe_{a_3} and Cu_B by partially reduced intermediates derived from O_2 (13, (53)). The substantial turnover rate of the modified enzyme thus suggests that this site is functionally intact.

Redox reactions of the modified enzyme. The absence of pHMB-induced changes at the metal center sites other than Cu_A is reflected in the behavior of the modified enzyme in its reactions with reductants and with O_2 . Like those in the native enzyme, all four of the metal center sites in the pHMB-modified oxidase are reduced by sodium dithionite and can subsequently be rapidly reoxidized by O_2 . It should be noted that the lack of inhibition observed in the single-turnover experiments is consistent with the observations of Tsudzuki, et al. (20), who noted essentially no decrease in the rate of turnover of cytochrome oxidase when the enzyme was modified by pCMB. As previously discussed, the reaction conditions we have used for the pHMB modification probably cause modification of a larger number of sulfhydryl groups than occurred in the earlier work. This may account for the greater inhibition of the turnover kinetics which we observe; however, it is also possible that some of the inhibition is due to chemical effects of the pHMB other than local modification of the Cu_A site.

The most striking difference between the chemical properties of the native and pHMB-modified enzyme preparations involves their reactions with reductants. The

EPR-visible Cu^{2+} centers of both preparations are rapidly and completely reduced by sodium dithionite. Unlike Cu_A in the native enzyme, however, there is no detectable reduction of the pHMB-modified copper center when the enzyme containing it is treated with either ascorbate/cytochrome c or NADH/PMS. One possible explanation for this effect of the pHMB modification is a change in the thermodynamic properties of the site. Specifically, the modification might lower the reduction potential of the copper center to such an extent that it can no longer be significantly reduced by ascorbate or NADH, but can be reduced when the much more powerful reductant sodium dithionite is used under otherwise identical conditions. This would be the case if the standard reduction potential of the modified copper center falls in or near the range delimited by the potentials of dithionite ($E^{\circ'} = -0.527 \text{ V}$ (54)) and of NADH ($E^{\circ'} = -0.320 \text{ V}$ (54)). This range of potentials is substantially lower than that typical of copper proteins (55, 56), but is in the region in which the potentials of many small organocopper complexes occur (57). An alternative explanation for the failure of both ascorbate/cytochrome c and NADH/PMS to reduce the modified copper center is that the electron transfer from these reductants to the copper center is significantly slower in the modified enzyme, but that electron transfer from

dithionite is not substantially affected. Although such a change in the kinetic properties of the enzyme cannot be entirely discounted, it seems unlikely that it would be sufficient to explain the observed effects of pHMB modification on the redox processes. In this context, the experimental observation that no reduction of the modified copper EPR signal intensity occurs even after 50 h of treatment with NADH/PMS is particularly germane. If production of reduced copper is actually taking place under these circumstances, it can only be doing so at a rate many orders of magnitude slower than that in the native enzyme (50).

Catalytic turnover of the pHMB-modified enzyme. In the nearly twenty years since Gibson and Greenwood (6) demonstrated that the redox state of Cu_A can change as rapidly as that of Fe_a in response to reaction of the enzyme with reducing or oxidizing substrates, the importance of this center in cytochrome oxidase electron transfer reactions has become increasingly well established. In the cytochrome oxidase derivative described in this chapter, the Cu_A center has been converted into a form which is no longer redox active with the enzyme's substrate, ferrocyanochrome c. It is therefore not surprising that the preparation of this derivative is accompanied by the loss of the majority of the

catalytic cytochrome oxidase activity present in the native enzyme. As described in the Results Section, however, the oxygen consumption measurements demonstrate the presence of a significant residual turnover activity in the modified enzyme which amounts to approximately 20% of that of the native enzyme. Since the modified copper center is not significantly reduced by ascorbate/cytochrome c , it is unlikely that this center can catalyze intramolecular electron transfer reactions at a significant rate under the conditions of the activity measurements, in which ascorbate is the strongest reductant present. For a modified copper center with a standard reduction potential more than 0.5 V below those of Fe_a and cytochrome c , virtually no net flux of electrons through the site is expected, even if the rate of reduction of the oxygen binding site by the copper is substantially increased because of the increase in the free energy change associated with this reaction. [The effect on the reaction rate of changing the potential of the electron transfer catalyst is analogous to that encountered when mediators of various potentials are used to catalyze electron transfer between solution species and electrodes; this phenomenon is discussed by Clark (58).] The presence of residual turnover activity must therefore reflect the presence in the modified enzyme of a Cu_A -independent electron transfer pathway from cytochrome c to Fe_a and to

the oxygen binding site. In view of the fact that the modified enzyme appears to be largely unperturbed by the modification (with the exception of the changes at Cu_A), it is probable that such a pathway exists in the native enzyme as well. These observations therefore strongly suggest that direct electron transfer (without the mediation of Cu_A) between cytochrome c and Fe_a can occur at a rate which is at least as large as one-fifth of the overall turnover rate of the unmodified enzyme.

The existence in the native enzyme of a branched electron transfer pathway, having the major flow of electrons occurring from Cu_A to the oxygen binding site and a minor flow from Fe_a, was proposed by Clore, et al. (8) as the model which best fitted the data from their careful EPR and optical kinetics studies of the low temperature intermediates in the reaction of reduced cytochrome oxidase with O₂. Recent studies using a similar technique in our laboratory have confirmed that a linear (unbranched) pathway is insufficient to explain the observed kinetics and have extended the observations into later stages of the electron transfer cycle and over a broader range of temperatures (59). As in the study described above, electron transfer from Cu_A²⁺ to the oxygen binding site was observed to be the dominant pathway with a smaller but significant (c. 30% of

the total) amount of transfer occurring from Fe_a^{3+} . No significant change in the ratio of the rates of the two pathways was observed over a substantial temperature range [170 - 195 K].

The observation of electron transfer kinetics consistent with a minor Cu_A -independent electron transfer pathway together with the direct demonstration of such a pathway in the pHMB-modified enzyme creates a strong case that direct Fe_a^{3+} to oxygen binding site electron transfers can in fact occur in cytochrome c oxidase in respiring mitochondria. Although it is possible that such transfers merely represent a small "leakage" pathway which is of little physiological significance, we favor an alternative interpretation. The electrochemical hydrogen ion gradient which is generated by cytochrome oxidase turnover is produced by two distinct mechanisms: by consumption of H^+ from the matrix of the mitochondrion during the conversion of O_2 to H_2O , and by proton pumping, in which the large amounts of energy liberated under physiological conditions by the reduction of O_2 by cytochrome c are used to fuel the (energetically unfavorable) transfer of H^+ ions from the matrix side of the mitochondrial inner membrane to the cytosolic side. We have proposed, on the basis of a wide variety of experimental data about the structures and reactions of the metal center

sites, that the cytochrome oxidase proton pump is localized at the Cu_A site and is driven by electron transfer through this site (16). If this were the case, the presence of a minor electron transfer pathway which bypasses Cu_A would cause a small decrease in the efficiency of coupling; however, the existence of such a pathway would confer the advantage of allowing catalytic turnover of the enzyme under a much wider range of physiological conditions. This is because the change in free energy associated with the overall cytochrome c oxidase reaction (electron transfer, oxygen reduction, and proton pumping) must become less negative as the energization of the membrane increases; if the electrochemical proton gradient becomes too large, the free energy change will become zero and the reaction will no longer proceed spontaneously. If an electron transfer pathway which bypasses the proton pump is present, however, turnover under this condition and even under those of somewhat higher energization will be possible because an energy-requiring step (proton pumping) is eliminated from the catalytic cycle. Thus, the bypass pathway which only a small fraction of the electrons use under non-energized conditions would become dominant under highly energized conditions. The fraction of the total electron transfer rate occurring through each of the two pathways would also vary if some of the four successive electron transfers to the

O₂ binding site which are necessary to reduce O₂ to H₂O produce more energy than do others (60). In both cases, such an arrangement allows the enzyme to tailor its coupling efficiency to changes in the relationship between the amount of energy available from electron transfer reactions and the amount needed to pump protons. This type of compromise between energy efficiency and turnover rate may be necessary for the efficient overall functioning of the metabolic pathway (see Chapter IV).

The reaction between pHMB and cytochrome oxidase under the conditions described in this chapter represents the first reported chemical modification of the Cu_A site which is not accompanied by extensive denaturation and inactivation of the protein. We anticipate that this derivative of the enzyme will prove to be a valuable tool in future studies of the role that Cu_A plays in the catalytic mechanism of cytochrome oxidase.

FOOTNOTES

¹Abbreviations and symbols used in this chapter: pHMB, sodium p-hydroxymercuribenzoate; pCMB, sodium p-chloromercuribenzoate; EPR, electron paramagnetic resonance; PMS, phenazine methosulfate; Fe_a, the low-potential heme site of cytochrome c oxidase; Cu_A, the low-potential copper site of cytochrome c oxidase; Fe_a₃, the high-potential heme site of cytochrome c oxidase; Cu_B, the high-potential copper site of cytochrome c oxidase.

²The protein chemical modification reactions of pHMB and pCMB are essentially identical because both compounds rapidly form the same equilibrium mixture of chemical species when dissolved in neutral aqueous solutions containing millimolar concentrations of Cl⁻ (61, 62). It is therefore likely that the differing effects of the pCMB treatment described by Tsudzuki, et al. (20) and of the pHMB treatment described in the present work arise from the differences between the reaction times and reagent concentrations used in the two sets of experiments rather than from chemical differences between the pCMB and pHMB reagents.

REFERENCES

1. Malmström, B.G. (1980) in Metal Ion Activation of Dioxygen (Spiro, T.G., Ed.) pp. 181-207, Wiley, New York.
2. Capaldi, R.A., Malatesta, F., Darley-USmar, V.M. (1983) Biochim. Biophys. Acta **726**, 135-148.
3. Fiamingo, F.G., Altschuld, R.A., Moh, P.P., Alben, J.O. (1982) J. Biol. Chem. **257**, 1639-1650.
4. Alben, J.O., Moh, P.P., Fiamingo, F.G., Altschuld, R.A. (1981) Proc. Natl. Acad. Sci. U.S.A. **78**, 234-237.
5. Brudvig, G.W., Blair, D.F., Chan, S.I. (1984) J. Biol. Chem. **259**, 11001-11009.
6. Gibson, Q.H., Greenwood, C. (1965) J. Biol. Chem. **240**, 2694-2698.
7. Beinert, H., Palmer, G. (1964) J. Biol. Chem. **239**, 1221-1227.
8. Clore, G.M., Andréasson, L-E., Karlsson, B., Aasa, R., Malmström, B.G. (1980) Biochem. J. **185**, 139-154.
9. Wikström, M., Krab, K., Saraste, M. (1981) Cytochrome Oxidase: A Synthesis, Academic Press, London.
10. Malkin, R., Malmström, B.G., Vänngård, T. (1968) FEBS Lett. **1**, 50-54.
11. Reinhammar, B.R.M. (1972) Biochim. Biophys. Acta **275**, 245-259.
12. Lemberg, M.R. (1969) Physiol. Rev. **49**, 48-121.
13. Blair, D.F., Martin, C.T., Gelles, J., Wang, H., Brudvig, G.W., Stevens, T.H., Chan, S.I. (1983) Chemica Scripta **21**, 43-53.
14. Beinert, H., Palmer, G. (1964) in Oxidases and Related Redox Systems (King, T.E., Mason, H.S., and Morrison, M., Eds.) Vol. 2, pp. 567-590, Wiley, New York.
15. Weintraub, S.T., Wharton, D.C. (1981) J. Biol.

Chem. 256, 1669-1676.

16. Chan, S.I., Bocian, D.F., Brudvig, G.W., Morse, R.H., Stevens, T.H. (1979) in Cytochrome Oxidase (King, T.E., et al., Eds.) pp. 177-188, Elsevier/North-Holland Biomedical Press, Amsterdam.
17. Stevens, T.H., Martin, C.T., Wang, H., Brudvig, G.W., Scholes, C.P., Chan, S.I. (1982) J. Biol. Chem. 257, 12106-12113.
18. Martin, C.T. (1985) PhD. Thesis, California Institute of Technology, Pasadena, California.
19. Martin, C.T., Scholes, C.P., Chan, S.I. (1986) manuscript in preparation.
20. Tsudzuki, T., Oriei, Y., Okunuki, K. (1967) J. Biochem. 62, 37-45.
21. Williams, G.R., Lemberg, R., Cutler, M.E. (1968) Can. J. Biochem. 46, 1371-1379.
22. Wainio, W.W., Nikodem, V. (1973) J. Bioenerg. 4, 579-590.
23. Brudvig, G., Chan, S.I. (1979) FEBS Lett. 106, 139-141.
24. Mann, A.J., Auer, H.E. (1980) J. Biol. Chem. 255, 454-458.
25. Darley-USmar, V.M., Capaldi, R.A., Wilson, M.T. (1981) Biochem. Biophys. Res. Comm. 103, 1223-1230.
26. Bickar, D., Bonaventura, J., Bonaventura, C., Auer, H., Wilson, M. (1984) Biochemistry 23, 680-684.
27. Brudvig, G.W., Stevens, T.H., Chan, S.I. (1980) Biochemistry 19, 5275-5285.
28. Hartzell, C.R., Beinert, H. (1974) Biochim. Biophys. Acta 368, 318-338.
29. Markwell, M.A.K., Haas, S.M., Bieber, L.L., Tolbert, N.E. (1978) Anal. Biochem. 87, 206-210.
30. Cadman, E., Bostwick, J.R., Eichberg, J. (1979) Anal. Biochem. 96, 21-23.
31. Tsibris, J.C.M., Tsai, R.L., Gunsalus, I.C.,

- Orme-Johnson, W.H., Hansen, R.E., Beinert, H. (1968) Proc. Natl. Acad. Sci. U.S.A. 59, 959-965.
32. Orme-Johnson, W.H., Beinert, H. (1969) Anal. Biochem. 32, 425-435.
33. Ernst, R.R. (1966) Adv. Magn. Res. 2, 1-135.
34. Savitzky, A., Golay, M.J.E. (1964) Anal. Chem. 36, 1627-1639.
35. Atherton, N.M. (1973) Electron Spin Resonance: Theory and Applications, Ellis Horwood, Chichester, England.
36. Aasa, R., Vänngård, T. (1975) J. Magn. Res. 19, 308-315.
37. van Gelder, B.F., Beinert, H. (1969) Biochim. Biophys. Acta 189, 1-24.
38. Aasa, R., Albracht, S.P.J., Falk, K-E., Lanne, B., Vänngård, T. (1976) Biochim. Biophys. Acta 422, 260-272.
39. Hoffman, B.M., Roberts, J.E., Swanson, M., Speck, S.H., Margoliash, E. (1980) Proc. Natl. Acad. Sci. U.S.A. 77, 1542-1546.
40. Peisach, J., Blumberg, W.E. (1974) Arch. Biochem. Biophys. 165, 691-708.
41. Vänngård, T. (1972) in Biological Applications of Electron Spin Resonance (Swartz, H.M., Bolton, J.R., & Borg, D.C., Eds.) pp. 411-447, Wiley-Interscience, New York.
42. Beinert, H., Shaw, R.W., Hansen, R.E., Hartzell, C.R. (1980) Biochim. Biophys. Acta 591, 458-470.
43. Peisach, J. (1978) in Frontiers of Biological Energetics (Dutton, P.L., Leigh, J.S. & Scarpa, A., Eds.) Vol. 2, pp. 873-881, Academic Press, New York.
44. Wertz, J.E., Bolton, J.R. (1972) Electron Spin Resonance: Elementary Theory and Practical Applications, McGraw-Hill, New York.
45. Griffith, J.S. (1971) Mol. Phys. 21, 141-143.
46. Kent, T.A., Young, L.J., Palmer, G., Fee, J.A., Münck, E. (1983) J. Biol. Chem. 258, 8543-8546.

47. Stevens, T.H., Brudvig, G.W., Bocian, D.F., Chan, S.I. (1979) Proc. Natl. Acad. Sci. U.S.A. 76, 3320-3324.
48. Brudvig, G.W., Stevens, T.H., Morse, R.H., Chan, S.I. (1981) Biochemistry 20, 3912-3921.
49. Halaka, F.G., Babcock, G.T., Dye, J.L. (1981) J. Biol. Chem. 256, 1084-1087.
50. Antalis, T.M., Palmer, G. (1982) J. Biol. Chem. 257, 6194-6206.
51. Callahan, P.M., Babcock, G.T. (1983) Biochemistry 22, 452-461.
52. Chan, S.I., Stevens, T.H., Brudvig, G.W., Bocian, D.F. (1980) in Frontiers in Protein Chemistry (Liu, T-Y., Yasunobu, K.T., and Mamiya G., Eds.) pp. 117-129, Elsevier, Amsterdam.
53. Malmström, B.G. (1983) in 34th Colloquium-Mosbach 1983: Biological oxidations pp. 189-200, Springer-Verlag, Berlin.
54. Loach, P.A. (1976) in Handbook of Biochemistry and Molecular Biology, 3rd Ed. (Fasman, G.D., Ed.) Vol. 1, pp. 122-130, CRC Press, Cleveland.
55. Addison, A.W. (1983) in Copper Coordination Chemistry: Biochemical & Inorganic Perspectives (Karlin, K.D. and Zubieta, J., Eds.) pp. 109-128, Adenine Press, Guilderland, New York.
56. Brill, A.S., Martin, R.B., Williams, R.J.P. (1964) in Electronic Aspects of Biochemistry (Pullman, B., Ed.) pp. 519-557, Academic Press, New York.
57. Patterson, G.S., Holm, R.H. (1975) Bioinorg. Chem. 4, 257-275.
58. Clark, W.M. (1960) Oxidation-Reduction Potentials of Organic Systems, Williams & Wilkins, Baltimore.
59. Blair, D.F., Witt, S.N., Chan, S.I. (1985) J. Am. Chem. Soc. 107, 7389-7399.
60. Malmström, B.G. (1982) Annu. Rev. Biochem. 51, 21-59.

61. Boyer, P.D. (1954) J. Am. Chem. Soc. 76, 4331-4337.
62. Webb, J.L. (1966) Enzyme and Metabolic Inhibitors Vol. 2, pp. 729-985, Academic Press, New York.

Chapter III

The Proton Pumping Site of Cytochrome c Oxidase:
A Model of Its Structure and Mechanism

Cytochrome c oxidase is the terminal enzyme in the mitochondrial respiratory chain. The enzyme catalyzes the conversion of O_2 to $2 H_2O$ in a reaction that consumes $4 H^+$ from the interior of the mitochondrion and 4 electrons (donated by ferrocytochrome c) from its exterior. The consumption of positive and negative charges from opposite sides of the mitochondrial inner membrane contributes to the formation of a proton electrochemical gradient $(\Delta\tilde{\mu}_H)^1$ across this membrane which fuels ATP synthesis and other energy-requiring biochemical processes (1, 2). The overall dioxygen-reduction reaction, including the steps which contribute to the formation of $\Delta\tilde{\mu}_H$, is exoergonic under physiological conditions, even in resting mitochondria in which it is opposed by a large existing $\Delta\tilde{\mu}_H$ (3).

It is generally agreed that cytochrome oxidase is a redox-linked proton pump; that is, that transfer of electrons through the enzyme from cytochrome c to dioxygen is accompanied by removal of protons from the interior of the mitochondrion (in addition to those consumed by O_2 reduction) and ejection of these ions to the exterior (4, (5). If one H^+ is pumped for every H^+ consumed by dioxygen reduction, then the two processes will contribute approximately equally to the formation of $\Delta\tilde{\mu}_H$.

A great deal is known both about the structure of the enzyme and about various aspects of its catalytic mechanism. The enzyme contains two separate transition metal oxidation/reduction sites -- Fe_a and Cu_A -- which are the initial acceptors of electrons from the heme of ferrocytochrome c (Fe^{2+}). The electrons subsequently move by intramolecular electron transfer processes to an oxygen-binding site consisting of two additional metal ions -- Fe_{a_3} and Cu_B -- in close proximity to one another. The structure of the redox centers, the rates of electron transfers between them, and the mechanism of O_2 reduction at the Fe_{a_3} - Cu_B site have been the subjects of intensive study over the last two decades (6, 7, 8).

Experimental study of cytochrome oxidase proton pumping has also received increasing attention since the pioneering work of Wikström and co-workers during the late seventies. Although energy conservation by the enzyme has often been studied in mitochondrial preparations, several laboratories (9, 10, 11, 12) have reconstituted purified cytochrome oxidase preparations into artificial phospholipid vesicles. These preparations display H^+ -pumping activity in vitro and have proven to be a most useful system in which to study the enzymology of the proton pump. Experiments with these systems have shown that the stoichiometry of the

proton pump can approach one H^+ pumped per electron transferred under certain conditions (13), and have investigated its kinetics. These experiments have also figured prominently in attempts to identify various components of the oxidase as essential parts of the proton pump, but no clear conclusions regarding the location of the proton pump or the nature of its chemical mechanism have as yet emerged. The H^+ -pumping process is, however, the subject of several theoretical analyses, as well as a few speculative mechanistic proposals. The former include expositions of the theoretical and practical constraints upon active transport systems in general (14, 15), as well as treatments specifically devoted to redox-linked energy transduction [e.g., (16)]. One of the values of such studies is that they together provide some information concerning the tasks which an enzyme must perform if it is to function effectively as a biological energy transducer. Recently, we considered the mechanism of a redox-linked proton pump model that incorporated these tasks and then employed electron transfer rate theory to evaluate the performance of this system at steady state (17).

Several groups have proposed mechanistic models of the cytochrome oxidase proton pump (7, 18, 19, 20, 21). Each of these has focused on some features used to accomplish

pumping (e.g., redox-linked modulation of the affinities of proton-binding groups) while not proposing specific means to achieve other equally necessary tasks (e.g., control of electron flow to and from the pump site). While some of the proposals are true fundamental chemical mechanisms involving particular structures in the oxidase molecule (19, 20), others have more the character of generalized state schemes with little or no structural detail (7, 21).

In the present work, we propose a structure and a complete, detailed chemical mechanism for the cytochrome oxidase proton pump. This mechanism employs chemical reaction steps localized at a single redox site within the enzyme. We then quantitatively evaluate the expected effectiveness of the system as a proton pump. Our intention in proposing this model is not to make a definitive statement regarding the detailed nature of the cytochrome c oxidase proton pump. Given the paucity of experimental evidence on the structural constituents of the pump, such a pronouncement would clearly be premature. We instead intend it as an example of how the substantial amount of information known about the proton pump can be accommodated in a detailed and complete mechanism involving specific chemical transformations localized at a single redox center.

The proposed model incorporates a novel redox-linked transition metal ligand substitution reaction. The use of this reaction leads in a straightforward manner to explicit mechanisms, localized to the pump site, for the processes thought to be necessary to achieve efficient redox-linked H^+ pumping. These processes, which have been discussed in an earlier work (17) for the case of a simple model energy transducer, include: 1) modulation of the energetics of protonation/deprotonation reactions and modulation of the energetics of redox reactions by the structural state of the pumping site; 2) control of the rates of the pump's electron transfer reactions with its physiological electron donor and electron acceptor during the turnover cycle (gating of electrons); and 3) regulation of the rates of the protonation/deprotonation reactions between the pumping site and the aqueous phases on the two sides of the membrane during the reaction cycle (gating of protons). Because an explicit mechanism is proposed for each of these processes, a realistic assessment can be made of how well the model pump would function as a redox-linked energy transducer. This is accomplished via analyses of the thermodynamic properties and steady-state kinetic behavior expected of the model. The goal of these studies is to learn how an enzyme which relies on the mechanism described here would be expected to perform both in the mitochondrion and in in

vitro experiments performed on artificial cytochrome oxidase vesicles. Finally, we propose several experimental tests to investigate how similar the cytochrome oxidase proton pump is to the model presented here.

THE ENVIRONMENT, STRUCTURE, AND FUNCTION
OF THE CYTOCHROME OXIDASE PROTON PUMP

The mitochondrial inner membrane. Because it spans the mitochondrial inner membrane, a cytochrome oxidase molecule has a surface exposed to the mitochondrial matrix (m-side) and a surface exposed to the solution between the inner and outer membranes of the mitochondrion (c-side). This c-side aqueous phase is connected to the cytoplasm of the cell by pores in the mitochondrial outer membrane which freely pass small inorganic and organic solutes. This solution is near pH 7 in mammalian cells. The difference in proton electrochemical potential across the inner membrane corresponds to a protonmotive force (Δp) of approximately 240 mV (2). Approximately 75% of Δp is electrical in origin and corresponds to a difference in electrostatic potential between the two sides of the membrane ($\Delta \Psi$) of up to 180 mV (22). The remainder of Δp is due to a difference in H^+ concentration on the two sides of the membrane; the pH of the m-side can be 1 unit or more higher than that on the c-side.

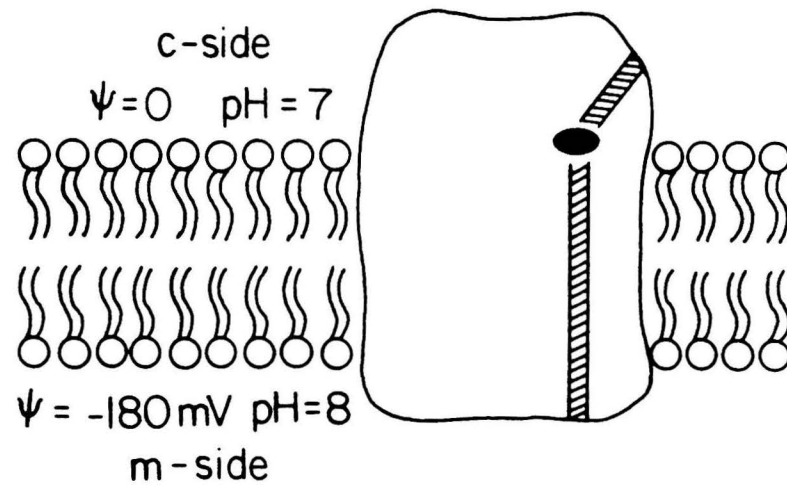
Organization of the proton pump and proton channels within the protein. In proton pumping enzymes such as bacteriorhodopsin (23) and cytochrome oxidase, the reactions

that drive proton pumping occur at specific cofactor sites. In the simplest types of pumping mechanism, the pumping processes also occur at or near the cofactor site in order to facilitate a more direct chemical interaction between the driving and driven processes [see discussions in (24, 5, 25, 26)]. Since a proton pump must take up H^+ from one side of the membrane and discharge it to the other, a mechanism must exist for proton transfer between the pump site and the aqueous phases on the two sides of the membrane. Such a mechanism must be capable of operating at least as rapidly as the maximum pump turnover rate.

An example of such an arrangement is shown in Fig. 1. This illustration depicts a localized proton pump in the interior of a transmembrane protein like cytochrome oxidase. The pump is connected to the two sides of the membrane by proton conducting channels. Nagle, Morowitz, and co-workers have proposed a structural model for such channels (27) which they calculate could easily accommodate the proton flux rates typical of proton pumping enzymes [$10^2 - 10^3 \text{ sec}^{-1}$] (28, 29). If the pump site is close enough to one of the aqueous phases to allow rapid diffusion of protons between the pump and that phase, only a single specialized channel structure connecting the pump to the exterior of the membrane is needed.

Figure 1

The environment of a localized proton pump in an enzyme in the mitochondrial inner membrane. The circle represents the proton pumping site; the shaded strips represent proton-conducting channels.



The redox center associated with the cytochrome oxidase proton pump. Determining which of the four transition metal centers in cytochrome oxidase is the redox element associated with the proton pump would be an excellent first step towards elucidating the molecular mechanism of proton pumping. Unfortunately, there is almost no existing data which significantly aids in this task. A notable exception is a recently published study by Casey and Wikström on proton pumping in mitochondria treated with respiratory inhibitors (30). This work provides evidence suggesting that Fe_a and Cu_A are more plausible candidates for the pumping site than are the metal ions of the oxygen binding site. It is difficult at present to determine whether it is Fe_a or Cu_A which is more likely to be the pumping site. It has been argued that the substantial pH dependence which has been reported for the midpoint reduction potential (E_m) of Fe_a is circumstantial evidence for involvement of this site in proton pumping [e.g., see (7)], particularly since the dependence of the Cu_A potential on pH is small (31). However, a recent spectroelectrochemical study showed that E_m for Fe_a is also only weakly dependent on pH (32, 33). It should be noted that there is no theoretical justification for concluding that the redox center associated with the proton pump must necessarily display a

strongly pH-dependent E_m . We recently presented an analysis of a simple proton pump model which showed efficient proton pumping even under conditions in which the E_m of the pump-associated redox element was nearly independent of pH in the range accessible to measurements (17). In our opinion, the available circumstantial evidence somewhat favors Cu_A over Fe_a as the redox site associated with the proton pump (34), [this point is discussed in more detail at the end of this chapter]. However, any conclusions on the subject must be regarded as tentative until directly relevant experimental results are available.

Electron donor to the pump site. When ferrocytochrome c is added to an anaerobic preparation of oxidized cytochrome oxidase, both Cu_A and Fe_a are reduced very rapidly (35). This observation is consistent either with a mechanism in which both Fe_a and Cu_A are reduced independently through two separate electron transfer pathways from ferrocytochrome c, or with mechanisms in which cytochrome c can only reduce one member of the $[Fe_a, Cu_A]$ pair directly and the other member is reduced only indirectly by electron transfer through the first member. The latter mechanisms require that electron transfer between Fe_a and Cu_A be at least as rapid as enzyme turnover. There is evidence that this is not the case [at least under conditions where $\Delta\mu_{H^+} = 0$] (36, 37, 38), and

cytochrome c is therefore probably the most important electron donor to both Fe_a and Cu_A . The standard reduction potential ($E^{\circ'}$) of cytochrome c is 225 mV (39), which is fairly close to those measured for Fe_a and Cu_A (32, 33, 40).

Electron acceptor from the pump. The metal centers which are candidates for the redox center linked to the proton pump, Fe_a and Cu_A , both transfer electrons directly to the cytochrome oxidase O_2 -binding site (41, 42, 43). The reduction of O_2 to $2 \text{H}_2\text{O}$ requires four electron transfers to this site. The individual standard reduction potentials for the four electron transfers are not known; however, the maximum total energy available from the four electron transfers is limited by the reduction potential of the $\text{O}_2/\text{H}_2\text{O}$ couple [$E^{\circ'} = 800 \text{ mV}$] (3).

Number of protons pumped by cytochrome oxidase per electron transferred. Measurements from several laboratories (11, 12, 13) show that cytochrome c oxidase reconstituted into phospholipid vesicles pumps protons with a protons pumped/electrons transferred ratio (H^+/e^-) near to, but less than, one. There is an unfortunate tendency among enzymologists to assume that apparent stoichiometries such as H^+/e^- are fixed properties of enzyme mechanisms

which are invariant under different reaction conditions (e.g., changes in substrate concentrations). This assumption is clearly unjustified in the case of cytochrome oxidase. Measurements of Δp and of proton/electron flux ratios in mitochondria show that the degree of coupling between electron transfer and proton pumping varies with Δp and with substrate concentration (44, 45). A similar phenomenon is observed with the oxidase vesicles: the measured H^+/e^- decreases as the number of enzyme turnovers over which the measurement was made increases (11, 10). These observations are consistent with the notion that the proton pumping stoichiometry varies with Δp : in the experiments the vesicles are initially de-energized (i.e., $\Delta p = 0$ initially), and the average Δp is expected to increase as the number of turnovers increases. This interpretation is supported by the recently reported observation that the decrease in H^+/e^- with increasing number of turnovers is smaller when pumping is measured in the presence of high valinomycin concentrations (13). Under these conditions, the permeability of the lipid bilayer to protons is increased [J. Gelles and S.I. Chan, unpublished observations] and Δp is therefore expected to be lower. We recently pointed out that a decrease in H^+/e^- with increasing $\Delta\psi$ can readily be attributed either to the expected effects of driving force on electron transfer

reaction rates (17) and/or to the existence of a branched electron transfer pathway within the enzyme (43, 42).

CONSTRAINTS ON KINETICS AND THERMODYNAMICS
IN A REDOX-LINKED PROTON PUMP MECHANISM

In order to be considered an acceptable model for the proton pump of cytochrome c oxidase, a proposed mechanism should be consistent with available experimental data relating to the enzyme. Unfortunately, nearly all of the experimental evidence available is more pertinent to the overall performance of the pump than to the details of the pump reaction mechanism, and therefore does not place strong constraints on possible models. An acceptable model must be chemically and physically reasonable, however. We now discuss several principles that have arisen from theoretical studies of biological energy transduction in general and from analysis of electron transfer linked H^+ pumping in particular. These are formulated here as specific principles or features which are thought to be needed in any pump which functions as a useful biological energy transducer.

Requirement for gating of protons and gating of electrons. Any spatially localized proton pump contains reaction steps in which protons bind to the pump site and others in which they are released. In order to achieve vectorial proton transport, the pumping mechanism must

control these proton transfers so that proton uptake by the site will occur preferentially from the correct source and/or proton discharge will occur preferentially to the correct destination. This control of the relative rates of proton transfer reactions with the two sides of the membrane, called "gating of protons" in a previous discussion (17), has been widely acknowledged to be a necessary pump feature in discussions of proposed models for the oxidase proton pump. In only two instances, however, are specific chemical mechanisms described to achieve it (18, 20), the authors of other models proposing that gating is achieved via undefined protein conformational changes which are coupled to the state of the pump site in an unspecified manner. Furthermore, it has been less widely noted that there exists an analogous requirement for control of the relative electron transfer rates between the pump and its redox partners (16). This is a consequence of the fact that a redox-linked proton pump which serves as a conduit for the transfer of electrons from a low reduction potential donor (e.g., cytochrome c) to a high reduction potential acceptor (e.g., the oxygen binding site) must modulate the rates of the electron transfers to and from these electron transfer partners in order to couple the free energies of the electron transfers into processes at the pump site. This "gating of electrons" is discussed extensively in a

previous work (17), in which we used electron transfer rate theory to explore the mechanisms by which a redox-linked proton pump might achieve such gating and the effects of varying the efficiency of the gating of electrons on the performance of a model pump.

Desirability of linkage between the pump state and the energetics of oxidation/reduction or protonation/deprotonation reactions. A question which has been discussed extensively in the literature of biological energy transduction concerns the extent to which an effective energy transducer must vary its affinity for its substrates during turnover. In active transport systems, for example, it is frequently supposed that the pumping enzyme will strongly bind the species to be transported on the uptake side of the membrane and then convert to a state in which the substrate is bound more weakly and is exposed to the discharge side. It has been demonstrated by several authors that this property is not an absolute requirement for active transport; however, analyses of the steady-state kinetics of particular pump mechanisms show that efficiency and/or kinetic performance are usually improved when at least some degree of thermodynamic linkage between substrate binding and pump state is incorporated [(15) and references therein; (17)]. For an electron transfer driven proton pump,

thermodynamic linkage will manifest itself as changes in the pK_a of a proton-binding group or groups and/or as changes in the reduction potential of the redox center associated with changes in the state of the pump site. The effects of varying the size of these changes on the performance of a simple proton pump model were examined in an earlier study (17).

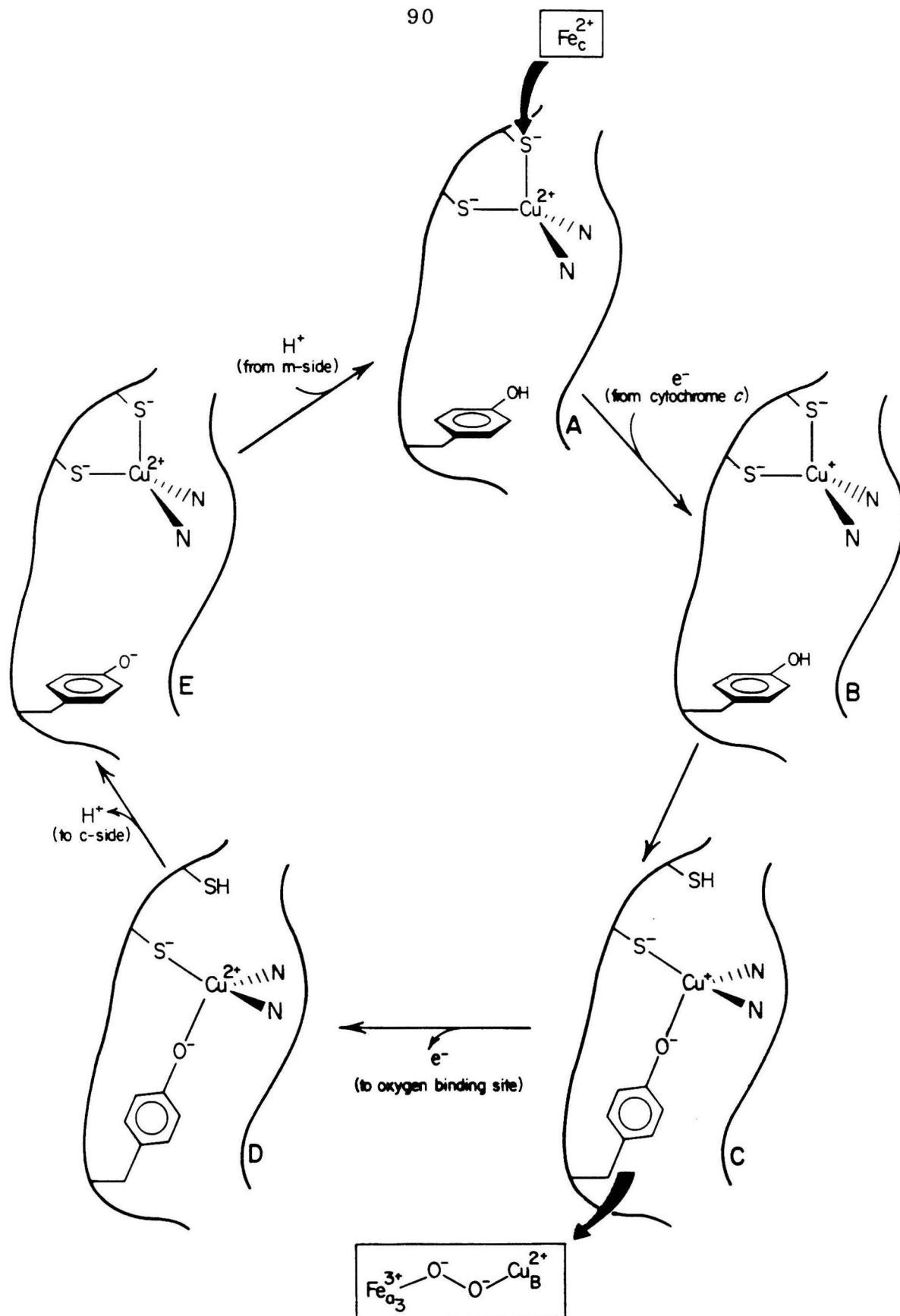
A MODEL OF THE CYTOCHROME OXIDASE PROTON PUMP

We now describe a possible chemical mechanism for H^+ pumping by cytochrome c oxidase (Fig 2). This model proposes that Cu_A is the localized site of redox-linked proton translocation. As discussed above, there is currently no evidence which allows one to distinguish clearly between Cu_A and Fe_a as the site of proton pumping in cytochrome oxidase. We have chosen to use Cu_A in this model because its structure is more compatible with the type of chemical mechanism being proposed; however, many features of the model are applicable to a proton pump involving any transition metal center. We discuss the application of several of these ideas to Fe_a in a subsequent section.

Redox-linked ligation structure changes at the H^+ -pumping site. We recently proposed (46, 34) that the results of spectroscopic studies on the oxidized Cu_A site are consistent with an unusual coordination structure in which the Cu^{+2} ion is ligated by two cysteine thiolate anions and by two nitrogen atoms (one or both derived from histidine imidazole groups) arranged in a distorted tetrahedral geometry. This structure is represented in the initial state of the pump model (Fig 2A). The molecular orbital analysis of this ligation geometry (34) implies that it is

Figure 2

Chemical mechanism of the proton pump model. The openings at the top and bottom of each diagram represent the ends of the proton conducting channels leading to the c-side and m-side of the membrane, respectively. The heavy arrows in parts A and C represent pathways of electron transfer.



unstable relative to typical copper protein [e.g., blue copper (47)] active site structures when reduced to Cu^+ . We propose that the four copper ligands in Fig. 2A are held rigidly in place by the protein backbone so that a more stable geometry cannot be achieved through movement of these ligands, but that a more stable structure can be attained when the reduced Cu_A site (Fig. 2B) undergoes a facile intramolecular ligand exchange reaction. This reaction causes the Cu^+ ion to move relative to the protein so that it may bond to an appropriately placed tyrosine phenolate while the topmost cysteine ligand is displaced to yield the structure depicted in Fig. 2C. The ligation geometry is now roughly trigonal planar, but the copper is displaced slightly out of the equatorial plane formed by the two nitrogen and the cysteine due to the bond with the oxygen of the tyrosine side chain. When the site is reoxidized by transfer of an electron to the oxygen-binding site, the distorted trigonal structure is unstable for the resulting Cu^{+2} ion (Fig. 2D) and rapidly converts back to the original structure (Fig. 2A). This oxidation/reduction-driven ligation change at Cu_A site forms the basis of the H^+ -pumping mechanism proposed below.

Proton transfer at the H^+ -pumping site. The Cu_A site in cytochrome c oxidase is not readily accessible to exogenous

reagents and does not bind inhibitor ligands [(43) and references therein]. Attempts to examine the accessibility of the site to solvent protons by spectroscopic techniques have yielded inconclusive results [C.T. Martin and S.I. Chan, unpublished data]. As described above, proton pumps like cytochrome oxidase are likely to incorporate a proton-conducting channel or channels which facilitate transfer of protons between the two sides of the membrane and the proton pumping site(s).

The model assumes that the Cu_A active site (i.e., the Cu ion and its polar ligands) is located within a hydrophobic pocket in the interior of the enzyme and that proton-conducting channels which connect to the respective sides of the membrane approach this pocket on opposite sides.² The termini of the two channels are represented in Fig. 2 by the gaps in the outline surrounding the site: the bottom gap connects to the mitochondrial matrix and the top to the exterior. Any active transport system must incorporate a barrier to prevent passive diffusion of the solute being transported down its concentration gradient (i.e., in a direction opposite the pumping direction). The effectiveness of such a barrier is of particular concern in a localized proton pump model with channels like that schematized in Fig. 1, since the entire protonmotive force

driving proton leakage across the membrane (Δp) may be applied to the small distance separating the ends of the two channels at their approaches to the pump (7). In the present model this barrier is provided primarily by the hydrophobic protein environment which surrounds the active site. The partial positive charge on the copper ion may also play a role in preventing proton leakage through the site. The model relies on these properties to restrict movements of protons through the site so that the only possible movements are those facilitated by binding of the protons to particular amino acid side chains associated with the pumping site.

The model shown in Fig. 2 achieves the translocation of protons via protonation and deprotonation of two functional groups: the tyrosine phenolate side chain adjacent to the end of the channel connected to the mitochondrial matrix (bottom of the site) and the cysteine thiolate side chain adjacent to the end of the channel leading to the cytosol (top of the site). A crucial feature of the model is that each of these groups can bind a proton strongly when it is not a ligand to the Cu ion, but only weakly when it is coordinated to the Cu ion (i.e., the ligated structures are conjugate bases of rather strong acids). The magnitude of these changes in the proton affinities of the two groups and

their expected effects on the titration behavior of the pump site are discussed in more detail below. It is assumed that in the environment of the site, the pK_a of the cysteine or tyrosine group in the conformation in which it is not a copper ligand is rather high so that it constitutes a proton binding site of high affinity. The redox-linked sequential conversion of the pump between forms in which each of the two groups is alternately a ligand to the copper or an effective proton binding site (but never both simultaneously) is used to effect the vectorial proton transfers essential to the pumping mechanism.

Chemical mechanism of the proton pump model. State A of Fig. 2 is expected to be the dominant species in the oxidized enzyme at equilibrium. Due to its high pK_a , the phenolic group, which is next to the proton channel connected to the m-side of the membrane, is predominantly in the protonated form. The site will be converted to state B when it is reduced by ferrocyclochrome c. As described above, it is strongly driven energetically and kinetically facile for this Cu^+ to adopt the more favored distorted trigonal geometry of state C. Since the phenol side chain in state B is protonated, the rapid ligand exchange at the copper is accompanied by transfer of the proton to the upper cysteine group. This transfer is facilitated by the partial

negative charge on the pentacoordinate "S_N2-like" transition state expected for the ligand substitution reaction, and by the high proton affinity of the unligated thiolate anion. The proton transfer could proceed via a mechanism in which proton movement in the correct direction is facilitated by hydrogen bonding of the tyrosine to one of the adjacent Cu ligands. When the resulting species (state C) is subsequently reoxidized by transfer of an electron to the oxygen binding site, it then assumes the structure of state D. This Cu⁺² species can re-form the favored tetragonally distorted tetrahedral geometry upon deprotonation of the thiol group adjacent to the channel which is connected to the c-side of the membrane. This deprotonation will occur via ejection of the proton to the adjacent channel, rather than back to the tyrosine phenolate, because of repulsion by the net positive charge now present on the copper-ligand complex. Even if the thiol group in Fig. 2D has a high pK_a, the reaction converting state D to state E may be energetically favorable since it combines an energetically favored ligand substitution with the energetically unfavored deprotonation. The subsequent conversion of state E to the starting state A will also be energetically favored because it consists of the protonation of a group (tyrosine phenolate) which has a high pK_a. This reaction returns the system to a state identical to the initial state except that

one electron has been transferred from cytochrome c to the oxygen binding site and one proton has been transferred from the m-side to the c-side.

Thermodynamic linkage in the proton pump model. One of the ways in which energetic linkage between the oxidoreduction and protonation/deprotonation steps of an electron transfer linked proton pump manifests itself is by differences in standard reduction potential of the pump-associated redox center in different states of the pump reaction mechanism. As noted earlier, it is in principle possible to achieve active transport without any such linkage, but the constraints on the rates of individual reaction steps in a real pump often necessitate energetic linkage if a satisfactory compromise is to be struck between the rate and the efficiency at which a pump functions. This point has been explained lucidly by Tanford (15), who cites several theoretical analyses of the subject. It has also been raised specifically in connection with the cytochrome oxidase proton pump (7) [but in contrast see (21)]. The conclusion is supported by the results of our previous study of a redox-linked energy transducer, in which we examined the performance of an abstract four-state proton pump model (17). This study demonstrated that optimal performance under near maximal loads was achieved when the pump accepted

electrons with a standard reduction potential near to that of the electron donor to the site and gave them up at a potential near that of the electron acceptor from the site. In the model of Fig. 2, we propose that the distorted tetrahedral redox couple of states A and B has a reduction potential near that of cytochrome c, while that of the distorted trigonal couple of states C and D has a potential closer to that of the O_2/H_2O couple at the oxygen binding site. The differences between the two ligation structures which might contribute to this large change in potential are discussed below.

Several previously proposed proton pump models (19, 20, 7) are based on a four-state paradigm (17) in which a protonatable group is associated with a redox center in such a way that its affinity for protons is modulated by the oxidation state of that center. The model of Fig. 2 can be viewed as relying upon a similar principle in which the proton affinities of two proton binding sites alternate between low and high values. In both cases, the changing $pK_a(s)$ of proton binding group(s) are another manifestation of the presence of thermodynamic linkage through the state of the pump between the oxidation/reduction and protonation/deprotonation reaction pathways.³

Ion transport mechanism of the proton pump model.

Tanford (15) used the term "alternating access models" to describe the class of active ion transport mechanisms in which ion translocation is achieved by alternately exposing a particular ion binding site to the two sides of the membrane. He noted that nearly all proposed mechanisms for active transport enzymes fell into this class. In contrast, the transition metal ligand substitution reaction proposed here as a basis for the cytochrome oxidase proton pump leads to a different type of ion transport mechanism. In this case, each of the two binding sites always remains in communication with a particular side of the membrane. Ion translocation (conversion of state B to state C) occurs because of a chemical reaction at the pump which displaces the H^+ from one site and allows it to bind to the other. As previously discussed, this process may be catalyzed by the adjacent copper ligands to ensure that proton transfer occurs to the topmost cysteine rather than to the m-side proton transport channel. The other ligand exchange reaction in the mechanism (conversion of state D to state E) may also involve catalysis of the proton transfer reaction, in this case a directional displacement of the proton by the copper ion.

The model proposed in the present work uses a novel but

conceptually simple mechanism involving two groups which can alternately serve as proton binding sites or as transition metal ligands. We will now discuss how such an arrangement leads straightforwardly to explicit chemical mechanisms for the gating of proton and electron transfers and show how these gating processes minimize futile cycle reactions that would otherwise lead to inefficient coupling at the pump site. Because the gating mechanisms are explicit, their effectiveness can be ³⁰⁰⁻³⁵⁰quantitated to determine if the model will function effectively as a proton pump under real conditions.

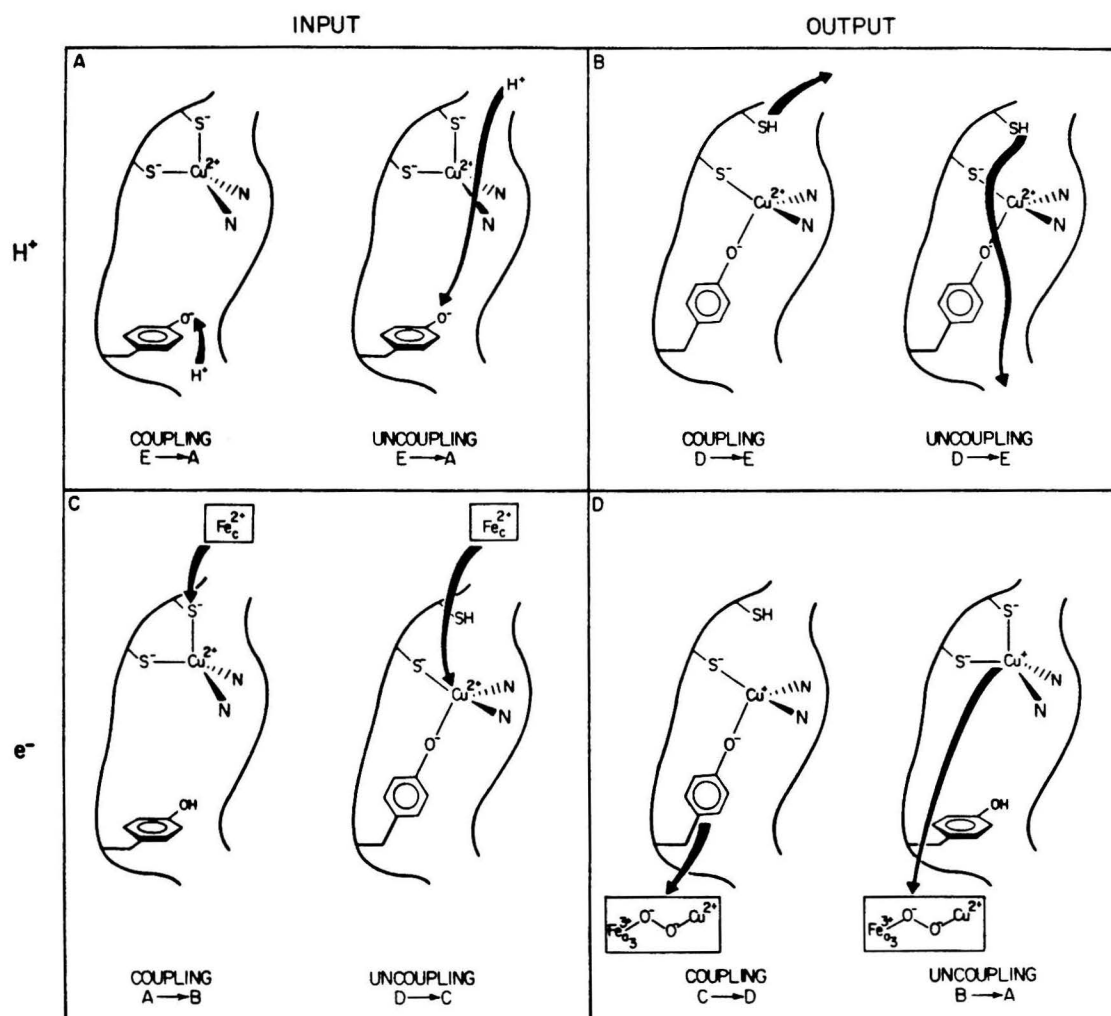
THE GATING OF ELECTRON AND PROTON FLOWS
IN THE MODEL PUMP MECHANISM

There are four types of transfer processes which must be considered in the analysis of gating in a redox-linked proton pump. These are the electron transfers to and from the pump and the proton transfers to and from the pump. Fig. 3 depicts some of the relevant reaction steps in the cytochrome oxidase proton pump model. Each section of the figure (3A through 3D) depicts a pair of proton or electron transfer reactions. One member of each pair, denoted "coupling", is a necessary part of the energy transduction mechanism for the pump and appears as a reaction step in the model pump mechanism of Fig. 2. For example, the deprotonation of the uppermost cysteine group to the channel leading to the c-side of the membrane, shown as the "coupling" reaction on Fig. 3B, is the reaction step converting species D to species E in Fig. 2.

The "uncoupling" reactions diagrammed in Fig. 3, in contrast, do not correspond to any reaction steps in the proton pumping mechanism shown in Fig. 2. Each of these uncoupling steps will, if added to the mechanism of Fig. 2., produce a reaction scheme which contains a "futile cycle" pathway in which the exoergonic flow of electrons from the

Figure 3

Comparison of "coupling" and "uncoupling" reactions of the model pump. Each diagram contains an arrow indicating the source and destination of a proton or electron transfer which interconverts the states of Fig. 2 specified by the letters at the bottom of the diagram. The left half of the figure refers to reactions involving proton and electron input to the pump, the right side to proton and electron output.



donor to the acceptor will occur without a corresponding endoergonic movement of protons from the m-side to the c-side of the membrane. Consider, for example, the "uncoupling" reaction of Fig. 3B: like its "coupling" analog, it converts the species of Fig. 2D into that of Fig. 2E. It does so, however, by expelling the proton to the m-side of the membrane rather than to the c-side. (Note that the free energy of expulsion to the m-side is more favorable because the pH of that phase is higher than that of the c-side.) A reaction cycle like that of Fig. 2 but using this "uncoupling" reaction to convert between states D and E would merely pick up protons from the c-side and expel them there again -- no net proton pumping would occur.

A similar loss of net pumping activity would be caused by the inclusion in the reaction cycle of the "uncoupling" electron-transfer reactions shown in Figs. 3C and 3D. For example, consider the effect of allowing the Fig. 3D "uncoupling" reaction to occur immediately after conversion of species A to species B in Fig. 2. This reaction would regenerate species A by transferring the electron received from Fe_c^{2+} in the previous step to the oxygen binding site, without any of the intervening steps which lead to H^+ pumping in the coupled reaction cycle. The presence of a highly exoergonic "short circuit" of this type, in which net

flow of electrons through the site occurs without associated proton flux, would clearly reduce or eliminate proton pumping by the model pump.

It is apparent from the foregoing discussion that the inclusion of means to reduce or eliminate unwanted "uncoupling" reactions is essential in a proton pump model. The need for control of these reactions is particularly acute because "uncoupling" reactions will be more energetically favored than the corresponding "coupling" reactions (17).⁴ In order to function effectively as a proton pump, the site must maintain the ratio of the rates of the "uncoupling" to "coupling" reactions at a low value. In the following sections, we discuss how this is achieved for the electron- and proton-transfer reactions in the pump model and estimate the values of the rate constant ratios.

Estimation of the relative rate constants for the "coupling" and "uncoupling" proton-transfer reactions. One of the advantages of a ligand substitution reaction of the type we have used as the basis for the proton pump model is that such a process provides a relatively straightforward mechanism by which effective proton gating may be achieved. The "coupling" reactions of Figs. 3A and 3B both involve transfers of protons between a group at the pump site and

the end of a proton-conducting channel which is immediately adjacent to that group. Proposed structural models for proton channels (27, 48, 49) consist of a series of X-H (X = O, N, S) bonds arranged in a hydrogen bonded chain. We propose that the thiol and phenol proton-binding groups in the model pump are positioned in a way that allows them to hydrogen bond to the terminal X-H group in the respective proton channels. The proton transfer reaction could then occur along the hydrogen bond:



and



The rates for such reactions have been studied both experimentally and theoretically in a large number of systems. In a series of calculations on model systems intended to simulate such transfers between fixed groups in the interior of proteins, Scheiner (29) obtained activation energies for proton transfer of approximately 2-10 kcal/mol, implying that the rates of such reactions can be quite rapid at physiological temperatures.

In contrast, the "uncoupling" reactions in Figs. 3A and 3B both involve proton transfer from the protonatable group to the channel at the opposite side of the pumping site. These reactions involve the complete cleavage of an S-H or O-H bond and the formation of two charged species in a non-solvating environment with a relatively low dielectric constant. As such, they will require several times the activation energy of the hydrogen-bond mediated proton transfer reaction. One can formulate a crude estimate of this quantity by considering the free energy for the heterolytic bond cleavage of RS-H [approximately 350 kcal/mol (50)] and conservatively assuming that the bond cleavage within the protein requires only one-tenth as much energy, owing to stabilization of the transition state by hydrogen bonding and/or dielectric interactions with the surrounding site. We therefore conclude that the ratio of the rate constants for the "coupling" and "uncoupling" reactions could be 1.2×10^{18} [i.e., $\exp\{(35 - 10) / RT\}$] or more at 300K. This extremely large factor is more than adequate to insure that effective proton gating can be accomplished by the mechanism proposed in the pumping model. In particular, we note that it is sufficient to overcome a statistical factor which may work against gating in a model of this type. As noted earlier, the proton channels are expected to communicate the full transmembrane $\Delta\tilde{\mu}_H^+$ to the

immediate vicinity of the pump site. This could make the effective pH at the end of the matrix channel as much as 4 units larger than that of the cytoplasmic one in resting mitochondria [based on $\Delta p = 240$ mV (2)] (51, 1). In an ensemble of pumps, therefore, the population with matrix channels in a protonatable state might be as much as 10^4 times as large as the population of protonatable cytosolic channels [see (27) for a discussion of channel state changes]. Despite the magnitude of this factor, however, it is not enough to overcome the enormous difference in the intrinsic rates of the two reactions. We are therefore confident that there will be no difficulty in achieving proton "gating ratios" [the ratios of the rate constants of the "uncoupling" and "coupling" reactions (17)] of 10^{-8} or less for the reaction pairs discussed above.

Estimation of the relative rate constants for the "coupling" and "uncoupling" electron transfer reactions.

Because of the low mass of electrons and the low activation free energies for electron transfers involving redox-active enzyme cofactors (i.e., the low barrier height opposing electron tunneling), electron movement can occur by tunneling through proteins in a spatially delocalized manner which does not require the involvement of particular chemical groups along the transport pathway. Control of

electron transfer rates to achieve gating of electrons is therefore likely to pose a more difficult problem than the analogous control of proton transfers, and must clearly be addressed in any complete proton pump model. This issue has been neglected in previously proposed models of the cytochrome oxidase proton pump. We will now consider several factors influencing the relative rates of the "coupling" and "uncoupling" electron transfer reactions depicted in Figs. 3C and 3D.

The theory of electron transfer developed by Marcus (52) predicts that the rate constant k of a fixed-distance intramolecular electron transfer reaction is given by

$$k = \kappa \nu e^{(-\Delta G^*/RT)}$$

$$\Delta G^* = \frac{\lambda}{4} \left[1 + \frac{\Delta G^{\circ'}}{\lambda} \right]^2 \quad (1)$$

In these equations, λ is the total energy associated with the nuclear reorganizations which accompanies the oxidation of the electron donor and the reduction of the electron acceptor; κ is the transmission coefficient which expresses the degree of electronic coupling between the wavefunctions of the electron donor and acceptor; ν is a frequency factor; and ΔG^* and $\Delta G^{\circ'}$ are the free energy of activation and the

standard free energy difference for the reaction, respectively.

As with the proton-transfer reactions described above, the "uncoupling" electron-transfer reactions are considerably more exoergonic than the "coupling" ones. This concept is related, but not identical, to the fact that the "uncoupling" electron transfer reactions will have a larger difference in standard reduction potential between the electron donor and acceptor. We emphasize that this conclusion is not a specific consequence of the pump model being discussed, but that it arises from the general principle, discussed above, that a practical compromise between efficiency and turnover rate in a real pump necessitates some matching of the reduction potentials of the electron input and output states of the pump with those of its electron transfer partners (15, 7). Based on the E° values of the high and low potential conformations of the pumping site [which are estimated in a discussion below], we predict a difference of 350 mV between the "coupling" and "uncoupling" reactions in both Fig. 3C and Fig. 3D. This corresponds to a difference in the standard free energy changes (ΔG° 's) of the two reactions of 8.6 kcal/mol. Eq. 1 predicts a specific relationship between the rate of the electron transfer reaction and its driving force. For the

types of electron transfer under consideration in the present study, this relationship is closely approximated⁶ by

$$\text{Rate} \propto e^{(-\Delta G^{\circ}/2RT)} \quad (2)$$

Using eq. 2, it can readily be calculated that, if all other conditions are equal, the "uncoupling" reactions will predominate over their "coupling" analogs by an intrinsic rate advantage of $1.4 \times 10^3:1$; i.e., the pump is essentially completely uncoupled. Clearly, an effective proton pump must be constructed so that the other factors that influence electron transfer rates are not equal for the two types of processes: the reaction mechanism must permit the "coupling" processes to more than make up for the rate advantage accorded to the "uncoupling" processes by the difference in driving force.

One means that is used in the pump mechanism of Fig. 2 to promote the rates of the "coupling" reactions relative to those of the "uncoupling" reactions is changing the relative distances between the redox center of the pump and its electron transfer partners. The transmission coefficient κ in eq. 1 is thought to vary exponentially with distance (53, 54, 55, 56):

$$\kappa \propto e^{(-2\alpha R)}, \quad (3)$$

where R is the donor-acceptor distance and α is a parameter describing the rate at which the amplitudes of the donor and acceptor wavefunctions diminish with distance. Measurements of electron transfer rates through chemically modified blue copper proteins by Gray and co-workers suggest that a value of $\alpha \cong 0.7 \text{ \AA}^{-1}$ is appropriate for the electron transfer reactions in the model pump [(57, 58) and references therein]. This value is also consistent with that determined by theoretical studies (53), but is somewhat higher than that measured in experiments involving some heme proteins, which yield $\alpha \cong 0.5 \text{ \AA}^{-1}$ for the reactions with moderate driving forces which are appropriate to the present discussion [reviewed by Mayo et al. (57)]. It should be noted that the distance used for the parameter R is the shortest distance between ligand atoms of the electron donor and acceptor or between π -systems connected to such atoms (52, 55, 56) [such π -systems are thought to impose no significant barrier to electron movement]. In the model pump under discussion, there will be substantial differences between the R parameters for the "coupling" and "uncoupling" reactions if the electron transfer partners are located in the directions from the site indicated in Fig. 2 [viz., Fe_c above the top of the site (Fig. 2A) and $\text{Fe}_{a_3}/\text{Cu}_B$ below the

bottom of the pump (Fig. 2C)]. We have concluded through the use of crystallographic data and molecular models of the pump site that the difference in R between the "coupling" and "uncoupling" reactions is greater than or equal to 3.0 Å for electron input [Fig. 3C] (46), and greater than or equal to 5.6 Å for electron output [Fig. 3D]. Using the relationship of eqs. 1 and 3, we find that these distance changes would result in "uncoupling": "coupling" rate constant ratios of 1.5×10^{-2} and 4.0×10^{-4} , respectively, if all other factors affecting electron transfer rates were equal. These parameters are the "gating ratios" described in a previous publication (17). Note that the parameter R in eq. 3 is contained in an exponential, so that an increase of 3.0 Å results in a rate decrease to 1.5×10^{-2} of the original rate regardless of what the total distance traversed by the electron transfer reaction is (as long as the distance is not so short that the reaction becomes nearly adiabatic).

The structural change associated with the ligand substitution reaction at the proton pump site can provide another mechanism to decrease the rates of the "uncoupling" reactions relative to those of the corresponding "coupling" reactions. This is because the orientation of the copper ion orbital involved in the electron transfer reactions may

change relative to the electron transfer partners of the site when the ligand substitution takes place. Because electron transfer rates depend strongly on the overlap between donor and acceptor orbitals (55), such reorientation might contribute to gating of electrons (e.g., by decreasing the rate of the "uncoupling" reaction in Fig. 3C relative to that of the "coupling" reaction). The total gating would then be larger than that estimated above on the basis of distance changes alone. The additional gating contributed by this effect unfortunately cannot be calculated in the absence of detailed information concerning the structure of the enzyme and its metal centers.

In addition to the driving force and distance factors, Marcus theory predicts (eq. 1) that changes in the reorganizational energy (λ) will have a major effect on the rates of thermally-activated electron transfer reactions. This term refers to the energy required to displace the atomic nuclei in the system from their initial equilibrium positions to the equilibrium configuration which they will assume after the electron transfer. The substantial effect of the reorganizational energy on electron transfer rates in proteins has been amply demonstrated [see (57), for example]. The case of blue copper centers in proteins is particularly relevant to the present discussion. These

sites, which have very small reorganizational energies, display rapid long-range electron transfer kinetics. It has been proposed that the reorganizational energies in these systems are small because the metal ions are relatively shielded from the polar solvent and also because their ligands are held in a protein "rack" which minimizes ligand movements accompanying oxidoreduction of the copper (59). It is natural to suppose that these structural features represent an evolutionary specialization of these proteins which allows them to function efficiently in their roles as biological electron-transfer catalysts. We propose that the same is true for the two conformations of the model proton pump, and we have therefore drawn Fig. 2 to show no visible changes in the ligation structure of the copper accompanying the electron transfer processes converting state A into state B and state C into state D. We wish to emphasize that the conformational changes which convert state B into state C and state D into state E are not associated with the electron transfer reactions directly but instead occur from the intermediates which are the products of these reactions; these structural changes therefore do not make a contribution to the reorganizational energies associated with the electron transfers.

Despite their pronounced effect on the overall rates of

electron transfer processes, changes in reorganizational energies cannot make a major improvement to the gating of electron transfers in the type of redox-linked proton pump under consideration. This conclusion (17) arises from the fact that changes in the reorganizational energy associated with the pump site itself (as opposed to changes in the reorganizational energies associated with the sites which are electron transfer partners of the pump) will necessarily have opposite effects on the gating of input and output electron transfer processes. For example, if the reorganizational energy of the states A and B redox couple (Fig. 2) is lowered relative to that of the states C and D redox couple, electron transfers involving the A-B couple will be accelerated relative to those involving the C-D couple. This will result in an increase in the efficiency of gating of electron input to the pump by promoting the rate of the "coupling" reaction in Fig. 3C over that of the "uncoupling" one. However, the same change in reorganizational energy would necessarily have the undesired effect of promoting the "uncoupling" reaction over the "coupling" one for the electron output process (Fig. 3D). It is apparent that modification of the reorganizational energies, while not allowing substantial increases or decreases in the overall amount of gating of electrons in the system, can affect the relative amounts of gating on the

two sides of the pump.

The total reorganizational energy for an electron transfer reaction can be thought of as the mean of the reorganizational energies of the oxidant and the reductant (52). Since this energy is relatively low for cytochrome c (57), the system may be able to tolerate a correspondingly higher reorganizational energy for the electron input conformation (Figs. 2A-B) and/or a reduced driving force and/or increased total electron transfer distance for electron input to the pump and still operate at an adequate rate. Electron transfers to the oxygen binding site, in contrast, may in general involve larger reorganization energies due to the structural changes at that site during O₂ reduction (6).

QUANTITATIVE EVALUATION OF THE BEHAVIOR OF THE
PROTON PUMP MODEL AT EQUILIBRIUM

Having described the ways in which individual structural and functional features of the proposed pump model could contribute to energy conservation, we now turn to an evaluation of the overall performance expected of the model. Our objective in conducting such an analysis is to determine whether the behavior of the pump model is consistent with experimentally determined properties of Cu_A and of the cytochrome oxidase proton pump. To this end, we will first discuss the expected thermodynamic properties (reduction potentials, pK_a s, etc.) of the model pump, and then derive equations describing its behavior under equilibrium conditions (such as those present during electrochemical titrations on the enzyme) and under steady-state turnover conditions (such as those present during steady-state kinetic studies on mitochondria or membrane reconstituted oxidase preparations).

pK_a values of the model pump. The pump model has two deprotonatable chemical groups, a cysteine thiol and a tyrosine phenolic hydroxyl. The solution pK_a s for these amino acids (8.3 and 10.0, respectively) insure that their side chains exist in neutral aqueous solution largely in the

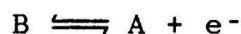
protonated form; however, environmental conditions at the pumping site may shift these pK_a s to higher or lower values. A particularly profound change in the acid/base properties of these groups is expected upon coordination to the copper ion, since it has a strong preference for the anionic (conjugate base) forms. Water and alkyl alcohols coordinated to Cu^{2+} , for example, exhibit pK_a s seven or more units below their solution values (60). We are not aware of any copper proteins in which acidic amino acid side chain ligands are coordinated to Cu when protonated; in particular, the well-studied protonation of the his₈₇ imidazole ligand in plastocyanin is not an example of such a system, since that reaction is accompanied by dissociation of the ligand from the Cu^+ (61). The magnitude of the expected pK_a shift, together with the assumption that the copper ion in the model pump is restricted to the two coordination geometries discussed in connection with the reaction cycle, implies that in the physiologically-relevant pH range the model pump can exist only in a deprotonated form or a form in which one but not both of the cys and tyr ligands is protonated. We therefore need consider only four different pK_a values: those of the cysteine in the oxidized and reduced forms of the distorted trigonal conformation (Figs. 2D and 2C), and those of the tyrosine in the oxidized and reduced forms of the distorted tetrahedral conformation

(Fig. 2A and 2B). These parameters are referred to as $pK_a(\text{cys},o)$, $pK_a(\text{cys},r)$, $pK_a(\text{tyr},o)$, and $pK_a(\text{tyr},r)$ in the following analysis.

As was noted in the discussion of the reaction cycle of the pump model, we require both the cysteine and the tyrosine to be relatively weak acids so that their conjugate bases avidly bind protons during the conversions of state E to state A and state B to state C. We therefore propose $pK_a(\text{cys},o) = 10$ and $pK_a(\text{tyr},o) = 11$; these values are reasonable ones for cysteine and tyrosine side chains confined to a largely solvent-free environment of moderately low polarity. The reduced species are likely to be weaker acids than the corresponding oxidized species due to the more positive charge on the copper in the latter, but this effect on the pK_a s is expected to be much smaller than the coordination effect discussed above. We have therefore used values of $pK_a(\text{cys},r) = 11$ and $pK_a(\text{tyr},r) = 12$ in the analysis that follows, giving $pK_a(\text{cys},o) - pK_a(\text{cys},r) = pK_a(\text{tyr},o) - pK_a(\text{tyr},r) = 1$. Even higher values for $pK_a(\text{cys},r)$ and $pK_a(\text{tyr},r)$ would be unlikely to significantly change the results of the calculations presented below.

Standard reduction potentials of states of the model pump. As was discussed earlier, the redox center associated

with an electron transfer driven proton pump may have a standard reduction potential that varies with the state of the pumping site. In the model pump mechanism (Fig. 2), the distorted tetrahedral redox couple



is proposed above to have a potential close to that of cytochrome c [$E^{\circ'} = 225$ mV (39)] in order to achieve effective performance of the pump. Similarly, we propose that the potential of the distorted trigonal redox couple



(Fig. 2) is closer to that of the potential of the oxygen binding site under aerobic conditions, which presumably approximates that of the O_2/H_2O couple [$E^{\circ'} = 800$ mV]. We will refer to the potentials of these two conformations of the site as $E_I^{\circ'}$ and $E_{II}^{\circ'}$, respectively.

The known standard reduction potentials of copper proteins vary over a range of more than 600 mV (62). Even those within a particular structurally related class of sites, the blue coppers, range from 184 mV [lacquer tree stellacyanin] to 767 mV [Polyporus laccase] (61). These differences could

be due to changes in one of the ligand groups and/or to differences in the ligation geometry induced by the protein structure (59). In the analysis that follows, we have used values of $E_{\text{I}}' = 225 \text{ mV}$ and $E_{\text{H}}' = 575 \text{ mV}$; these choices are reasonable for the structures proposed for the two conformations given the aforementioned wide range of potentials attained by copper proteins. This choice of potentials allows a substantial difference between E_{H}' and E_{I}' (which, as discussed previously, is desired for optimal performance of the pump) while still reserving a total of 225 mV [i.e., $800 - 575$] of standard reduction potential to drive electron transfer to and from the pump site at rates sufficient to accommodate the observed electron transfer rate through Cu_A [70-80% (43, 42) of the steady-state turnover rate of 200 s^{-1} at $\Delta\tilde{\mu}_{\text{H}^+} = 0$].⁷

Behavior of the pump model in an electrochemical/pH titration. If the model under consideration is to be a viable proposal for the structure and function of the cytochrome oxidase proton pump, its predictions must coincide with the observable properties of the Cu_A site. A property which is frequently discussed in relationship to proton pumping is the dependence of the midpoint reduction potential of the site upon pH.

The standard reduction potential of the Cu_A site observed in spectroelectrochemical measurements at 25°, pH 7 is 285 mV for the state of the enzyme in which the Fe_a center is oxidized and the oxygen binding site is reduced and bound by CO (40). Cu_A interacts anticooperatively with Fe_a in such a way that its potential is reduced to approximately 245 mV when Fe_a is reduced (40). Furthermore, the measured potential is almost independent of pH in the range 6.1-8.5 (31). This is not the behavior expected of a simple site in which oxidoreduction is strongly coupled to protonation/deprotonation of an acidic group with a pK_a in the physiological range -- in such cases a strongly (approximately -60 mV / pH unit) pH-dependent midpoint potential should be observed (63). Such strong coupling is not observed in either Fe_a or Cu_A at pH values near neutrality and, as previously discussed, is not a requirement for redox-linked proton pumping (17, 21).

We have derived (Appendix I) the following expression for the fraction of pump sites in the reduced state at equilibrium as a function of pH and applied reduction potential [E_h , in the nomenclature used by Dutton (63)]:

$$f_{red} = \frac{1 + K_3 + K_3K_6 + K_5}{1 + K_1 + K_1K_4 + K_2K_3 + K_2K_3K_7 + K_3 + K_3K_6 + K_5}, \quad (4)$$

where

$$K_1 = 10^{(\{E_h - E_l'\} / 60 \text{ mV})} \quad (4a)$$

$$K_2 = 10^{(\{E_h - E_h'\} / 60 \text{ mV})} \quad (4b)$$

$$K_3 = K_{p\ t} \quad (4c)$$

$$K_4 = 10^{\{pH - pK_a(\text{tyr}, o)\}} \quad (4d)$$

$$K_5 = 10^{\{pH - pK_a(\text{tyr}, r)\}} \quad (4e)$$

$$K_6 = 10^{\{pH - pK_a(\text{cys}, o)\}} \quad (4f)$$

$$K_7 = 10^{\{pH - pK_a(\text{cys}, r)\}} \quad (4g)$$

The symbols $pK_a(\text{cys}, o)$, $pK_a(\text{cys}, r)$, $pK_a(\text{tyr}, o)$, $pK_a(\text{tyr}, r)$, E_l' , and E_h' have already been defined. $K_{p\ t}$ refers to the equilibrium constant for the proton transfer reaction



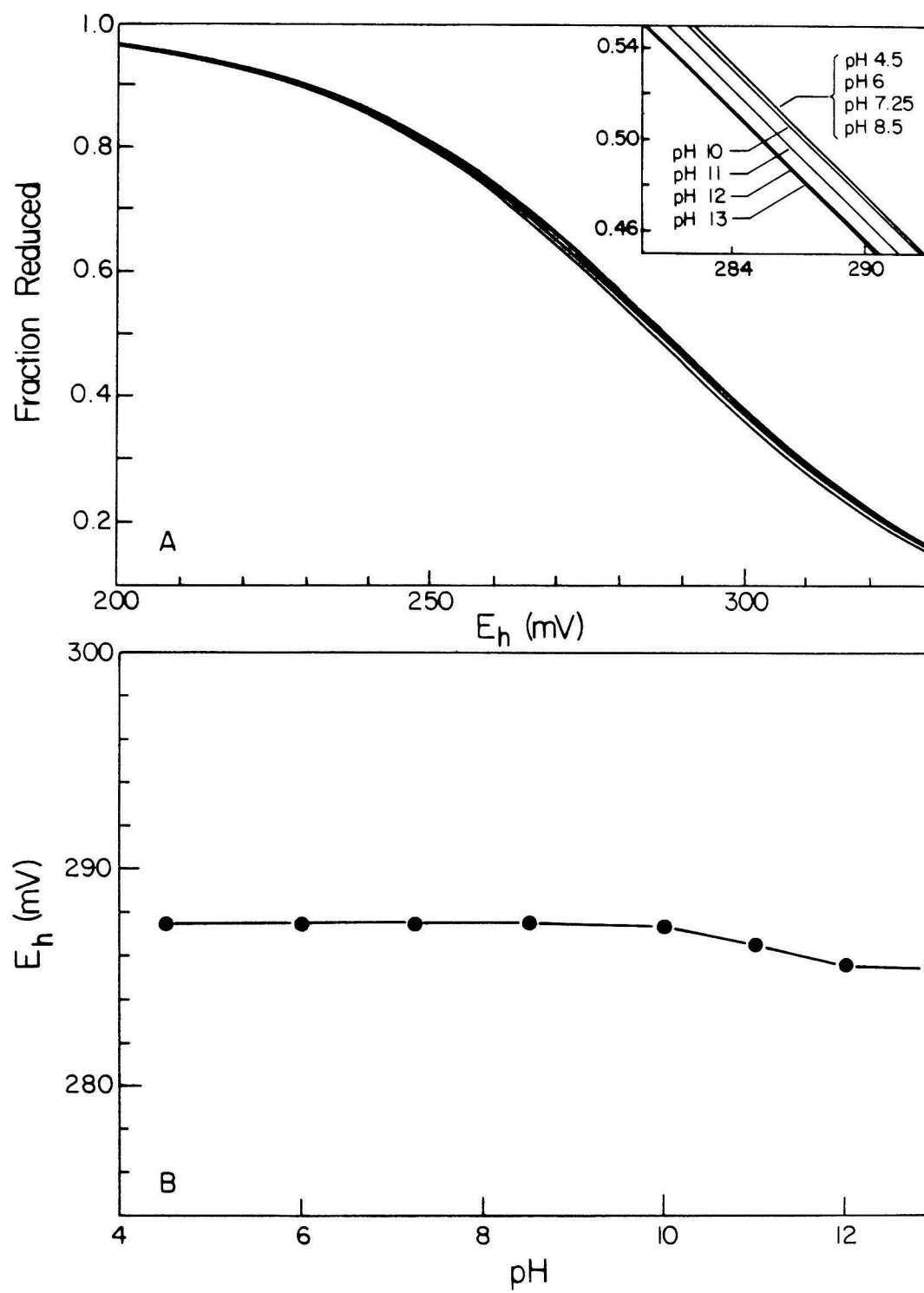
where the letters refer to the states in Fig. 2. $K_{p\ t}$ is expected to be greater than 1, since (as previously discussed) the functioning of the model depends on the distorted tetrahedral conformation being more stable for

Cu^{+2} and the trigonal conformation being more stable for Cu^+ .

Figure 4A shows titration curves generated with eq. 4 by varying E_h while holding the pH at one of a set of several values. The values used for $\text{pK}_a(\text{cys},\text{o})$, $\text{pK}_a(\text{cys},\text{r})$, $\text{pK}_a(\text{tyr},\text{o})$, $\text{pK}_a(\text{tyr},\text{r})$, E_i' , and E_{ii}' were those discussed previously. The value used for K_{pt} [10] was chosen to give a midpoint potential at pH 7 [$E_{m,7} = 287 \text{ mV}$] close to that experimentally observed for Cu_A ; raising K_{pt} causes the calculated midpoint to move closer to E_{ii}' and further away from E_i' . The midpoint potentials for the curves in Fig. 4A are displayed in Fig. 4B. These values do not vary in the pH 6.1-8.5 range, in agreement with experiment. This behavior is a consequence of both the high pK_a s proposed for the protonatable groups and the fact that the ligand exchange mechanism allows the presence of one proton to stabilize both the oxidized and the reduced forms of the redox center site, albeit by binding to different sites. Having seen that the predicted equilibrium properties of the model pump site are congruent with those observed for Cu_A , we now turn our attention to the properties of the system under turnover conditions.

Figure 4

Calculated behavior of the model pump in electrochemical titrations at different pH values. A: Fraction of the pump sites in the Cu^+ state at equilibrium with varying electrochemical potentials relative to that of the neutral hydrogen electrode (E_h). Curves shown are for pH 4.5, 6, 7.25, 8.5, 10, 11, 12, and 13. Inset: Magnified view of the central sections of the curves. B: The midpoint potentials (E_m) of the titration curves in A, plotted as a function of their pH values. Parameter values: $E_i' = 225$ mV, $E_h' = 575$ mV, $K_{pt} = 10$, $\text{pK}_a(\text{tyr},o) = 11$, $\text{pK}_a(\text{tyr},r) = 12$, $\text{pK}_a(\text{cys},o) = 10$, $\text{pK}_a(\text{cys},r) = 11$.



QUANTITATIVE EVALUATION OF THE BEHAVIOR
OF THE MODEL PROTON PUMP DURING STEADY STATE-TURNOVER

To be biologically useful, a cytochrome c oxidase molecule must function with adequate efficiency and must operate at a reasonable rate. The former requirement arises from the fact that inefficient operation would waste energy; the latter is because the biosynthesis of the oxidase molecule has particular energy, time, space, and material costs. When one considers the variations in pump performance caused by alterations of the design of the pump or changes in its operating environment (e.g., changes in $\Delta\tilde{\mu}_H$), the maximum efficiency will not in general occur under the same conditions as the maximum rate.

Consequently, optimal performance will entail a compromise between these two factors. The best compromise between efficiency and rate may differ from organism to organism and from tissue to tissue; it may also undergo temporal variations with the level of metabolic activity in some cell types. In the foregoing sections of this chapter I have described the proton pump model and demonstrated that it is consistent with experimentally determined properties of cytochrome oxidase. We will now turn our attention to the actual performance of the model pump, which we examine by calculating the turnover rate and free energy transduction

efficiency expected during steady-state turnover at different membrane electrochemical potentials.

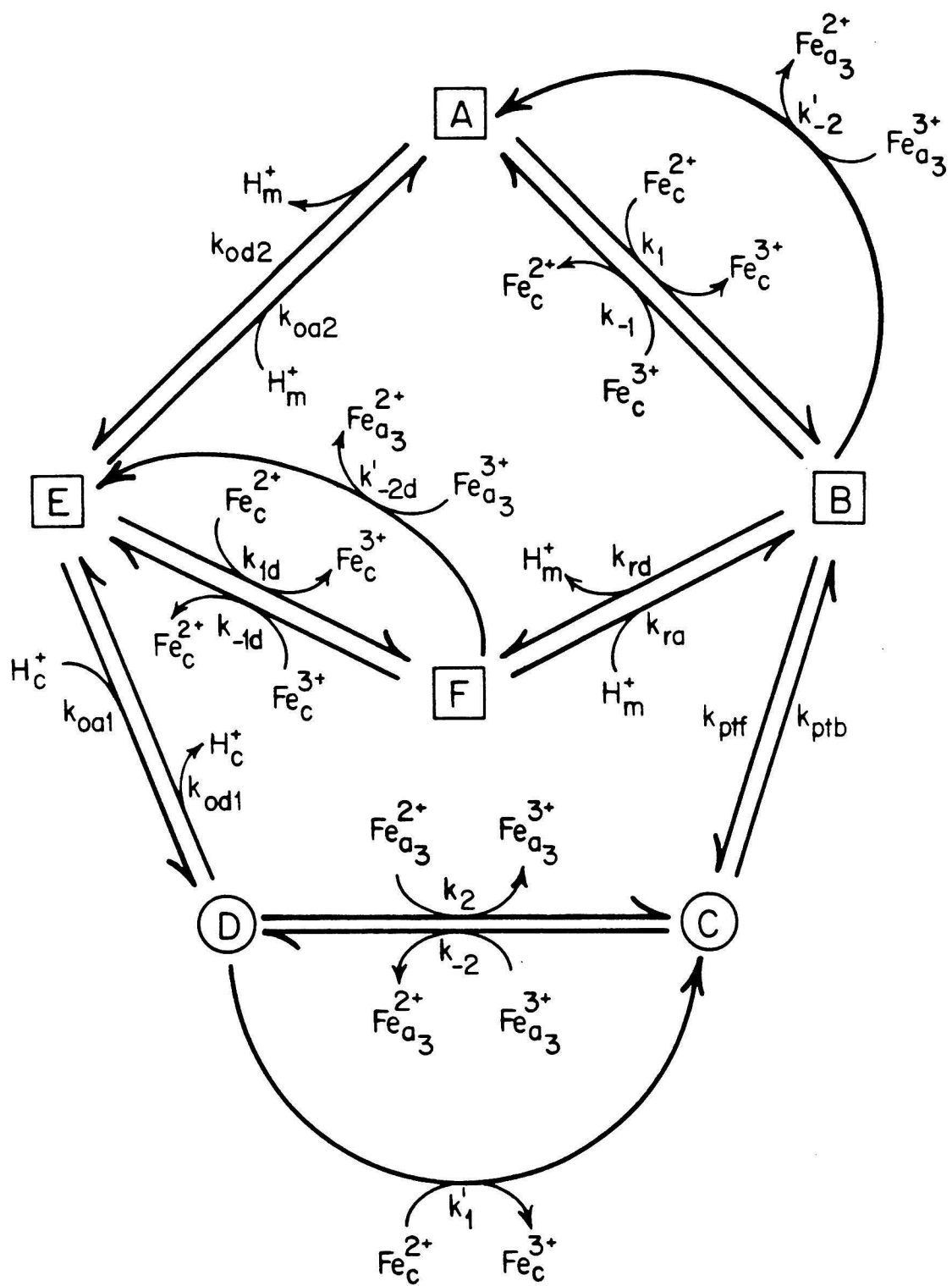
Reaction scheme for the steady-state analysis. The reactions included in the steady-state analysis and the designations used for the rate constants are shown in Fig. 5. Curved arrows connecting states and primed rate constants refer to "uncoupling" electron transfer pathways. As previously (17), the reverse reactions of these processes are not included in the analysis because they are substantially endoergonic electron transfers and are not expected to occur at significant rates. "Uncoupling" proton transfer reactions are also not considered in the analysis since, as discussed earlier, the pump model incorporates very efficient proton gating mechanisms. The states labelled A through E correspond to states with the same letter in Fig. 2. Clockwise passage among the states leads to electron transfer driven proton pumping. As discussed previously, the pK_a s of the tyrosine and cysteine are expected to be well below the physiological pH range when they are coordinated to the copper; therefore, no states with protonated copper ligands have been included in the analysis. For the sake of completeness, however, a state in which the copper ion is reduced and both the cysteine and tyrosine are deprotonated (state F in Fig. 5) was included.

Figure 5

Reaction scheme for the steady-state calculations.

Letters inside squares refer to states with the distorted tetrahedral copper ligation structure; those in circles refer to states with the distorted trigonal structure.

States A through E refer to the correspondingly lettered state in Fig. 2; state F is an additional state described in the text. The curved arrows connecting states A-B, D-C, and F-E represent "uncoupling" electron transfer pathways.



This state has exactly the same structure as that shown in Fig. 2B, except that the tyrosine side chain is in the form of the deprotonated phenolate anion. As described in the above discussion of the equilibrium behavior of the model pump, the pK_a of this group is proposed to be extremely high [$pK_a(\text{tyr},r) = 12$]. This state is not significantly populated under most of the conditions described below, and its absence would probably not alter any of the conclusions derived from the following analysis.

Parameters used in the steady-state calculations. Table I lists the names and meanings of the parameters used in the steady-state calculation and the numerical values used for these parameters in the initial analysis. The first group of parameters in Table I relate to thermodynamic properties of the model pump and have already been discussed in the context of the equilibrium behavior of the model pump. The reader will note that the pK_a values for the cysteine group do not directly enter into the analysis.⁸ The second group of parameters contains some of the factors which are needed to calculate the driving force for the electron transfer reactions to and from the pump site under varying conditions of membrane potential. These properties of cytochrome oxidase have been characterized experimentally, and the values used for each of these parameters are derived from

Table I: Parameters used in the steady state analysis of the pump model

Parameter	Value ^a	Description
<u>Thermodynamic properties of the model pump</u>		
E_H°	575 mV	Standard reduction potential of high potential (distorted trigonal) conformation of pump site in the protonated form.
E_L°	225 mV	Standard reduction potential of low potential (distorted tetrahedral) conformation of pump site in the protonated form.
$pK_a(\text{tyr},o)$	11	pK_a of the unligated tyrosine side chain when copper is oxidized.
$pK_a(\text{tyr},r)$	12	pK_a of the unligated tyrosine side chain when copper is reduced.
K_{pt}	10	Equilibrium constant for the conformational change from the reduced, protonated form of the distorted tetrahedral conformation to the same form of the distorted trigonal conformation.
<u>Factors affecting the electron transfer rates to and from the pump</u>		
E_c°	225 mV	Standard reduction potential of cytochrome <u>c</u> (39).
$f_{red}(c)$	0.5	Fraction of cytochrome <u>c</u> in the reduced state. ^b
$[Fe_c]$	1	Concentration of cytochrome <u>c</u> relative to that of cytochrome oxidase (2).
$E_{a_3}^\circ$	800 mV	Effective standard reduction potential of the O_2 -bound oxygen binding site (3).
$f_{red}(a_3)$	0.5	Fraction of the oxygen binding site in the reduced state. ^b
$f\psi$	0.75	Fraction of the membrane proton motive force due to $\Delta\psi$ (64, 1).
f_x	0.	Fraction of the membrane dielectric traversed by the electron transfer from cytochrome <u>c</u> to the pump site (72).
<u>Factors specifying relative rates of pump site reactions</u>		
PP_i	$1 \times 10^{15} \text{ s}^{-2}$	Product of the proton association and dissociation rate constants on the input side of the pump (used to calculate rate constants k_{ra} , k_{rd} , k_{oa2} , and k_{od2})
PP_o	$1 \times 10^{15} \text{ s}^{-2}$	Product of the proton association and dissociation rate constants on the output side of the pump (used to calculate rate constants k_{oa1} and k_{od1})

EP _i	1×10 ⁴ s ⁻²	Product of the forward and backward isoergonic ^c electron transfer rate constants on the input side of the pump (used to calculate rate constants k ₁ , k ₋₁ , k _{1d} , and k _{-1d}).
EP _o	1×10 ⁴ s ⁻²	Product of the forward and backward isoergonic ^c electron transfer rate constants on the output side of the pump (used to calculate rate constants k ₂ and k ₋₂).
PK _{pt}	1×10 ¹¹ s ⁻²	Product of the forward and backward rate constants for the conformational change from the reduced, protonated form of the distorted tetrahedral conformation to the same form of the distorted trigonal conformation (used to calculate rate constants k _{ptf} and k _{ptb}).
L _i	see text	Isoergonic ^c rate constant for the leak reaction involving cytochrome <u>c</u> (used to calculate the rate constant k _{1'}).
L _o	see text	Isoergonic ^c rate constant for the leak reaction involving the oxygen reduction site (used to calculate the rate constant k _{2'}).

^aIndicated value used unless otherwise specified in figure legend.

^bFraction reduced values were chosen so that the cytochrome c and oxygen reduction site potentials are those appropriate to typical experimental conditions (3).

^cDefined in text.

the studies referenced in Table I. The reader should be aware that some of these values vary rather markedly depending upon the experimental conditions employed in the study of the mitochondria (2, 64); the numbers used are fairly typical for an experiment using submitochondrial particles. The third group of parameters relate to the relative rates of the proton transfer, ligand substitution, and electron transfer reactions involved in turnover of the pump. The values chosen for these parameters are such that the long distance electron transfer reactions to and from the pump are the slowest and will therefore control the overall turnover rate of the system. As noted in the discussion of proton gating, the proton transfers between the protonatable groups at the pump site and their adjacent proton channels are expected to have small activation barriers. Their rate constant products are therefore made correspondingly large. The rate constant product for the ligand substitution reaction, which includes a proton transfer reaction which might be expected to require more activation energy than those just discussed, is set at a value intermediate between those for the other proton transfers and those for the electron transfers. It was noted during the course of the calculations that this value could be varied over a substantial range without having a discernible effect on the outcome of the calculation, as

long as it was not made so slow as to limit the overall turnover rate (data not shown). The leak rate constants L_i and L_o are expressed as individual rate constants rather than products of forward and reverse rate constants since the highly endoergonic reverse reactions are neglected because they are very slow. Therefore, the "gating ratios" which were calculated in the section discussing the gating of electrons in the model pump represent the quantities $L_i / (EP_i)^{1/2}$ and $L_o / (EP_o)^{1/2}$ for the "uncoupling": "coupling" reaction rate constant ratios of Figs. 3C and 3D, respectively.

Procedure used to calculate model pump performance at steady state. The calculation of the steady-state properties of the system was conducted using a procedure developed for and described in our earlier work (17); we present here a summary of the method and the assumptions upon which it is based. Each calculation was performed at a series of different $\Delta\tilde{\mu}_H^+$ values in order to examine the way in which the performance of the system varied at different steady-state transmembrane proton electrochemical potentials. Since the cytoplasm of cells has a high buffering capacity relative to the interior of the mitochondrion, the pH of the cytoplasm was fixed at 7 and the pH of the matrix was varied according to the ΔpH

component of $\Delta\tilde{\mu}_{H^+}$. Since the proton channels leading to the pump may traverse the dielectric of the membrane, the effective proton concentrations presented by the channels to the pump were adjusted using the theory derived by Mitchell (51, 1), which assumes that the channel protons remain at thermodynamic equilibrium with protons in the connected aqueous phase. The rate constants for the proton transfer and conformational change reactions of Fig. 5 were then calculated from the appropriate pK_a or equilibrium constant and the rate constant products. The calculation of the rate constants for the electron transfer reactions is more complex because these values depend on the difference in the standard reduction free energies between the electron transfer partners (eq. 1) and this energy difference varies with membrane $\Delta\psi$ (52). As in our previous study (17), the electron transfer rate constants are expressed initially as isoergonic rate constants (i.e., the rate constants expected for the electron transfer when $\Delta G^{\circ'} = 0$) which are then scaled to the values appropriate to the relevant $\Delta G^{\circ'}$ using eq. 2. As previously (17), the oxygen binding site is treated as a simple one-electron acceptor; in the present study, the electron transfers from the cytosol to the oxygen binding site are treated as if crossing the membrane $\Delta\psi$ in its entirety, since each electron transfer to the site is assumed to be coupled to the uptake of one H^+ from the

mitochondrial matrix.

Given the values for the rate constants, we calculate the steady-state electron transfer rate, proton pumping rate, efficiency, and concentration of each state of Fig. 5 using the formulas derived in Appendix II. It should be noted that the efficiency values in this work, in contrast to those in the preceding study (17) which focused on the performance of an isolated idealized transducer, are efficiencies for the complete cytochrome oxidase reaction, including the contribution to $\Delta\tilde{\mu}_H^+$ production by the consumption of protons from the mitochondrial matrix by O_2 reduction. The electron transfer rates include electron transfer through the pump site only; the effect on the efficiency of electron transfers which bypass this site is not considered.

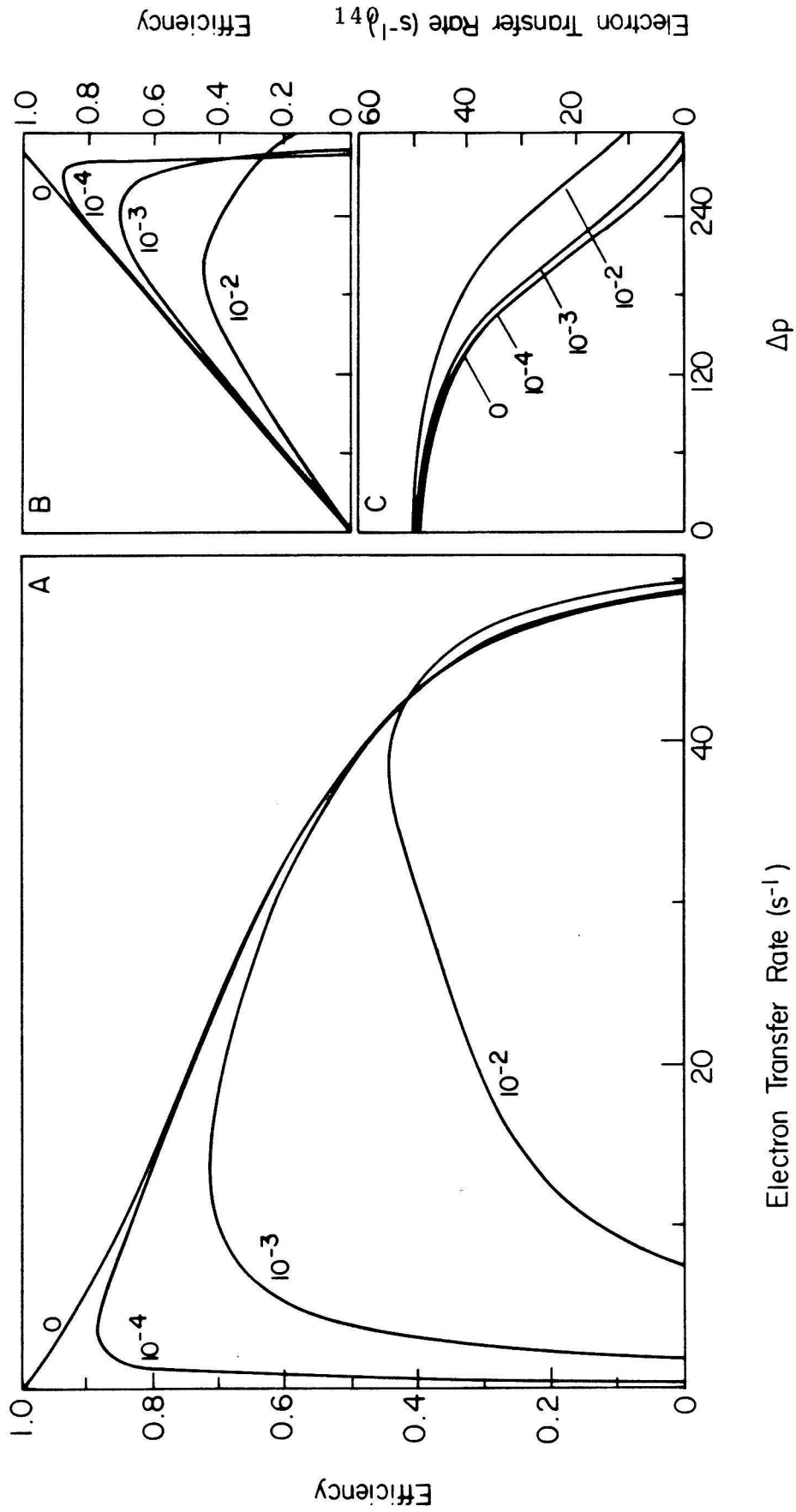
Results of the steady-state calculation for the pump model. The rate versus efficiency results of the steady-state calculation using the parameter values in Table I are shown in Fig. 6A. The figure shows four calculations, each with different gating ratios, which were obtained by varying the isoergonic leak rate constants while holding fixed the other parameters listed in Table I. Each point on an individual curve was generated by calculating the efficiency

and the rate corresponding to a particular $\Delta\mu_H^+$, giving the results shown in Figs. 6B and 6C. The pairs of rate and efficiency values were then used to produce Fig. 6A. The type of presentation used in Fig. 6A is particularly valuable in examining performance aspects of the pump because it allows direct visualization of the different conditions required for maximum efficiency, maximum rate, and maximum power output. It can therefore be helpful in understanding the compromises between these measures of performance that may be needed under particular metabolic conditions (17, 65).

The qualitative features of the performance of the model pump are similar to those obtained with a simpler model transducer described in our earlier work (17), and the reader is referred to that work for a detailed discussion of some of the behavioral properties of this type of system. We summarize several significant points here: First, the efficiency is highest when there are no leaks and, as expected, decreases as the leaks become increasingly severe (Fig. 6A). The loss of efficiency caused by the leaks is more severe at higher membrane potentials (Fig. 6B) since the free energy difference between the pumping cycle (including the "coupling" pathways) and the futile cycles (including the "uncoupling" pathways) becomes larger as the

Figure 6

Energy transduction efficiency and electron transfer rate in the steady-state reaction scheme. Calculations were performed for gating ratios ["uncoupling": "coupling" isoergonic electron-transfer rate constant ratios; see text] of 0, 10^{-4} , 10^{-3} , and 10^{-2} which were attained using leak rate constants $L_i = L_o = 0$, 10^{-2} , 10^{-1} , and 1 s^{-1} , respectively. The other parameter values were those given in Table I.



membrane potential increases. Second, increasing the the leak rates has only a small effect on the efficiency in the physiologically relevant range of membrane potentials [$\Delta p = 240$ mV in resting mitochondria (2)], and virtually no effect on the maximum attainable power output of the system, until the gating ratio falls below 10^{-3} . It should be noted that since the gating ratios are expressed in terms of the isoergonic rate constants, a gating ratio of 10^{-3} corresponds to a substantial flux through the "uncoupling" pathways [20% and 9% of the flux through the coupling pathways on the input and output sides of the pump, respectively, when $\Delta p = 240$ mV]. Third, efficiency is only weakly dependent on rate over the physiologically relevant range of membrane potentials, but the rate versus potential curves are strongly sloped in this region. It has long been known that the transition from resting [state 4] to phosphorylating [state 3] mitochondria is accompanied by a large increase in electron transfer rates but only a small [$\Delta\Delta p \cong 30$ mV (1)] reduction in the membrane potential. The behavior of the model is consistent with such changes and shows that the transition can occur with only a minor decrease in operating efficiency. Fourth, the system exhibits "respiratory control" of the same magnitude as that observed in experiments using cytochrome oxidase reconstituted into artificial lipid vesicles (66). This

manifests itself as an approximately ten-fold increase in electron transfer rate upon going from a maximally coupled system to an uncoupled ($\Delta p = 0$) one.

It would be of great interest to compare the maximum steady-state efficiency attained by the model pump with that measured experimentally for cytochrome oxidase. Unfortunately, accurate efficiency values are not known for cytochrome oxidase, because of the difficulties involved in measuring the stoichiometry of proton translocation under the steady-state conditions where Δp can also be determined. The analogous problem with measurements of the overall efficiency of the respiratory chain is discussed by Stucki (65).

Concentrations of reaction intermediates at steady state.

In several theoretical studies of active transport processes, considerable attention has been given to the relative concentrations of the different states in the reaction cycle during steady-state turnover. Jencks (14) and Tanford (15), in their discussions of simple models for active transport enzymes, have each emphasized the importance of various properties of the reaction cycle which will tend to maintain reaction cycle intermediates at equal concentrations in the steady state. These concepts have

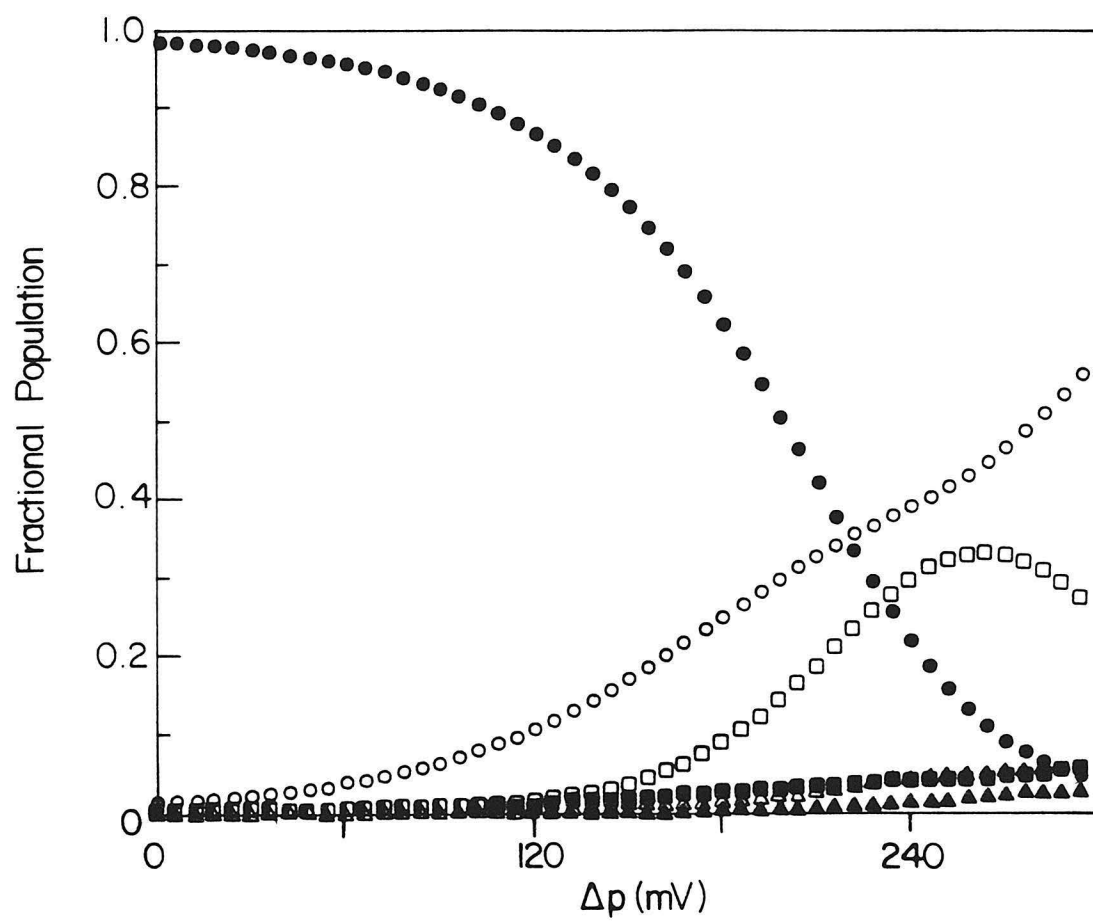
been applied to the cytochrome oxidase proton pump by Malmström (21). The benefit of equal intermediate concentrations is primarily that in such circumstances no single step in the reaction cycle disproportionately limits the overall rate.

We believe that the importance of these ideas has been overemphasized to the extent that workers in the field may erroneously assume that they represent general principles or "rules" (21) to which an active transport system must adhere if it is to achieve adequate performance. This is not the case. The principles are based on analysis of a single class of simple pump mechanisms, and they are relevant to rate alone, which as discussed above is only one of several factors relevant to assessing the performance of a proton pump (65). Efficiency and power output are also important performance criteria, and they will in general be maximal under different conditions than rate will be (Fig. 6).

Fig. 7 illustrates that the concentrations of intermediates in the cytochrome oxidase pump model are grossly unequal under conditions in which the pump achieves maximum efficiency. In the high efficiency region near $\Delta p = 240$ mV, the intermediates A through E can be divided into two groups based on their concentrations. (Species F is not

Figure 7

Fractional population of the states of the model pump. Figure shows the relative concentrations of states A (●), B (■), C (○), D (△), E (□), and F (▲) of the model pump in the steady-state calculation with gating ratios of 10^{-3} shown in Fig. 6 [$L_i = L_o = 10^{-1} \text{ s}^{-1}$; other parameter values are those in Table I].



considered because, as mentioned earlier, it does not make a substantial contribution to the behavior of the system.) Species A, C, and E are each present with a fractional concentration of about $1/3$, while B and D are present at approximately an order of magnitude lower concentrations. The two groups are distinguished by the fact that the latter consists of the states which are sources for the leak reactions [k_1 and k_{-2} in Fig. 5]. It is readily understandable that attempts to increase the concentrations of these species to the point that they are equal with those of the other species would drastically increase the flux of electrons through the leak pathways with a consequent large decrease in the efficiency of energy conservation. The fact that the "uncoupling" pathways have so little effect on the efficiency of the system over a wide range of Δp values (compare the gating ratio 0 and 10^{-3} curves in Fig. 6B in the $\Delta p = 0$ to 200 mV range) is partly due to the fact that the pump can maintain the leak source species at low concentrations throughout this range of conditions.

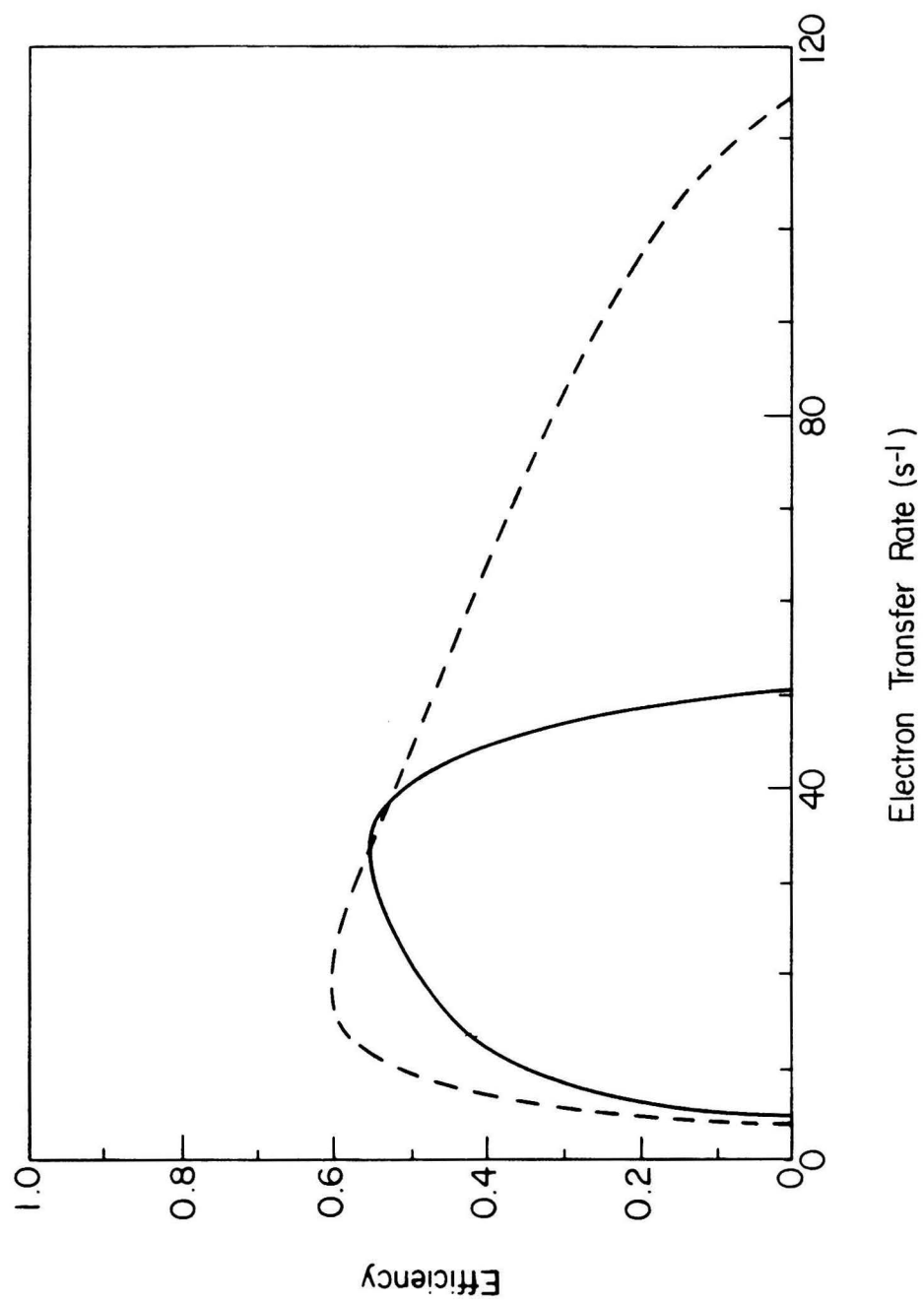
Steady state analysis incorporating the effects of electron transfer distance changes in the model pump. In the discussion of gating earlier in this chapter, we concluded that differences in the electron transfer distances for the "coupling" and "uncoupling" electron

transfer reactions would give electron gating ratios of approximately 1.5×10^{-2} on the input side and 4.0×10^{-4} on the output side of the pump. The solid line in Fig. 8 shows the results of a steady-state calculation using these values. The major conclusion from these data is that the design of the model pump is a workable one: reasonably efficient proton pumping will take place at physiological values of $\Delta\tilde{\mu}_H^+$ when the physical and chemical parameters of the pump have the values estimated in discussions above. It is important to note that the magnitude of efficiency calculated in Fig. 8 may be an underestimate of the true efficiency obtained in the model pump since, as discussed earlier, we have not attempted to include contributions to the gating from changes in the relative orientations of the donor and acceptor wavefunctions.

The rate constants for the input and output "uncoupling" electron transfer reactions in the calculation are very different, reflecting the asymmetry in the conformationally-induced distance changes for the input and output electron transfer processes. It was previously noted that changes in the reorganizational energies of the two conformations of the pump site, while not increasing the efficiency of gating in the pump as a whole, can affect the relative efficiencies of gating in the input and output

Figure 8

Free energy transduction efficiency and electron transfer rate of the model pump. Parameter values are those in Table I, except as noted. Solid line: Performance with symmetrical input and output isoergonic electron transfer rate constant products and with the gating ratios expected from the electron transfer distance changes in the model pump [input gating ratio = 1.5×10^{-2} ; output gating ratio = 4.0×10^{-4} ; $EP_i = EP_o = 10^{+4} \text{ s}^{-2}$; $L_i = 1.5 \text{ s}^{-1}$; $L_o = 0.039 \text{ s}^{-1}$]. Dashed line: Performance after symmetry of the input and output gating ratios is restored by adjusting the reorganizational energies of the two conformations of the pump site [input gating ratio = output gating ratio = 2.4×10^{-3} ; $EP_i = 6.1 \times 10^{+4} \text{ s}^{-2}$; $EP_o = 1.6 \times 10^{+3} \text{ s}^{-2}$; $L_i = 0.60 \text{ s}^{-1}$; $L_o = 0.096 \text{ s}^{-1}$].



electron transfer processes. This has the effect of changing the way that the gating is apportioned between the input and output sides of the pump. If the two ligation structures of the site have appropriately chosen unequal reorganizational energies, these can compensate for the inequality in the gating by distance changes of the electron input and output processes. The effect of such an adjustment is shown by the dashed curve in Fig. 8: the maximum attainable efficiency, and the maximum power, are increased by restoring symmetry to the electron transfer gating processes (17).

STRUCTURAL REQUIREMENTS OF THE PROTON PUMP MODEL

As mentioned previously, there is little experimental data about the identity of the metal center associated with the cytochrome oxidase proton pump, about the structural features of the pump site, or about the chemical mechanism of the pump. Nevertheless, we have in this chapter proposed a detailed model of the proton pump in cytochrome oxidase. Our purpose is to provide a sufficiently comprehensive description of the model to demonstrate that it is a workable design for a proton pump. We anticipate that the concreteness of the model will aid understanding of the mechanistic features required for proton pumping and will provoke the formulation of new experimental approaches to the study of proton pumping in cytochrome oxidase. In this context, it should be noted that some structural features of the model pump are based on experimental observations of cytochrome oxidase structure while others have no empirical basis but are included to fulfill a particular role in the pump mechanism. Several of the latter type of features could be substantially altered without significantly affecting model function. We now conclude our discussion of the pump model by distinguishing the structural features which were included to make the model consistent with experimentally determined properties of the cytochrome

oxidase molecule from those which were included only to complete the description of the mechanism.

The redox center associated with the pump. As noted earlier, the cytochrome oxidase proton pump is probably associated with Fe_a or Cu_A , but there is little information which allows one to distinguish between these two possibilities. There is substantial evidence that Fe_a and Cu_A lie on two parallel pathways for electron transfer from cytochrome c to the oxygen binding site [see (34) and references therein]. In the detergent-solubilized enzyme, the Cu_A pathway accounts for 70-85% of the total flux of electrons through the enzyme (43, 42, 41). The observation that it is Cu_A , and not Fe_a , which is on the major electron transfer pathway through the enzyme suggests that Cu_A is the site of the proton pump (34). In this view, the pathway through Fe_a represents a pump bypass which has little significance at low $\Delta\tilde{\mu}_H+$ but becomes more prominent as $\Delta\tilde{\mu}_H+$ increases (43, 42, 17). This arrangement has the advantage of maintaining a high power output for the respiratory chain over a wide range of conditions (67).

Since it is our opinion that Cu_A represents the best candidate for the redox site associated with the cytochrome oxidase proton pump, we have formulated the model described

in this chapter using this metal center. However, in view of the tentativeness of the evidence linking Cu_A and the pump, it is of interest to consider the extent to which the ideas discussed in this chapter are applicable to proton pump models involving Fe_a . A ligand exchange mechanism of the type proposed here might be applied in some form to any pump linked to a transition metal redox center. However, it should be noted that the range of chemical reactions undergone by heme cofactors in proteins is rather limited due to the stability of the porphyrin-iron complex. Axial ligand substitution reactions are the only reactions commonly observed at heme protein active sites which result in major changes in the site structure. Even allowing such substitutions, it is difficult to formulate a pumping mechanism for Fe_a without invoking substantial protein conformational changes to achieve the necessary gating of protons and electrons. Previously published cytochrome oxidase pump models commonly attribute one or more necessary pump functions to rather vaguely specified protein conformational changes. Reliance on global conformational change mechanisms does not in itself affect the feasibility of such mechanisms, but it does make their feasibility much more difficult to assess. We are currently conducting experiments to directly examine the role of Cu_A in proton pumping.

The structures of the Cu_A site in the proton pump model.

An essential and testable feature of the model proposed in this chapter is that the structure of the Cu_A site in the stable oxidized form of the enzyme (Fig. 2A) is different from that in the stable reduced form (Fig. 2C). A great deal is known about the structure of Cu_A²⁺ from studies exploiting the characteristic EPR and optical absorptions of this species (6). Recent work indicates that Cu_A²⁺ has two nitrogen ligands (one or both of which are histidine imidazole side chains) and one or (more likely) two cysteine thiolate ligands (68, 69, 46). The ligation structure and geometry shown in Fig. 2A will produce an electronic structure consistent with the known properties of the site and which explains its spectroscopic features, some of which are quite unique (69, 46, 34). It should be noted that many of the detailed features of this structure are not essential to the functioning of the proton pump model. In particular, the model does not require the presence of two cysteines since the role of the topmost ligand in Fig. 2A could be filled by other amino acid side chains (e.g., tyrosine, lysine) which are chemically suited to be copper ligands and which have the necessary high pK_a.

Much less is known about the stable reduced structure of

the enzyme because Cu_A^+ has no known EPR or optical absorptions. Although some information about the structure of the Cu_A^{+1} site is provided by x-ray spectroscopy (70, 71), the interpretation of these data is complicated by the overlap of the spectral features from Cu_A and Cu_B . Because of these difficulties, the identity of the ligands to Cu_A^+ is not presently known. In particular, there is no evidence for (or against) the presence of a tyrosine ligand. The choice of a tyrosine as a ligand to the distorted trigonal conformation of the model site was somewhat arbitrary and other amino acids with similar acid/base and ligation properties (e.g., cysteine) might function equally well. Experiments which provide more definitive information about the structure of Cu_A^+ would be valuable both as a test of the specifics of the model and of the general concept of a pump mechanism involving a ligand substitution at Cu_A .

SUMMARY

The model for proton pumping in cytochrome c oxidase proposed in this chapter is the first such model which includes explicit chemical mechanisms for all of the processes necessary to achieve redox-linked proton pumping. In particular, it incorporates mechanisms for the gating of both protons and electrons, as well as reactions which modulate the reduction potential of the redox site associated with the pump. All three of these processes are facilitated by a novel transition metal ligand exchange mechanism at the pumping site. In addition to describing the model, we have also presented quantitative analyses of the properties of the pump at equilibrium and during steady-state turnover. The equilibrium calculation demonstrates that the behavior expected of the model pump in an electrochemical titration is the same as that observed for the Cu_A center: a nearly pH-independent midpoint potential of approximately 290 mV. The steady-state analysis shows that the model pump is expected to function efficiently and with good power output under physiological conditions, and that its properties under conditions of varying load are similar to those observed in experiments on respiring mitochondria and on purified cytochrome oxidase reconstituted into artificial lipid vesicles.

Although the analysis presented here concerns only a single model of a redox-linked proton pump, it leads to some important general conclusions regarding the mechanistic features of such pumps. The first is that a workable proton pump mechanism does not require large protein conformational changes. This chapter presents an example of a workable mechanism involving only small structural changes at the pump site. Another general conclusion is that a redox-linked proton pump need not display a pH-dependent midpoint potential. The model presented here shows virtually no change in its electrochemical titration curve over a wide range of pH. A final conclusion is that mechanisms for redox-linked proton pumps that involve transition metal ligand exchange reactions are quite attractive because such reactions readily lend themselves to the linked gating processes necessary for proton pumping. It is our hope that the model of the cytochrome oxidase proton pump presented here will stimulate workers in the field to perform experimental tests of the model; and, if it fails these tests, to propose new and more accurate models.

Appendix I:

STATE POPULATIONS OF THE MODEL PUMP AT EQUILIBRIUM

States of the model pump which are not significantly populated during steady-state turnover may become so under equilibrium conditions. To insure the completeness of the analysis, we have considered all eight states representing the possible combinations of oxidized or reduced copper, distorted tetrahedral or distorted trigonal ligation geometry, and protonated or deprotonated proton binding site (Fig. 9). As with all of the analyses in this chapter, states in which the tyrosine or cysteine side chains are protonated while acting as copper ligands are not included since such structures have very low pK_as.

The terms K₁ through K₉ represent the ratios of the equilibrium concentrations of the products to those of the reactants of the reactions indicated by arrows in Fig. 9:

$$K_1 = [A] / [B]$$

$$K_2 = [D] / [C]$$

$$K_3 = [C] / [B]$$

$$K_4 = [E] / [A]$$

$$K_5 = [F] / [B]$$

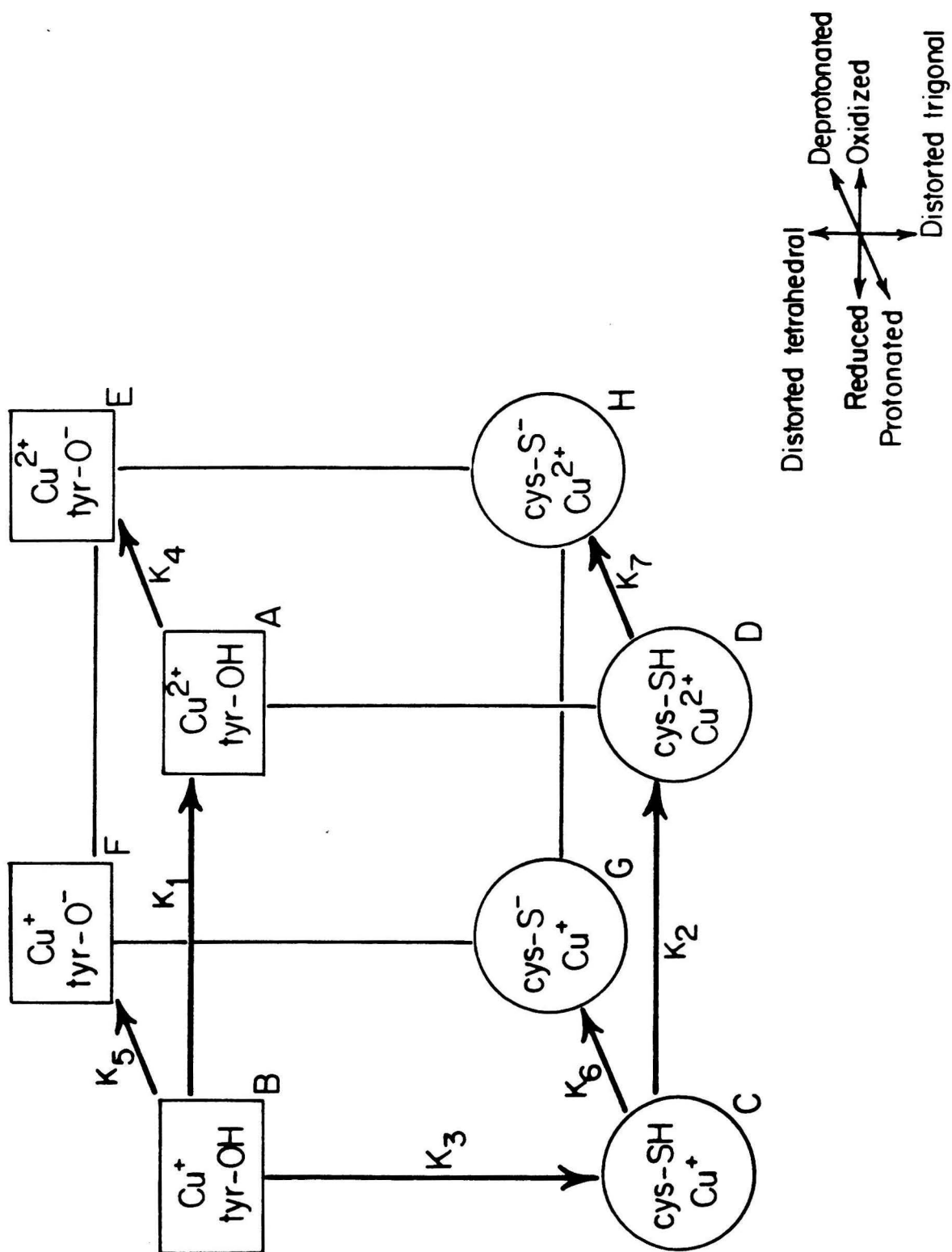
$$K_6 = [G] / [C]$$

$$K_7 = [H] / [D]$$

where the letters in square brackets represent the

Figure 9

States of the model pump considered in the equilibrium concentrations calculation. The three orthogonal axes of the cube represent oxidation or reduction of the copper, protonation or deprotonation of the appropriate proton binding site, and the distorted tetrahedral (squares) or distorted trigonal (circles) ligation structure. Constants K_1 through K_7 represent the concentration ratio of the species at the head of the indicated arrow to the species at its tail.



concentrations of each of the species A through H relative to the total concentration of all eight species. (A through F designate the same species that they do in Figs. 2 and 5. The numerical values of K_1 through K_7 can be calculated from the thermodynamic parameters of the model using eqs. 4a through 4g in the text. Note that K_1 and K_2 pertain to oxidation reactions and their values therefore depend on E_h , and that K_4 , K_5 , K_6 , and K_7 pertain to deprotonation reactions and therefore depend on pH.

The concentration equations can be written as the matrix equation

$$\begin{bmatrix} 1 & 1 & 1 & 1 & 1 & 1 & 1 & 1 \\ -1 & K_1 & 0 & 0 & 0 & 0 & 0 & 0 \\ 0 & 0 & K_2 & -1 & 0 & 0 & 0 & 0 \\ 0 & K_3 & -1 & 0 & 0 & 0 & 0 & 0 \\ K_4 & 0 & 0 & 0 & -1 & 0 & 0 & 0 \\ 0 & K_5 & 0 & 0 & 0 & -1 & 0 & 0 \\ 0 & 0 & K_6 & 0 & 0 & 0 & -1 & 0 \\ 0 & 0 & 0 & K_7 & 0 & 0 & 0 & -1 \end{bmatrix} \begin{bmatrix} [A] \\ [B] \\ [C] \\ [D] \\ [E] \\ [F] \\ [G] \\ [H] \end{bmatrix} = \begin{bmatrix} 1 \\ 0 \\ 0 \\ 0 \\ 0 \\ 0 \\ 0 \\ 0 \end{bmatrix}.$$

Solving for the concentration vector yields

$$\begin{bmatrix} [A] \\ [B] \\ [C] \\ [D] \\ [E] \\ [F] \\ [G] \\ [H] \end{bmatrix} = \begin{bmatrix} K_1 Q \\ Q \\ K_3 Q \\ K_2 K_3 Q \\ K_1 K_4 Q \\ K_5 Q \\ K_3 K_6 Q \\ K_2 K_3 K_7 Q \end{bmatrix} ,$$

where

$$Q = \frac{1}{1 + K_1 + K_1 K_4 + K_2 K_3 + K_2 K_3 K_7 + K_3 + K_3 K_6 + K_5} .$$

The fraction of the pump molecules in any of the reduced forms is

$$\begin{aligned}
 f_{red} &= [B] + [C] + [F] + [G] \\
 &= \frac{1 + K_3 + K_3 K_6 + K_5}{1 + K_1 + K_1 K_4 + K_2 K_3 + K_2 K_3 K_7 + K_3 + K_3 K_6 + K_5} ,
 \end{aligned}$$

as given by eq. 4 in the text.

Appendix II:

THE TURNOVER RATE AND EFFICIENCY
OF THE MODEL PUMP AT STEADY STATE

At steady state, the system of reactions schematized in Fig. 5 is described by the following set of equations for the various species concentrations:

$$[A] + [B] + [C] + [D] + [E] + [F] = 1 \quad (A1)$$

$$\begin{aligned} & (k_1 [Fe_c] f_{red}(c) + k_{od2}) [A] - \\ & (k_{-1} [Fe_c] \{1-f_{red}(c)\} + k'_{-2} \{1-f_{red}(a_3)\}) [B] - \\ & k_{oa2} [H\ddot{m}] [E] = 0 \quad (A2) \end{aligned}$$

$$\begin{aligned} & -k_1 [Fe_c] f_{red}(c) [A] + \\ & (k_{-1} [Fe_c] \{1-f_{red}(c)\} + k'_{-2} \{1-f_{red}(a_3)\} + k_{ptf} + k_{rd}) [B] - \\ & k_{ptb} [C] - \\ & k_{ra} [H\ddot{m}] [F] = 0 \quad (A3) \end{aligned}$$

$$\begin{aligned} & -k_{ptf} [B] + \\ & (k_{ptb} + k_{-2} \{1-f_{red}(a_3)\}) [C] - \\ & (k_2 f_{red}(a_3) + k'_1 [Fe_c] f_{red}(c)) [D] = 0 \quad (A4) \end{aligned}$$

$$\begin{aligned}
& -k_{od2} [A] - \\
& k_{od1} [D] + \\
& (k_{oa2} [H_m] + k_{oa1} [H_c] + k_{1d} [Fe_c] f_{red}(c)) [E] - \\
& (k_{-1d} [Fe_c] \{1-f_{red}(c)\} + k'_{2d} \{1-f_{red}(a_3)\}) [F] = 0 \quad (A5)
\end{aligned}$$

$$\begin{aligned}
& -k_{rd} [B] - \\
& k_{1d} [Fe_c] f_{red}(c) [E] + \\
& (k_{-1d} [Fe_c] \{1-f_{red}(c)\} + k'_{2d} \{1-f_{red}(a_3)\} + k_{ra} [H_m]) [F] = 0 \quad (A6)
\end{aligned}$$

where the symbols in square brackets refer to the concentrations of the named species relative to the enzyme concentration, except for $[H_m]$ and $[H_c]$ which are the absolute H^+ concentrations on the m-side and c-side of the membrane, respectively. Other symbols are the parameters defined in Table I and the rate constants shown in Fig. 5.

Eqs. A2 through A6 can be combined into the matrix equation

$$\begin{bmatrix}
c_{11} & c_{12} & 0 & 0 & c_{15} & 0 \\
c_{21} & c_{22} & c_{23} & 0 & 0 & c_{26} \\
0 & c_{32} & c_{33} & c_{34} & 0 & 0 \\
c_{41} & 0 & 0 & c_{44} & c_{45} & c_{46} \\
0 & c_{52} & 0 & 0 & c_{55} & c_{56}
\end{bmatrix}
\begin{bmatrix}
[A] \\
[B] \\
[C] \\
[D] \\
[E] \\
[F]
\end{bmatrix}
=
\begin{bmatrix}
0 \\
0 \\
0 \\
0 \\
0 \\
0
\end{bmatrix}$$

where the c_{nm} s are defined by reference to eqs. A2 through A6.

By generating appropriate linear combinations of the rows, this matrix equation may be rearranged to a form in which all of the species concentrations are given relative to that of species A:

$$\begin{bmatrix} C_{21} & C_{22} & 0 & 0 & 0 & 0 \\ C_{31} & 0 & C_{33} & 0 & 0 & 0 \\ C_{41} & 0 & 0 & C_{44} & 0 & 0 \\ C_{51} & 0 & 0 & 0 & C_{55} & 0 \\ C_{61} & 0 & 0 & 0 & 0 & C_{66} \end{bmatrix} \begin{bmatrix} [A] \\ [B] \\ [C] \\ [D] \\ [E] \\ [F] \end{bmatrix} = \begin{bmatrix} 0 \\ 0 \\ 0 \\ 0 \\ 0 \\ 0 \end{bmatrix} \quad (A8)$$

where the constants C_{nm} are given by the following equations:

$$\begin{aligned} C_{61} = & C_{11}C_{55} (C_{12}C_{45}C_{23}C_{34} - C_{15}C_{44}C_{33}C_{22} + C_{15}C_{44}C_{23}C_{32}) - \\ & (C_{12}C_{55} - C_{15}C_{52}) \\ & (C_{11}C_{45}C_{23}C_{34} - C_{15}C_{41}C_{23}C_{34} - C_{15}C_{44}C_{33}C_{21}) \end{aligned} \quad (A9a)$$

$$\begin{aligned} C_{66} = & -C_{56}C_{15} (C_{12}C_{45}C_{23}C_{34} - C_{15}C_{44}C_{33}C_{22} + C_{15}C_{44}C_{23}C_{32}) + \\ & (C_{12}C_{55} - C_{15}C_{52}) (C_{15}C_{46}C_{23}C_{34} + C_{15}C_{44}C_{33}C_{26}) \end{aligned} \quad (A9b)$$

$$C_{21} = C_{11}C_{55} (C_{15}C_{46}C_{23}C_{34} + C_{15}C_{44}C_{33}C_{26}) - \\ C_{56}C_{15} (C_{11}C_{45}C_{23}C_{34} - C_{15}C_{41}C_{23}C_{34} - C_{15}C_{44}C_{33}C_{21}) \quad (A9c)$$

$$C_{22} = (C_{12}C_{55} - C_{15}C_{52}) (C_{15}C_{46}C_{23}C_{34} + C_{15}C_{44}C_{33}C_{26}) - \\ C_{56}C_{15} (C_{12}C_{45}C_{23}C_{34} - C_{15}C_{44}C_{33}C_{22} + C_{15}C_{44}C_{23}C_{32}) \quad (A9d)$$

$$C_{31} = C_{61} - C_{66} \frac{C_{11}C_{22}C_{55} - C_{12}C_{21}C_{55} + C_{15}C_{52}C_{21}}{-C_{12}C_{26}C_{55} + C_{15}C_{52}C_{26} - C_{15}C_{22}C_{56}} \quad (A9e)$$

$$C_{33} = -C_{66} \frac{-C_{12}C_{23}C_{55} + C_{52}C_{23}C_{15}}{-C_{12}C_{26}C_{55} + C_{15}C_{52}C_{26} - C_{15}C_{22}C_{56}} \quad (A9f)$$

$$C_{41} = C_{11}C_{45}C_{55}C_{46} - C_{11}C_{45}C_{45}C_{56} - C_{15}C_{41}C_{46}C_{55} + \\ C_{15}C_{41}C_{45}C_{56} + C_{15}C_{46}C_{41}C_{55} - \\ \{C_{11}C_{45}C_{26}C_{33} - C_{15}C_{41}C_{26}C_{33} + C_{15}C_{46}C_{21}C_{33}\} \\ \{ \frac{C_{12}C_{45}(C_{55}C_{46} - C_{45}C_{56}) - C_{15}C_{46}C_{52}C_{45}}{C_{12}C_{45}C_{26}C_{33} + C_{15}C_{46}C_{22}C_{33} - C_{15}C_{46}C_{23}C_{32}} \} \quad (A9g)$$

$$C_{44} = -C_{15}C_{44}C_{55}C_{46} + C_{15}C_{44}C_{45}C_{56} + C_{15}C_{46}C_{44}C_{55} \\ - \{-C_{15}C_{44}C_{26}C_{33} - C_{15}C_{46}C_{23}C_{34}\} \\ \{ \frac{C_{12}C_{45}(C_{55}C_{46} - C_{45}C_{56}) - C_{15}C_{46}C_{52}C_{45}}{C_{12}C_{45}C_{26}C_{33} + C_{15}C_{46}C_{22}C_{33} - C_{15}C_{46}C_{23}C_{32}} \} \quad (A9h)$$

$$C_{51} = C_{61} + C_{66}(C_{52}C_{11}) / (C_{12}C_{56}) \quad (A9i)$$

$$C_{55} = C_{66}(C_{52}C_{15} - C_{12}C_{55}) / (C_{12}C_{56}). \quad (A9j)$$

Using eq. A8, eq. A1 becomes

$$[-C_{21}/C_{22} - C_{31}/C_{33} - C_{41}/C_{44} - C_{51}/C_{55} - C_{61}/C_{66} + 1] [A] = 1. \quad (A10)$$

This equation thus gives the concentration of species A in terms of the total concentration of pumps. The concentrations of the other species may be likewise determined by using this equation in conjunction with eq. A8 (which gives the other species concentrations relative to that of species A). This is the source of the expressions used to calculate the species concentrations shown in Fig. 7.

The rate of proton translocation by the model pump is given by

$$k_{H^+} = k_{od1} [D] - k_{oa1} [H^+] [E], \quad (A11)$$

and the rate of electron transfer by

$$\begin{aligned}
k_{e-} = & k_1 [\text{Fec}] f_{\text{red}}(c) [A] + k_{1d} [\text{Fec}] f_{\text{red}}(c) [E] - \\
& k_{-1} [\text{Fec}] \{1 - f_{\text{red}}(c)\} [B] - \\
& k_{-1d} [\text{Fec}] \{1 - f_{\text{red}}(c)\} [F] + \\
& k_1' [\text{Fec}] f_{\text{red}}(c) [D].
\end{aligned} \tag{A12}$$

Substituting eqs. A8 and A10, the rates of proton translocation and electron transfer are then given by

$$k_{H+} = \frac{k_{od1} (-C_{41}/C_{44}) - k_{oa1} [H^+] (-C_{51}/C_{55})}{-C_{21}/C_{22} - C_{31}/C_{33} - C_{41}/C_{44} - C_{51}/C_{55} - C_{61}/C_{66} + 1} \tag{A13}$$

$$\begin{aligned}
k_{e-} = & \{k_1 [\text{Fec}] f_{\text{red}}(c) + \\
& k_{1d} [\text{Fec}] f_{\text{red}}(c) (-C_{51}/C_{55}) - \\
& k_{-1} [\text{Fec}] \{1 - f_{\text{red}}(c)\} (-C_{21}/C_{22}) - \\
& k_{-1d} [\text{Fec}] \{1 - f_{\text{red}}(c)\} (-C_{61}/C_{66}) + \\
& k_1' [\text{Fec}] f_{\text{red}}(c) (-C_{41}/C_{44})\} \\
& / \\
& \{-C_{21}/C_{22} - C_{31}/C_{33} - C_{41}/C_{44} - C_{51}/C_{55} - C_{61}/C_{66} + 1\} .
\end{aligned} \tag{A14}$$

These equations are used to calculate electron and proton transfer rates, and thus proton pumping efficiencies, as follows: It is assumed that every electron transfer to dioxygen leads to the translocation of a single charge in addition to any charge translocation due to proton pumping, since the protons consumed in dioxygen reduction originate in the matrix and the electrons originate in cytochrome c on

the cytosol side of the membrane. Defining the proton/electron flow ratio as

$$R = k_{H^+} / k_{e^-}, \quad (A15)$$

the overall efficiency of free energy transduction (η) is given by

$$\eta = \frac{(\Delta\tilde{\mu}_{H^+}) (1 + R)}{\Delta G_{e^-}}, \quad (A16)$$

where $\Delta\tilde{\mu}_{H^+}$ is the proton electrochemical potential across the membrane, and ΔG_{e^-} is the free energy available per electron transferred. This equation assumes that the consumption of an electron from the cytosol and a proton from the matrix is energetically equivalent to translocating a proton from the matrix to the cytosol; this will be true if the buffering capacity of the cytosol is large.

FOOTNOTES

¹Abbreviations and symbols used in this chapter: $\Delta\tilde{\mu}_H^+$, Transmembrane proton electrochemical potential; Δp , protonmotive force; Fe_c , the iron of cytochrome c; m-side, side of the mitochondrial inner membrane facing the matrix of the mitochondrion; c-side, side of the mitochondrial inner membrane facing the outer membrane; H^+/e^- , ratio of number of protons pumped to number of electrons transferred.

²A complete channel structure may not be necessary on the output side of the model pump since there is some evidence suggesting that Cu_A is located near the c-side surface of the enzyme (72).

³In the four-state paradigm, the change in the proton affinity of the site upon oxidoreduction must exactly equal the change in electron affinity upon protonation/deprotonation. This is because the four states form a closed thermodynamic cycle and standard free energy changes must be conserved around the cycle. For the more complex model presently under consideration, the same energy conservation argument holds; however, additional conformational change reactions are present in the cycle. This has the effect of eliminating the necessary correlation between reduction potential changes and pK_a changes since the total of the standard free energy changes for the two conformational change reactions will in general be nonzero.

⁴There are also additional "uncoupling" reactions which are energetically unfavored relative to the corresponding "coupling" reactions. We have not considered these because they are not likely to occur at significant rates.

⁵Mechanisms for the gating of protons also operate at other steps in the model pump catalytic cycle. An example is the deprotonation of the tyrosine side chain in state B. As previously discussed, the hydroxyl group proton must transfer to the cysteine group ("coupling" reaction), not to the m-side channel ("uncoupling" reaction).

⁶Under conditions where the reorganizational energy is large compared to the net free energy change for the reaction (52, 17).

⁷Whether a driving force this small is adequate to achieve the desired rate depends on several previously discussed properties of the system, primarily the reorganizational energy of the electron transfer partners, the distance separating them, and the structure of the intervening

medium. The approximate intersite distances for cytochrome oxidase electron transfers have been estimated at 13-15 Å [center to center] (73). The edge to edge distance relevant to electron transfer rates may be 5 Å or more lower. Little is known about the intervening medium or the reorganizational energies for these electron transfer processes. A comparison might be made to the work of Kostić, et al. (74), who measured a rate of 2 s^{-1} for an intramolecular electron transfer process in a ruthenated azurin species having a somewhat larger driving force (240 mV) and an equal or smaller intersite distance (11.8 Å, edge to edge). The two orders of magnitude difference between the rate measured in the azurin derivative and that needed in oxidase is not a significant discrepancy when one considers the extreme sensitivity of the rates to minor changes in the distance and reorganizational energy parameters. It should also be noted that electron transfer in the [artificial] ruthenium-azurin complex occurs through a portion of the protein selected by happenstance; in contrast, the medium between Cu_A and its electron transfer partners might be specialized [e.g. by the presence of appropriately oriented aromatic groups (55)] for rapid electron transfer.

$\text{pK}_a(\text{cys}, r)$ is only relevant to the production of a state which is the deprotonated form of state C in Fig. 2. This state is not considered in the analysis because it will not be significantly populated since $\text{pK}_a(\text{cys}, r)$ is large and the cysteine group in state C is in contact with the c-side channel where $\tilde{\mu}_H^+$ is high. $\text{pK}_a(\text{cys}, o)$ is relevant to the deprotonation of state D. In the pump mechanism (Fig. 2), the conversion of state D to state E includes both the deprotonation of state D to the c-side (which is very energetically unfavorable since $\text{pK}_a(\text{cys}, o) = 10$ and the c-side pH is 7) and the (energetically favorable) conversion of the Cu^{2+} ion from the distorted trigonal to the distorted tetrahedral structure. Since the states A through E of Fig. 5 form a closed cycle, the equilibrium constant for the conversion of D to E is not independent of the previously defined parameters but can be calculated from E_H' , E_I' , $\text{pK}_a(\text{tyr}, o)$, and $K_{P,t}$, which are related to the equilibrium constants for the other four reactions in the cycle. The pK_a for the reaction $\text{D} \rightleftharpoons \text{E} + \text{H}^+$ is given by $\text{pK}_a(\text{tyr}, o) - (E_H' - E_I')/60 \text{ mV} + \log_{10}(K_{P,t})$. The value of this quantity is 6.2 when the pump parameters have the values given in Table I; this implies that conversion of state D to state E by deprotonation to the c-side (pH 7) is energetically favorable.

REFERENCES

1. Mitchell, P. (1976) Biochem. Soc. Trans. 4, 399-430.
2. Wikström, M., Saraste, M. (1984) in Bioenergetics (Ernster, Ed.) pp. 49-94, Elsevier, Amsterdam.
3. Wikström, M., Krab, K., Saraste, M. (1981) Annu. Rev. Biochem. 50, 623-655.
4. Wikström, M. (1984) Nature 308, 558-560.
5. Wikström, M., Krab, K. (1979) Biochim. Biophys. Acta 549, 177-222.
6. Blair, D.F., Martin, C.T., Gelles, J., Wang, H., Brudvig, G.W., Stevens, T.H., Chan, S.I. (1983) Chemica Scripta 21, 43-53.
7. Wikström, M., Krab, K., Saraste, M. (1981) Cytochrome Oxidase: A Synthesis, Academic Press, London.
8. Malmström, B.G. (1980) in Metal Ion Activation of Dioxygen (Spiro, T.G., Ed.) pp. 181-207, Wiley, New York.
9. Krab, K., Wikström, M. (1978) Biochim. Biophys. Acta 504, 200-214.
10. Casey, R.P., Chappell, J.B., Azzi, A. (1979) Biochem. J. 182, 149-156.
11. Proteau, G., Wrigglesworth, J.M., Nicholls, P. (1983) Biochem. J. 210, 199-205.
12. Sarti, P., Jones, M.G., Antonini, G., Malatesta, F., Colosimo, A., Wilson, M.T., Brunori, M. (1985) Proc. Natl. Acad. Sci. U.S.A. 82, 4876-4880.
13. Thelen, M., O'Shea, P.S., Azzi, A. (1985) Biochem. J. 227, 163-167.
14. Jencks, W.P. (1980) Adv. Enzymol. 51, 75-106.
15. Tanford, C. (1983) Annu. Rev. Biochem. 52, 379-409.
16. Devault, D. (1971) Biochim. Biophys. Acta 225, 193-199.

17. Blair, D.F., Gelles, J., Chan, S.I. (1986) Biophys. J. in press.
18. Wikström, M. (1986) Curr. Top. Membr. Transp. 16, 303-321.
19. Chan, S.I., Bocian, D.F., Brudvig, G.W., Morse, R.H., Stevens, T.H. (1979) in Cytochrome Oxidase (King, T.E., et al., Eds.) pp. 177-188, Elsevier/North-Holland Biomedical Press, Amsterdam.
20. Babcock, G.T., Callahan, P.M. (1983) Biochemistry 22, 2314-2319.
21. Malmström, B.G. (1985) Biochim. Biophys. Acta 811, 1-12.
22. Rottenberg, H. (1979) Meth. Enzymol. 55, 547-569.
23. Ottolenghi, M. (1980) Adv. Photochem. 12, 97-200.
24. Wikstrom, M., Krab, K. (1980) Curr. Top. Bioenerg. 10, 51-101.
25. Wikström, M., Krab, K. (1978) in Energy Conservation in Biological Membranes, 29. Mosbach Colloquium (Schafer, G. & Klingenberg, M., eds.) pp. 128-139, Springer-Verlag: Berlin.
26. Mitchell, P. (1979) Eur. J. Biochem. 95, 1-20.
27. Nagle, J.F., Morowitz, H.J. (1978) Proc. Natl. Acad. Sci. U.S.A. 75, 298-302.
28. Nagle, J.F., Mille, M.M., Morowitz, H.J. (1980) J. Chem. Phys. 72, 3959-3971.
29. Scheiner, S. (1985) Accts. Chem. Res. 18, 174.
30. Wikstrom, M., Casey, R.P. (1985) J. Inorg. Biochem. 23, 327-334.
31. van Gelder, B.F., van Rijn, J.L.M.L., Schilder, G.J.A., Wilms, J. (1977) in Structure and Function of Energy Transducing Membranes (van Dam, K. and van Gelder, B.F., eds.) pp. 61-68, Elsevier/North Holland (Amsterdam).
32. Ellis, W.R., Wang, H., Blair, D.F., Gray, H.B., Chan, S.I. (1986) Biochemistry 25, 161-167.

33. Blair, D.F., Ellis, W.R., Wang, H., Gray, H.B., Chan, S.I. (1986) J. Biol. Chem. in press.
34. Li, P.M., Nilsson, T., Martin, C.T., Gelles, J., Blair, D.F., Morgan, J.E., Wang, H., Witt, S.N., Manthey, J., Chan, S.I. (1986) manuscript in preparation.
35. Antalis, T.M., Palmer, G. (1982) J. Biol. Chem. 257, 6194-6206.
36. Halaka, F.G., Barnes, Z.K., Babcock, G.T., Dye, J.L. (1984) Biochemistry 23, 2005-2011.
37. Greenwood, C., Brittain, T., Wilson, M., Brunori, M. (1976) Biochem. J. 157, 591-598.
38. Wilson, M.T., Greenwood, C., Brunori, M., Antonini, E. (1975) Biochem. J. 147, 145-153.
39. Dutton, P.L., Wilson, D.F., Lee, C-P. (1970) Biochemistry 9, 5077-5082.
40. Wang, H., Blair, D.F., Ellis, W.R., Gray, H.B., Chan, S.I. (1986) Biochemistry 25, 167-171.
41. Clore, G.M., Andréasson, L-E., Karlsson, B., Aasa, R., Malmström, B.G. (1980) Biochem. J. 185, 139-154.
42. Blair, D.F., Witt, S.N., Chan, S.I. (1985) J. Am. Chem. Soc. 107, 7389-7399.
43. Gelles, J., Chan, S.I. (1985) Biochemistry 24, 3963-3972.
44. Pietrobon, D., Azzone, G.F., Walz, D. (1981) Eur. J. Biochem. 117, 389-394.
45. Azzone, G.F., Zoratti, M., Petronilli, V., Pietrobon, D. (1985) J. Inorg. Biochem. 23, 349-356.
46. Martin, C.T., Scholes, C.P., Chan, S.I. (1986) manuscript in preparation.
47. Gray, H.B., Solomon, E.I. (1981) in Metal Ions in Biology (Spiro, T.G., Ed.). Wiley, New York. Vol. 3, 1-39.
48. Freund, F. (1981) Trends Biochem. Sci. 6, 142-145.

49. Kristof, W., Zundel, G. (1980) Biopolymers 19, 1753-1769.
50. Bartmess, J.T., McIver, R.T. (1979) in Gas Phase Ion Chemistry (M.T. Bowers, Ed.) Vol. 2, pp. 87-121, Academic: New York.
51. Mitchell, P. (1969) Exp. Theor. Biophys. 2, 159-216.
52. Marcus, R.A., Sutin, N. (1985) Biochim. Biophys. Acta 811, 265-322.
53. Hopfield, J.J. (1974) Proc. Natl. Acad. Sci. U.S.A. 71, 3640-3644.
54. Beratan, D.N., Hopfield, J.J. (1984) J. Am. Chem. Soc. 106, 1584-1594.
55. Scott, R.A., Mauk, A.G., Gray, H.B. (1985) J. Chem. Educ. 62, 932-938.
56. Guarr, T., McLendon, G. (1985) Coord. Chem. Rev. 68, 1-52.
57. Mayo, S.L., Ellis, W.R., Crutchley, R.J., Gray, H.B. (1986) Science in press.
58. Gray, H.B. (1986) Coord. Chem. Rev. in press.
59. Gray, H.B., Malmström, B.G. (1983) Comments Inorg. Chem. 2, 203-209.
60. Hanzlik, R.P. (1976) Inorganic aspects of biological and organic chemistry, Academic Press, New York.
61. Freeman, H.C. (1980) in Proc. XXI. Int. Conf. Coord. Chem (Lament, J.P., ed.) 29-51.
62. Addison, A.W. (1983) in Copper Coordination Chemistry: Biochemical & Inorganic Perspectives (Karlin, K.D. and Zubieta, J., Eds.) pp. 109-128, Adenine Press, Guilderland, New York.
63. Dutton, P.L. (1978) Meth. Enzymol. 54, 411-435.
64. Branca, D., Ferguson, S.J., Sorgato, M.C. (1981) Eur. J. Biochem. 116, 341-346.
65. Stucki, J.W. (1978) in Energy Conservation in Biological Membranes, 29. Mosbach Colloquium

(Schafer, G. and Klingenberg, M., Eds.) pp. 264-287, Springer-Verlag, Berlin.

66. Hunter, D.R., Capaldi, R.A. (1974) Biochem. Biophys. Res. Comm. 56, 623-628.
67. Blair, D.F., Gelles, J., Chan, S.I. (1986) manuscript in preparation.
68. Stevens, T.H., Martin, C.T., Wang, H., Brudvig, G.W., Scholes, C.P., Chan, S.I. (1982) J. Biol. Chem. 257, 12106-12113.
69. Martin, C.T. (1985) PhD. Thesis, California Institute of Technology, Pasadena, California.
70. Hu, V.W., Chan, S.I., Brown, G.S. (1977) Proc. Natl. Acad. Sci. U.S.A. 74, 3821-3825.
71. Powers, L., Chance, B., Ching, Y., Angiolillo, P. (1981) Biophys. J. 34, 465-498.
72. Millett, F., deJong, C., Paulson, L., Capaldi, R.A. (1983) Biochemistry 22, 546-552.
73. Brudvig, G.W., Blair, D.F., Chan, S.I. (1984) J. Biol. Chem. 259, 11001-11009.
74. Kostić, N.M., Margalit, R., Che, C-M., Gray, H.B. (1983) J. Am. Chem. Soc. 105, 7765-7767.

Chapter IV

Cu_A and Energy Transduction in Cytochrome c Oxidase

The work described in the preceding chapters, taken together with other recently published studies, supports several new conceptions about the functional role of the Cu_A site in cytochrome c oxidase. It is apparent that this center may play a primary role in proton pumping by the enzyme, and that its function in intramolecular electron transfer processes may be different from that previously proposed. In this chapter, I summarize the conclusions that have led to this reevaluation of the functional role of Cu_A . I also discuss the significance of results from Chapter II which form the basis of a new approach to studying the role of Cu_A in energy transduction by cytochrome oxidase. We have begun three experimental programs based on this method, and I summarize the goals, experimental design, and progress of these studies. I conclude the chapter by considering the physiological significance of these new conceptions about the role of Cu_A in energy transduction by cytochrome oxidase.

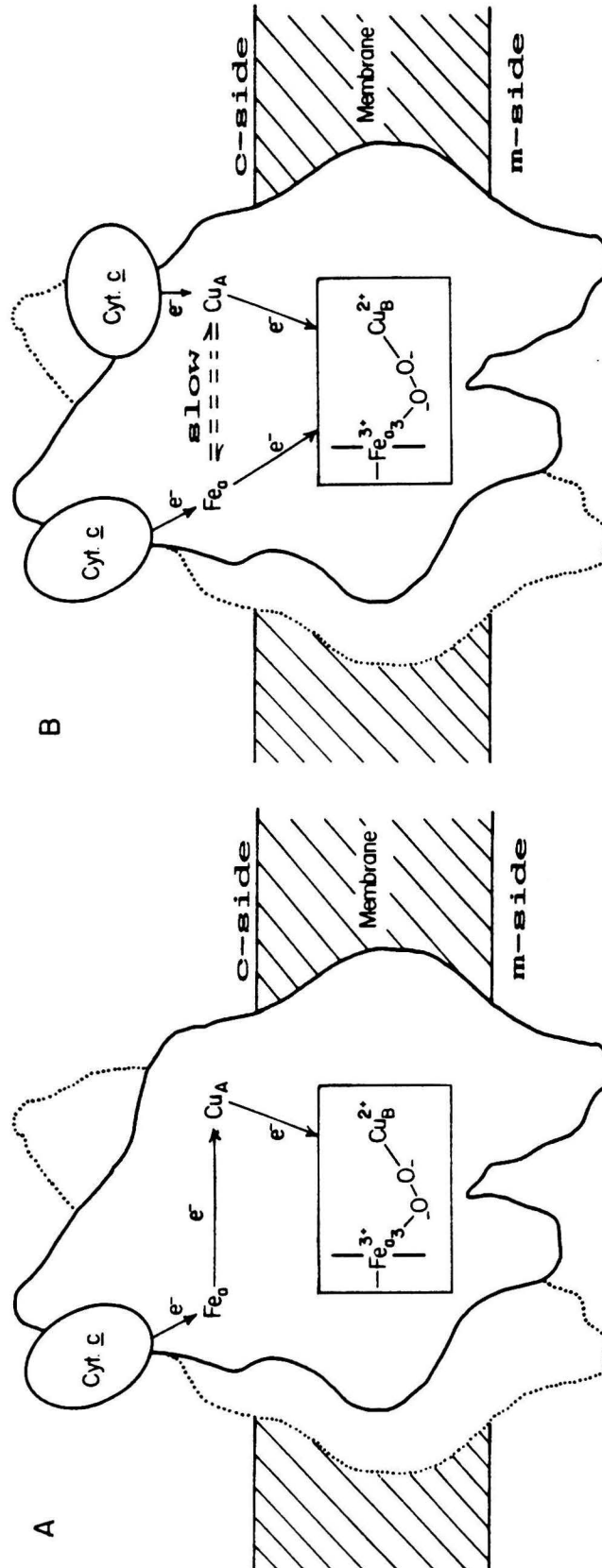
SUMMARY: RESULTS LEADING TO A REEVALUATION
OF THE ROLE OF Cu_A IN CYTOCHROME OXIDASE ENERGY TRANSDUCTION

Parallel electron transfer pathways. The locations and temporal sequences of intramolecular electron transfers in cytochrome oxidase have been the subject of controversy for more than twenty years (1, 2, 3). Electrons transferred to oxidase by cytochrome c rapidly reduce Fe_a and Cu_A . After subsequent electron transfer reactions, the electrons ultimately reach the oxygen binding site "electron sink." The early kinetic studies of the fast electron transfer reactions in cytochrome oxidase (4, 5) were interpreted in terms of a model (Fig. 1A) in which Fe_a and Cu_A are linked in series to comprise a pathway for electrons travelling from the heme of cytochrome c (Fe_c)¹ to $\text{Fe}_{a_3}/\text{Cu}_B$. In this view, which is still widely accepted (2, 1), Cu_A serves as an electron transfer mediator which facilitates movement of electrons from Fe_a near the cytochrome c binding site to $\text{Fe}_{a_3}/\text{Cu}_B$ at the O_2 binding site. However, because reduction and reoxidation of Fe_a and Cu_A take place concurrently and with similar rates, the interpretation of the kinetic data upon which this conclusion is based is ambiguous, and alternative models have been proposed (3).

Recent studies using two different experimental

Figure 1

Two models of the intramolecular electron transfer pathways in a cytochrome c-cytochrome oxidase complex. A: Sequential pathway model (1, 2). B: Parallel pathway model based on recent research results (see text).



approaches have supported a new interpretation of the fast kinetic data. In the new model (Fig. 1B) there are parallel electron transfer pathways from both Fe_a and Cu_A to $\text{Fe}_{a_3}/\text{Cu}_B$. One of the studies (6) is that described in Chapter II. This work demonstrates that, at least in the sodium *p*-hydroxymercuri-benzoate (pHMB)-modified enzyme, there is an electron transfer pathway between Fe_a and $\text{Fe}_{a_3}/\text{Cu}_B$ which does not involve oxidoreduction of Cu_A . If this pathway is present in the native enzyme as well, the model of Fig. 1A is clearly incomplete. The data of Chapter II show that the turnover of the pHMB-modified enzyme (involving direct Fe_a -to- $\text{Fe}_{a_3}/\text{Cu}_B$ electron transfer) occurs at about one-fifth the rate of that in the native enzyme. One possible interpretation of this observation is that the Fe_a -to- $\text{Fe}_{a_3}/\text{Cu}_B$ pathway being observed is the dominant pathway of electron transfer to the O_2 binding site in the native enzyme but that enzyme turnover is slowed by the pHMB treatment. An alternative interpretation is that the Cu_A -to- $\text{Fe}_{a_3}/\text{Cu}_B$ pathway is the major one in the native enzyme, accounting for as much as four-fifths of the electron flux to $\text{Fe}_{a_3}/\text{Cu}_B$, so that when this pathway is inhibited by the chemical modification of Cu_A only about one-fifth of the flux remains. [This analysis assumes that electron transfer to the O_2 binding site is the rate limiting step in the electron transfer pathway under the

conditions in which the measurements are made (7, 8).]

In a second type of study which has provided support for the model of Fig. 1B, reaction intermediates of the enzyme are trapped and the kinetics of electron transfer processes are monitored at cryogenic temperatures (9, 8). These studies show that, at least at low temperatures, both Fe_a and Cu_A are sources for a significant fraction of the electron transfers to $\text{Fe}_{a_3}/\text{Cu}_B$. Furthermore, they provide strong support to the second interpretation of the pHMB-modification work described above by demonstrating that the fraction of transfers to $\text{Fe}_{a_3}/\text{Cu}_B$ occurring via Fe_a is a minority (about 30% of the total) and that this fraction is independent of temperature over a fairly wide range (8). The conclusions that the enzyme has parallel electron transfer pathways to $\text{Fe}_{a_3}/\text{Cu}_B$ and that the Cu_A pathway is the predominant one both have major importance to understanding the mechanism of energy transduction in cytochrome oxidase, as is discussed further at the end of this chapter.

A related issue is the identification of electron transfer pathway(s) for the reduction of Fe_a and Cu_A by ferrocyanide C . As schematized in Fig. 1A, the traditional view has been that Fe_a (and only Fe_a) is the immediate electron acceptor from cytochrome C . The

experimental evidence supporting this view is concisely summarized by Brunori, et al. (1). The data of Chapter II which show that electron transfer between cytochrome c and Fe_a can occur without the involvement of Cu_A are consistent with this view. As is the case with electron transfers to $\text{Fe}_{a_3}/\text{Cu}_B$, recent data suggest that single pathway schemes may be inadequate to account for the observed properties of the system. Although it is well established that both Fe_a and Cu_A are reduced very rapidly upon mixing of an oxidase preparation with reductants (7), it is becoming apparent that electron transfer between Fe_a and Cu_A may be too slow to account for this reaction (10, 11). If this is the case, it is likely that there are independent pathways for reduction of Fe_a and Cu_A by cytochrome c, possibly involving separate cytochrome c binding sites. These results are particularly interesting because they suggest a mechanism for metabolic control of the efficiency of cytochrome oxidase energy transduction (discussed at the end of this chapter).

Evidence suggesting that Cu_A is the redox center associated with the cytochrome oxidase proton pump. The experiments of Wikström and Casey (12) suggest that the cytochrome oxidase proton pump is most likely associated with either Fe_a or Cu_A . Even prior to the publication of

these studies, it had been forcefully argued that Fe_a is the most plausible candidate of the four metal centers in oxidase to be associated with the proton pump. Wikström and colleagues presented a three-point rationale in support of this position (13, 3): 1) The oxidoreduction of Fe_a displays kinetic heterogeneity, and this is consistent with the presence of an equilibrium between two structures of the metal center with different electron transfer rates and different reduction potentials (14); 2) Fe_a has a strongly pH-dependent reduction potential; 3) Both the pH-dependence of the Fe_a reduction potential and the proton pumping activity of the enzyme are abolished by a treatment which removes subunit III of the enzyme; this subunit is thought to contain a proton channel which serves to transport H⁺ to the pump from the m-side of the membrane (15).

Further analysis and new experimental data, however, show that none of these three points are valid reasons for preferring Fe_a over Cu_A as the proton pumping site. The reasoning of the first point is equally applicable to Cu_A -- as Wikström et al. themselves point out, the "kinetic heterogeneity [displayed by Fe_a] is also 'mirrored' in the behavior of Cu_A..." (3). It is this strong similarity in the redox kinetics of the two sites which is responsible for past difficulties in distinguishing between the various

models of the intramolecular electron transfer pathways discussed in the previous section. As noted in Chapter III, the second point is contradicted by data from recent studies (16) which show only a minor pH dependence of the reduction potential of Fe_a . The third point is also undermined by recent experimental results. In contrast to the conclusions of earlier studies (15, 17), it has now been conclusively shown that oxidase preparations which lack subunit III can pump protons (18, 19, 20, 21). Subunit III is therefore unlikely to contain the proton-transport channel(s) or any component essential for the operation of the proton pump. Consequently, it is unclear whether the observed change in the pH-dependence of the Fe_a reduction potential upon subunit III depletion (15) has any relevance to a role for this site in proton pumping.

In Chapter III, we proposed a model for the cytochrome c proton pump based on Cu_A . The analysis of this model demonstrated that it is a clear counter-example to the presumption [e.g., (3)] that an electron transfer driven proton pump must exhibit a strongly pH-dependent midpoint potential. Furthermore, that chapter contains a quantitative analysis of the turnover rate and free energy transduction efficiency of the model pump which demonstrates its plausibility as a mechanism for the cytochrome oxidase

proton pump. None of the mechanisms based on Fe_a which have been proposed for the cytochrome oxidase proton pump (22, 3, 23) have been sufficiently complete to permit an analysis of their performance. It may be that the formulation of a complete pumping mechanism involving Fe_a represents a more formidable task than was the case for the Cu_A model because of the heme cofactor's comparatively limited repertoire of chemical reactivity.

As has been previously discussed, the number of protons pumped by cytochrome oxidase per electron transferred to O_2 (H^+/e^-) can approach unity in measurements on purified oxidase reconstituted into artificial lipid vesicles (24). If, as suggested above, the electron transfer pathways through Fe_a and Cu_A are independent, with the Cu_A pathway accounting for 20-30% of the total, the number of protons pumped per electron transferred through the pump site would be close to 1 if the pump site is Cu_A but 3-5 if it is Fe_a . The pumping of 3 or more protons in one electron transfer step would make such a step have a positive free energy change since under typical conditions there is only enough energy released by electron transfer from $\text{Fe}_c^{3+}/\text{Fe}_c^{2+}$ to $\text{O}_2/\text{H}_2\text{O}$ to translocate a maximum of 1.75 protons [not including the proton consumed in O_2 reduction] (25). The presence of such a strongly endoergonic step in the oxidase

turnover cycle, while not thermodynamically infeasible, would probably make the turnover process unacceptably slow. This consideration therefore favors Cu_A over Fe_a as the site of the cytochrome oxidase proton pump since proton pumping involving that center would be directly coupled to a larger fraction of the total number of electron transfers to $\text{Fe}_{a_3}/\text{Cu}_B$ and hence to a larger fraction of the available free energy.

THE FURTHER STUDY OF THE ROLE OF Cu_A
IN ENERGY TRANSDUCTION BY CYTOCHROME OXIDASE:

A. A Methodological Foundation.

Near the end of the last chapter of their comprehensive book about cytochrome oxidase, published five years ago, Wikström et al. (3) commented, " Cu_A is the most enigmatic redox center of the enzyme... no special function apart from that of a simple carrier of electrons has been obvious." It is clear that some of the reasons for the lack of information about this site are the experimental difficulties attendant to its study. Unlike Fe_a and Fe_{a_3} , Cu_A has only a weak optical absorption in its oxidized form and no known absorption in its reduced form. Much of the extensive characterization of the structure and chemistry of the $\text{Fe}_{a_3}/\text{Cu}_B$ site has been possible because of the ease with which the experimenter can introduce inhibitors (e.g., CO, NO, CN^- , N_3^-) which bind to and perturb the functioning of the site. For the case of Cu_A (and Fe_a), in contrast, the only means to chemically alter the site without destroying the enzyme structure (aside from one-electron oxidoreduction reactions) have been isotopic substitutions of ligand atoms [reviewed in (26)]. Although these alterations have been valuable tools in studying the structure of the site, they have not facilitated direct studies of the catalytic role of

Cu_A because they do not induce perturbations of the site's function or chemical reactivity.

The pHMB-modification reaction described in Chapter II chemically perturbs the Cu_A site and alters its electron transfer properties without significantly affecting the structures of the other enzyme metal centers. As described in the preceding sections of this chapter, this reaction has already helped to elucidate the intramolecular electron transfer pathways in cytochrome oxidase. However, the greatest significance of the pHMB-modification reaction may be its value as a tool in future experiments: it can be used directly study the role of Cu_A in the mechanism of free energy transduction by cytochrome oxidase. We have recently undertaken several such studies; I now summarize the goals of these projects and the progress that has been made in achieving them.

THE FURTHER STUDY OF THE ROLE OF Cu_A
IN ENERGY TRANSDUCTION BY CYTOCHROME OXIDASE:

B. Research in Progress.

Structural analysis of Cu_A^+ via x-ray spectroscopy of a Cu_A -depleted enzyme preparation. Both Cu_A and Cu_B are tightly bound to cytochrome oxidase and cannot be removed by treating the enzyme with chelators like EDTA or 1,10-phenanthroline derivatives except under denaturing conditions. Wharton and co-workers have reported removal of copper under conditions involving extremes of pH and chelator concentration [0.1 M bathocuproine sulfonate at pH 4.7 or 1 M KCN at pH 10] but such treatments result in major changes in the heme optical and EPR spectra and in loss of enzymatic activity (27, 28).

We recently postulated that the pHMB modification reaction described in Chapter II might be exploited to render Cu_A more susceptible to removal from the enzyme by chelators under mild conditions which would preserve the structure and function of the other metal center sites. We observe that treatment of the pHMB-modified enzyme with EDTA under conditions where the native enzyme is unaffected lead to conversion of most of the modified copper EPR signal to one resembling the spectrum of Cu^{2+} EDTA complexes. Removal

of small solutes from this sample by dialysis caused the loss of a majority of EPR-visible Cu^{+2} as assessed by double-integration of the 77K EPR spectrum. Work is currently in progress to increase the amount of Cu^{+2} removed by this treatment and to assess the structural and functional integrity of the other metal center sites in this preparation.

If the approach outlined above succeeds in the preparation of an enzyme derivative similar in properties to the pHMB-modified enzyme described in Chapter II but with Cu_A completely removed instead of merely chemically changed, we anticipate that such a derivative would be of great value in further studies of the functional role of Cu_A . In particular, it would provide an experimental method by which to test a major prediction of the proton pumping model of Chapter III. An important feature of the proposed pumping mechanism is that a reversible, redox-linked ligand substitution reaction occurs in such a way that the stable reduced form of Cu_A has different ligands from the stable oxidized form. As discussed in Chapter III, evidence for or against this change is difficult to obtain because of the scarcity of spectroscopic probes of the Cu_A^+ site. In principle, extended x-ray absorption fine structure (EXAFS) spectra of the enzyme would contain the information about a

change in ligation, especially if this change involves a change in the total number of sulfur atoms ligated to Cu (29). In practice, however, Cu EXAFS on cytochrome oxidase has revealed little more than mean copper-ligand distances and a limited amount of information about the types of copper ligands present (29, 30). Much of the difficulty in the interpretation of the data arises from the need to distinguish between the spectral contributions of Cu_A and Cu_B. In an attempt to deconvolute the spectral features of Cu_A and Cu_B, Powers et al. (31) assumed that the copper of stellacyanin was structurally similar to Cu_B and subtracted the EXAFS spectrum of this protein from that of cytochrome oxidase. The resulting difference was assumed to represent the EXAFS spectrum of Cu_A. Although such an approach is valid if Cu_B can be shown to resemble the Cu site of stellacyanin, its application in this case is questionable in view of the chemical and spectroscopic dissimilarities between stellacyanin [or any other blue copper protein] and Cu_B (32, 33).

EXAFS analysis of a Cu_A-depleted cytochrome oxidase preparation might be of great value in obtaining information about the ligation structures of Cu_A and Cu_B in cytochrome oxidase. If the spectroscopic and chemical properties of the Cu_B site are unaffected by the removal of Cu_A (as they

are apparently unaffected by the pHMB-modification of the Cu_A structure), the EXAFS spectra of the oxidized and reduced Cu_A -depleted enzyme would provide a great deal more information about the ligation structure of Cu_B in both oxidation states than studies on the native enzyme owing to the absence of the interfering Cu_A EXAFS. This experiment should readily reveal whether or not Cu_B has any sulfur ligands, which is at present a controversial issue (29). Of even greater potential value, however, is the information which this experiment might provide about the structure of Cu_A , particularly concerning the change of ligation upon oxidoreduction which is predicted by the proton pumping model of Chapter III. Subtraction of the spectra of oxidized and reduced Cu_A -depleted enzyme from those of oxidized and reduced native oxidase, respectively, should yield data on the Cu_A^{+1} and Cu_A^{+2} structures which are expected to be considerably more reliable than any previously obtained. We have already performed some preliminary x-ray absorption studies on partially Cu_A -depleted samples and are currently refining the depletion technique.

Proton pumping measurements on the pHMB-modified enzyme.

As discussed earlier, both the conclusion that Cu_A (and not Fe_a) lies on the major intramolecular electron transfer

pathway within cytochrome oxidase and the analysis of the pump model of Chapter III support the hypothesis that Cu_A is the redox center associated with the proton pump. If this hypothesis is correct, it is clear that the pHMB-modified enzyme should not pump protons since the structure of the Cu_A is disrupted and electron transfer from cytochrome c to O_2 through Cu_A is blocked in this preparation (Chapter II).

More than a year ago, we began a project to test whether the pHMB-modified oxidase contains a functional proton pump, and we have made significant progress toward answering that question. The experimental design is adopted from that used by several other laboratories for measurements of the proton pumping activity of cytochrome oxidase preparations. The method (34) requires that the purified oxidase preparation be reconstituted into sealed unilamellar phospholipid vesicles in such a way that the interior compartments of the vesicles are strongly buffered and the exterior compartment has little buffer (Fig. 2A). H^+/e^- can then be measured in this system by adding a known amount of ferrocycytochrome c and observing the ejection of protons from the vesicles by electrochemically monitoring the pH of the extravesicular medium. If only a small amount of ferrocycytochrome c is added (e.g., a ten-fold molar excess over the oxidase), the extravesicular acidification resulting from proton ejection

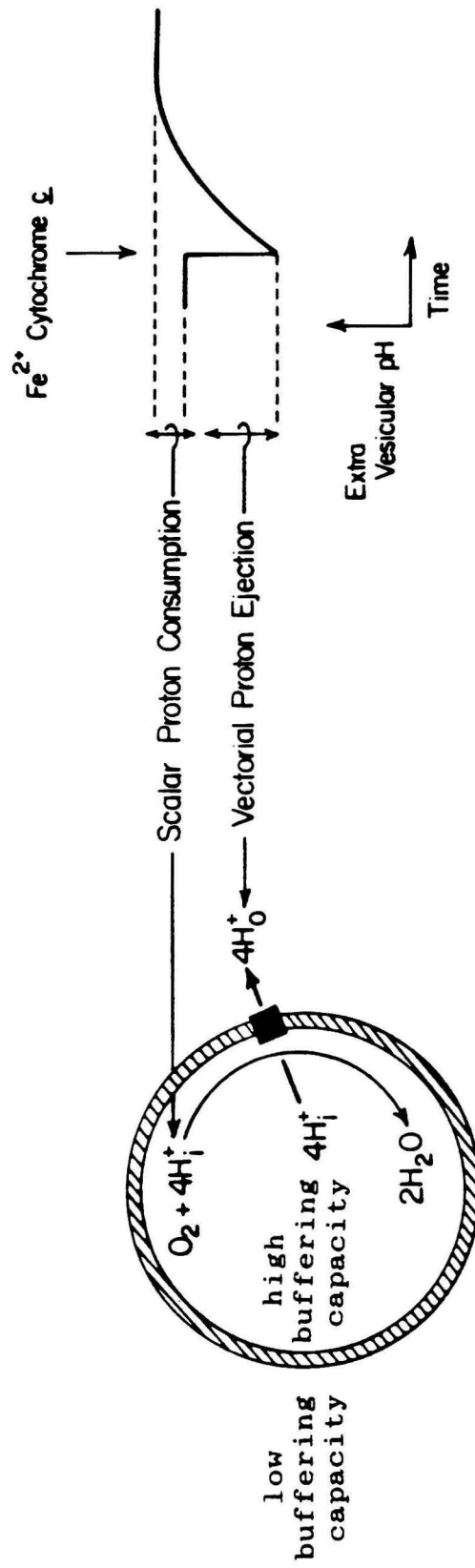
is complete in a short time (typically less than 1 s). This acidification transient is followed by a slow extravesicular alkalization caused by leakage of protons across the vesicle membranes driven by the transmembrane proton electrochemical potential gradient ($\Delta\tilde{\mu}_{\text{H}^+}$) generated by the oxidase turnover (Fig. 2B).

In order to accurately determine H^+/e^- by measuring the magnitude of the fast acidification phase, the rate of proton leakage must be sufficiently slow that the acidification and alkalization phases can be reliably measured. The preparation of well-sealed [i.e., proton impermeable] vesicles is therefore a prerequisite for a successful proton pumping measurement.

The vesicle preparation must also be almost completely free of oxidase molecules that have both the cytochrome c binding site(s) and the O_2 reduction site exposed to the extravesicular phase. In the mitochondrion, the former always face the c-side of the membrane and the latter faces the m-side. Structures with the incorrect topology (all sites facing the extravesicular phase) will be present in the vesicle preparation if it contains molecules that are not incorporated in membranes, that are incorporated in unsealed membranes, or that are bound to the surface of

Figure 2

An experiment to measure the proton pumping activity of cytochrome oxidase. Left: A schematic diagram of an phospholipid vesicle (hatched) with an incorporated cytochrome oxidase molecule (black square). The reactions shown in the diagram represent the proton pumping and oxygen reduction processes which take place when 4 equiv. of ferrocytochrome c are added to the extravesicular compartment. Subscripts i and o refer to protons inside and outside the vesicle, respectively. Right: Changes in the pH of the extravesicular compartment induced by addition of ferrocytochrome c. The rapid acidification upon addition of the cytochrome c is caused by ejection of protons from the vesicles by the pumping reaction. The slow alkalization is caused by diffusion of protons into the vesicle interior to partially replace those removed by the pumping and O_2 reduction reactions. The pH change induced by the scalar proton consumption is smaller than that induced by the vectorial proton ejection because the former reaction is buffered by the entire buffering capacity of the system while the latter is buffered only by the extravesicular buffering capacity.



membranes rather than inserted through them in the biologically appropriate fashion. Fig. 3 illustrates the way that the presence of these improperly reconstituted enzyme molecules will affect the proton pumping measurement. Curve A (identical to the curve in Fig. 2B) shows the transient acidification followed by slow alkalization expected from a system reconstituted with the correct topology. Note that the pH after the final equilibrium is attained is higher than the starting pH due to consumption of H^+ from the interior of the vesicles by the $4e^- + 4H^+ + O_2 \rightleftharpoons 2H_2O$ half-cell reaction. Curve E shows the behavior expected if, for example, all of the oxidase molecules are bound to vesicle exterior surfaces instead of properly inserted through the vesicle membranes. In this case, the initial alkalization transient is due to proton consumption by the O_2 -reduction half-cell reaction catalyzed by the oxidase molecules on the exterior of the vesicles. The subsequent slow acidification results from leakage of H^+ out of the vesicles to restore the pH equilibrium between the intravesicular and extravesicular compartments. If the preparation contains a mixture of correctly reconstituted and improperly reconstituted oxidase molecules, the observed pH-time curves (Fig. 2, curves B, C, and D) will be an appropriately weighted sum of the curves of the pure species (curves A and E). The important feature

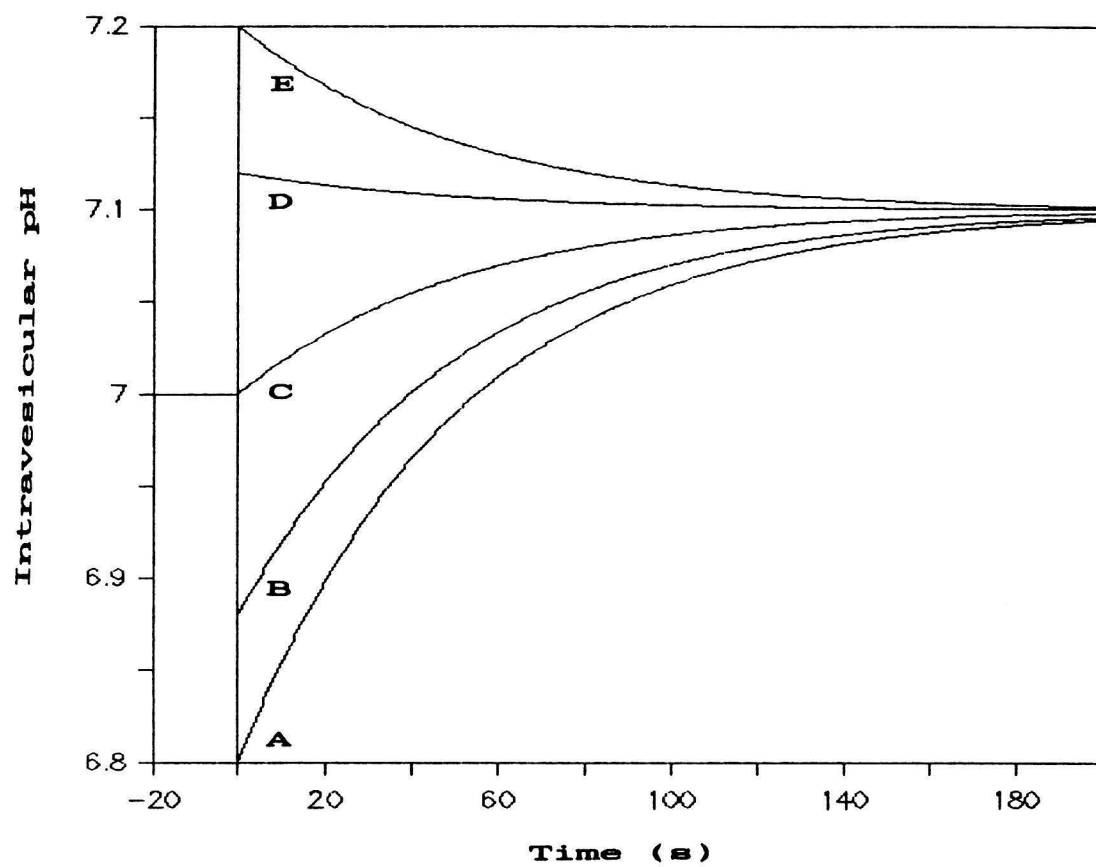
of this behavior is that, in the case where there is a small amount of unreconstituted enzyme (curve B), the curve has the same form as that from a properly reconstituted preparation, but the acidification has a smaller magnitude and this would result in underestimation of H^+/e^- .

Before the H^+/e^- measurement is performed on a vesicle-reconstituted oxidase preparation, it is useful to make a measurement of the respiratory control ratio (RCR) to help determine whether the reconstitution was successful. The RCR is the ratio of steady-state electron transfer rates of the preparation in the presence and absence of uncouplers (protonophores). When uncouplers are not present, electron transfer is substantially inhibited by the $\Delta\tilde{\mu}_H^+$ across the vesicle membranes. The inhibition does not occur, however when both the chemical and electrical components of $\Delta\tilde{\mu}_H^+$ are collapsed by the addition of uncouplers to the vesicle preparation (35, 36). RCRs of 10 or more have been reported for reconstituted cytochrome oxidase preparations (36).

We have succeeded in reconstituting both native and pHMB-modified cytochrome oxidase into phospholipid vesicles.² The RCR values for the samples tested are significantly greater than one (Table I), indicating that enzyme has been incorporated in the vesicle membranes. RCR

Figure 3

Effect of improperly reconstituted enzyme on a measurement of proton pumping activity. This figure depicts the extravesicular pH versus time curves calculated for cytochrome oxidase preparations which have been incorporated into vesicle membranes with varying degrees of success. For all five curves, the extravesicular pH was assumed to be 7 before a pulse of ferrocytochrome c was added at time = 0. Fluxes of proton leakage through the membrane were assumed to be proportional to the pH difference with a rate constant of 0.02 s^{-1} . Each curve was calculated for a system with a fraction of the enzyme reconstituted with the correct transmembrane orientation and the remainder incorrectly reconstituted in such a way that the molecules have both their O_2 binding sites and their cytochrome c binding sites exposed to the extravesicular compartment (see text). A: 100% correct. B: 80% correct, 20% incorrect. C: 50% each correct and incorrect. D: 20% correct, 80% incorrect. E: 100% incorrect.



values are influenced by a variety of factors other than the presence or absence of proton pumping, including the presence of unreconstituted enzyme, the rate of electron transfer, and the proton leak rate. It should be noted that the relatively low RCR value for the pHMB-modified enzyme does not necessarily indicate a lack of proton pumping, since the electron transfer rate in the modified enzyme is substantially lower than that in the unmodified preparations (Chapter II).

In addition to determining the RCR values, we have also made preliminary H^+/e^- measurements in each of the three types of samples. We have observed pumping in native enzyme samples only. We are presently trying to determine whether the lack of observed pumping in the other samples should be attributed to inhibition of the pump in the enzyme species being studied or to the presence of incompletely reconstituted enzyme molecules in the vesicle preparation.

If we succeed in demonstrating that the pHMB-modified enzyme does not pump protons, this will suggest that Cu_A must indeed be considered a likely candidate for the redox center associated with the cytochrome oxidase proton pump. It will not be possible, however, to directly attribute the loss of pumping to disruption of the Cu_A site by pHMB. As

Table I: Respiratory Control Ratios of Vesicle-Reconstituted Cytochrome Oxidase Preparations

Preparation ^a	Number of Samples	RCR ^c	
		Mean	Std. Dev.
native	10	7.4	3.0
unmodified control ^b	3	3.4	1.0
pHMB-modified	3	1.7	0.3

^aSamples prepared as described in Chapter II, Materials and Methods. ^bPrepared following the same procedure as pHMB-modified sample, but without addition of pHMB. ^cMethod: Respiratory controls ratios were determined by measuring the ratio of steady-state turnover rates in the presence and absence of 0.6 μ M carbonylcyanide *m*-chlorophenylhydrazone and 3.3 μ M valinomycin. Activity was measured by monitoring the rate of oxygen consumption using a Clark-type oxygen sensor at 30°. The assay contained 0.1 M K-HEPES pH 7.4, 15 mM sodium ascorbate, and 51 μ M cytochrome c. The volume of vesicles added to the assay was adjusted to give approximately equal activities in the coupled and uncoupled measurements in order to minimize errors resulting from any nonlinearities in the assay response.

discussed in Chapter II, it is likely that pHMB reacts with many thiol groups not associated with the Cu_A site, and it would be valuable to exclude the modification of these groups as a possible cause of the inhibition of pumping. We have therefore undertaken a third project to help determine more specifically whether the loss of pumping activity is associated with the disruption of Cu_A.

Identification of cysteine groups important to the Cu_A structure and to proton pumping activity. The results presented in Chapter II demonstrate that treatment with pHMB, a reagent that reacts predominantly with thiolate groups in proteins (37), causes a structural and functional change at the Cu_A site. Since the role of thiolate ligands in the coordination of Cu_A is well established (38, 39), it is reasonable to hypothesize that it is the modification by pHMB of one or more thiolate ligands of Cu_A which is responsible for the structural change associated with pHMB treatment. This assumption is supported by 1) the observation that other copper proteins with thiolate ligands undergo such reactions with mercurials (40), and 2) the observation that EDTA treatment of the pHMB-modified oxidase can remove the EPR-visible copper while the same treatment is completely ineffective in removing Cu_A from native oxidase. We are currently examining the stoichiometry and

location in the protein sequence of the S-*p*-carboxyphenylmercuricysteine residues in order to establish a correlation between this modification of enzyme thiol groups and the loss of the Cu_A^{2+} signal during the course of the reaction. We are optimistic that these experiments will produce readily interpretable results because of the work of Tsudzuki et al. (41) described in Chapter II. These workers noted that when oxidase was treated for a short time with low concentrations of *p*-chloromercuribenzoic acid, a reagent with similar chemical properties to pHMB in aqueous solution, all but 1-2 of the thiol groups in the enzyme are labelled with little accompanying loss of enzyme activity. We showed that no change in the Cu_A^{2+} EPR spectrum occurs under these conditions (Chapter II). We anticipate that the modification of oxidase with pHMB under the conditions described in Chapter II (which involve a much longer reaction time and a higher reagent concentration than that employed by Tsudzuki et al.) will be accompanied by modification of one or two additional thiols. If the modification of these additional thiols and the change in the Cu_A EPR spectrum can be shown to have identical time courses, this would suggest that the modification of these groups caused the change in the structure of Cu_A . The simplest explanation of this phenomenon would be that the

thiols in question are Cu_A ligands. Analysis of the location of these groups in the amino acid sequences of the protein subunits might therefore help to identify the particular cysteine(s) which are ligands to Cu_A.

The same approach could be used to study whether modification of particular cysteine groups is associated with a loss of proton pumping activity in the pHMB-modified enzyme. We hypothesize that such loss would follow the same time course as the modification of a cysteine group or groups associated with the loss of the Cu_A²⁺ EPR signal. A demonstration that this is the case would support the conclusion that inhibition of proton pumping is due to a modification of the pump site itself rather than, for example, blockage of a proton channel leading to the pump.

We have devised procedures to purify the subunits of cytochrome oxidase so that the extent of pHMB modification of each subunit can be assessed individually. This considerably simplifies the study of individual thiol modifications since no subunit of bovine oxidase contains more than two thiol groups (42). We are currently developing analytical techniques of the accuracy required to measure the extent of pHMB-modification of individual thiol groups. This task is complicated by the fact that pHMB

bound to thiol groups can readily exchange to free thiols when the protein is denatured, a factor which may account for apparent inconsistencies in previous studies of the reactions of mercurials with cytochrome oxidase (43). We have succeeded in eliminating this exchange reaction by using $\text{ICH}_2\text{CONH}_2$ to block free thiols after pHMB treatment.

BIOCHEMICAL AND PHYSIOLOGICAL IMPLICATIONS

The studies in this thesis focus on cytochrome c oxidase as an isolated enzyme. In the cell, however, oxidase is not isolated either spatially or functionally, but is instead a part of a complex metabolic pathway (the respiratory chain) which itself is only one component of the biochemical machinery of the mitochondrion. I conclude this chapter by considering some implications of the results presented here for the physiology and biochemistry of these more complex systems of which cytochrome c oxidase is a part.

At first glance, the suggestion that oxidase contains an electron transport pathway which bypasses the putative proton pumping site (Fig. 1B) might seem implausible. Why should an enzyme with a biological role of free energy transduction contain a mechanism which reduces its efficiency as an energy transducer? A possible answer to this question is related to a point discussed in Chapter III: The efficiency is not the sole determinant of the biological utility of a free energy transducer (44, 45). To illustrate this idea with an extreme example, it is easy to see that even a highly efficient energy transducer is of no value to an organism if it operates at zero rate. Finite rates entail some degree of thermodynamic irreversibility;

an irreversible energy transducer is an entropy producer and entropy production entails a loss of free energy.

The trade-off between rate and efficiency is of special concern in relation to electron transfer driven proton pumping in cytochrome oxidase. Electron transfer through oxidase, in addition to driving the enzyme's proton pump, is also required for two other processes which conserve free energy in a metabolically useful form by contributing to the $\Delta\tilde{\mu}_H^+$ across the inner mitochondrial membrane. The first such process is electron transfer through the redox elements which precede cytochrome oxidase in the respiratory chain. These elements include two sites of electrogenic proton translocation (13). The other important energy transduction process requiring electron transfer through oxidase is the consumption of electrons from the c-side and protons from the m-side in the cytochrome oxidase O_2 reduction reaction, which also contributes to $\Delta\tilde{\mu}_H^+$. Factors which increase the efficiency of the cytochrome oxidase proton pump and concomitantly slow its rate may nevertheless have an adverse effect on the total free energy transduction efficiency of the respiratory chain because electron transfer through oxidase is required for the efficient functioning of these other energy transducing processes.³ In particular, it should be noted that in resting mitochondria the elements of

the electron transport chain upstream from cytochrome oxidase are nearly at equilibrium (46, 47) while the oxidase reaction appears to be highly irreversible (48). These conclusions imply that the overall rate of electron transport depends strongly on the rate of oxidase turnover and will increase or decrease as the rate of electron transfer through oxidase increases or decreases. Consequently, allowing some of the electron transfers catalyzed by cytochrome oxidase to occur by a pathway which is not kinetically restricted by being coupled to the proton pump may be biologically useful under many circumstances. Such electron transfers could occur either through the pump [for example, by the "uncoupling" electron transfer pathways (Chapter III)] or around the pump [by the Fe_a -to- $\text{Fe}_{a_3}/\text{Cu}_B$ electron transfer pathway (Fig. 1B)]. To add concreteness to this discussion, I will conclude it by describing three particular circumstances under which an increased flow of electrons through cytochrome oxidase pathways not coupled to proton pumping may be advantageous.

One such circumstance is that of high transmembrane protonmotive forces (Δp). Δp reaches values of 200-240 mV in state 4 mitochondria (13). Under the conditions of a typical experiment, the differences in reduction potential ($\Delta E'$) traversed by an electron transferred from Fe_c^{2+} to O_2

is less than 550 mV (25). As discussed at the end of Chapter II, pumping of one proton for each electron transferred can no longer take place when Δp exceeds one-half of $\Delta E'$. Even at Δp values below this cut-off, pumping will be substantially slowed. In that circumstance, increasing the fraction of electron transfers through the enzyme which are not linked to proton pumping may be necessary in order to achieve an adequate electron transfer rate. It should be noted that no special control mechanism is necessary to achieve this effect. In the case of both electron leakage through the pump and electron leakage around the pump, an increase in Δp is expected to cause an increase in the fraction of the total electron transfer rate due to electron leakage [(45, 49); see also Chapter III]. This phenomenon represents a negative feedback system for the production of Δp and may play a role in membrane potential homeostasis.

A second condition under which increased transfer of electrons not coupled to proton pumping might be beneficial is that in which some electron transfers to the $\text{Fe}_{\text{a}_3}/\text{Cu}_{\text{B}}$ site are significantly slower than the others. Reduction of O_2 to H_2O requires four electron transfers to the site, and during each of these transfers a different intermediate (or intermediates) of O_2 reduction is present there. Because

these intermediates will in general have different standard reduction potentials (50) and redox reorganizational energies, one would expect the electron transfers to occur at different rates. This expectation has been confirmed experimentally by Blair et al. (8), who found that two O_2 -reduction intermediates at different levels of reduction were reduced by intramolecular electron transfer from Fe_a at substantially different rates. If one or more of the electron transfers to Fe_{a_3}/Cu_B represent a particularly severe kinetic obstacle (i.e., a strong limitation on the total electron transfer rate), then bypassing the proton pump at that step would be advantageous. This is because the driving force for an electron transfer which bypasses the pump is expected to be substantially greater than that for an electron transfer coupled to pumping, and the bypass reaction will therefore be faster if the other factors affecting the electron transfer rates are similar.

A final circumstance under which it may be advantageous to divert electron flow around the cytochrome oxidase proton pump is that in which the cell requires greater power output from the respiratory chain. As discussed in Chapter III, the optimal compromise between free energy transduction efficiency and power output of the respiratory chain depends strongly on the metabolic state of the cell. In a

metabolically quiescent tissue (e.g., resting muscle), the best compromise favors a high efficiency of energy transduction so that little energy is wasted. In an active tissue (e.g., contracting muscle) the rate at which the system produces energy will be more critical, and the best compromise will be closer to the condition of maximum power output [in the redox-linked proton pump, the maximum of the product of electron transfer rate and free energy transduction efficiency] (45). Shunting a portion of the electron transfers around the oxidase proton pump is likely to be advantageous in such circumstances. As discussed above, such a mechanism is expected to substantially increase the rate of electron transfer through oxidase and consequently through the entire respiratory chain while only having a comparatively small effect on the overall efficiency of the system because the proton pumping eliminated by the shunt is only one of several energy-conserving processes in the electron transport chain.

In order for the bypass of the oxidase proton pump to be a metabolic control point in the respiratory chain, there must be a mechanism for metabolic events external to the enzyme to control the ratio of electron transfer rates through the pumping and bypass pathways. Changes in Δp have already been suggested as a candidate for such a mechanism,

since changes in the magnitude of Δp , as well as changes in the relative amounts of the electrical and concentration components of Δp , will differentially affect the two pathways (Chapter III). In addition, an intriguing possibility is raised by the electron transfer scheme of Fig. 1B. This model suggests that changing the relative rates of cytochrome c oxidation at its two binding sites will change the fraction of the electrons that pass through the pump site. (This conclusion is independent of whether the pump is associated with Cu_A or Fe_a .) Consequently, the cell may directly influence the fraction of electron transfers that bypass the pump by inhibiting or promoting binding of cytochrome c to one or the other binding site. In this way, small regulator molecules could tune the performance of the respiratory chain to particular metabolic conditions.

SUMMARY

In this chapter, I have described several hypotheses concerning the chemical mechanisms of electron transfer and proton pumping by cytochrome oxidase which have arisen from the research described in this dissertation. I have also discussed some research projects which we have undertaken to test these hypotheses and to further explore experimental avenues arising from the work described in Chapters II and III. Finally, I have considered a group of ideas concerning the way in which the chemical properties of the enzyme are tailored to its physiological role as an energy transducer. Many of these ideas are speculative and require further study. Despite the fact that cytochrome c oxidase has been studied by legions of biochemists for more than fifty years, it is clear that there is a large amount of interesting biology and chemistry in this molecule which remains unexplored.

FOOTNOTES

¹Abbreviations and symbols used in this chapter: Fe_c , the heme of cytochrome c ; H^+/e^- , the number of protons pumped per electron transferred from Fe_c to O_2 ; RCR, respiratory control ratio; pHMB, sodium *p*-hydroxymercuribenzoic acid; $\Delta\tilde{\mu}_{\text{H}^+}$, transmembrane proton electrochemical potential gradient; Δp , transmembrane protonmotive force; EXAFS, extended x-ray absorption fine structure.

²The reconstitution procedure was a modification of that devised by Casey (34): A mixture of 2:2:1 (w/w/w) bovine heart phosphatidylcholine, soy phosphatidylethanolamine, and bovine heart cardiolipin, was prepared from stock solutions in CHCl_3 provided by Avanti Polar Lipids (Birmingham, AL). The solvent was evaporated under flowing N_2 and the residue dried in vacuo at least 12 h. For every 40 mg lipid, 1 ml of 0.1 M K-HEPES pH 7.4, 1% K-cholesterol was added and the mixture was sonicated for 35-45 min at 25% duty cycle with a Heat Systems, Inc. sonicator at power setting 6, medium tip. The sample was maintained at 0° under N_2 during the sonication. Native, unmodified control, and pHMB-modified samples were prepared as described in Chapter II. Enzyme samples (stored at -80°) were diluted into a 100 mM K-HEPES, pH 7.4 buffer containing a final concentration of 1.4-1.8% *n*-octyl- β -D-glucopyranoside and were incubated at 0° at least 1 h. The solution was then diluted with the sonicated lipid solution to a final enzyme concentration of 4 μM while keeping the lipid concentration above 30 mg/ml. The lipid-protein mixture (6 ml or less) was then dialyzed at 4° against the following buffers for the indicated time periods: 0.5 l 100 mM K-HEPES pH 7.4 (4 h), 1 l 10 mM K-HEPES pH 7.4, 20.2 mM K_2SO_4 , 69.8 mM sucrose, 20 g/l Amberlite XAD-2 (4 h), 1 l 1 mM K-HEPES pH 7.4, 22.3 K_2SO_4 , 76.7 mM sucrose, 20 g/l Amberlite XAD-2 (12 h), and 1 l 1 mM K-HEPES pH 7.4, 22.3 K_2SO_4 , 76.7 mM sucrose (1 h). The resulting vesicle suspensions could be stored up to 10 d at 0° without significant loss of respiratory control.

³Slowing the rate of electron transfer will only have a negative effect on the efficiencies of the free energy transducers when there are "slip" (i.e., uncoupling) processes. The presence of such processes in the energy transduction system of mitochondria is well documented (51). Even in systems without "slip" where the efficiency will not decrease, power output will still be adversely affected because of the decrease in rate.

REFERENCES

1. Brunori, M., Antonini, E., Wilson, M.T. in Metal Ions in Biological Systems (Sigel, H., Ed.), Marcel Dekker, New York.
2. Malmström, B.G. (1980) in Metal Ion Activation of Dioxygen (Spiro, T.G., Ed.) pp. 181-207, Wiley, New York.
3. Wikström, M., Krab, K., Saraste, M. (1981) Cytochrome Oxidase: A Synthesis, Academic Press, London.
4. Gibson, Q.H., Greenwood, C. (1965) J. Biol. Chem. 240, 2694-2698.
5. Beinert, H., Palmer, G. (1964) J. Biol. Chem. 239, 1221-1227.
6. Gelles, J., Chan, S.I. (1985) Biochemistry 24, 3963-3972.
7. Antalıs, T.M., Palmer, G. (1982) J. Biol. Chem. 257, 6194-6206.
8. Blair, D.F., Witt, S.N., Chan, S.I. (1985) J. Am. Chem. Soc. 107, 7389-7399.
9. Clore, G.M., Andréasson, L-E., Karlsson, B., Aasa, R., Malmström, B.G. (1980) Biochem. J. 185, 139-154.
10. Halaka, F.G., Barnes, Z.K., Babcock, G.T., Dye, J.L. (1984) Biochemistry 23, 2005-2011.
11. Greenwood, C., Brittain, T., Wilson, M., Brunori, M. (1976) Biochem. J. 157, 591-598.
12. Wikström, M., Casey, R.P. (1985) J. Inorg. Biochem. 23, 327-334.
13. Wikström, M., Saraste, M. (1984) in Bioenergetics (Ernster, Ed.) pp. 49-94, Elsevier, Amsterdam.
14. Brzezinski, P., Malmström, B.G. (1986) Proc. Natl. Acad. Sci. U.S.A. in press.
15. Penttillä, T. (1983) Eur. J. Biochem. 133, 355-361.
16. Blair, D.F., Ellis, W.R., Wang, H., Gray, H.B., Chan,

- S.I. (1986) J. Biol. Chem. in press.
17. Thelen, M., O'Shea, P.S., Petrone, G., Azzi, A.
(1985) J. Biol. Chem. 260, 3626-3631.
 18. Puettner, I., Carafoli, E., Malatesta, F. (1985) J. Biol. Chem. 260, 3719-3723.
 19. Sarti, P., Jones, M.G., Antonini, G., Malatesta, F., Colosimo, A., Wilson, M.T., Brunori, M. (1985) Proc. Natl. Acad. Sci. U.S.A. 82, 4876-4880.
 20. Solioz, M., Carafoli, E., Ludwig, B. (1982) J. Biol. Chem. 257, 1579-1582.
 21. Sone, N., Yanagita, Y., Hon-Nami, K., Fukumori, Y., Yamanaka, T. (1983) FEBS Lett. 155, 150-154.
 22. Wikström, M. (1986) Curr. Top. Membr. Transp. 16, 303-321.
 23. Babcock, G.T., Callahan, P.M. (1983) Biochemistry 22, 2314-2319.
 24. Thelen, M., O'Shea, P.S., Azzi, A. (1985) Biochem. J. 227, 163-167.
 25. Wikström, M., Krab, K., Saraste, M. (1981) Annu. Rev. Biochem. 50, 623-655.
 26. Blair, D.F., Martin, C.T., Gelles, J., Wang, H., Brudvig, G.W., Stevens, T.H., Chan, S.I. (1983) Chemica Scripta 21, 43-53.
 27. Weintraub, S.T., Wharton, D.C. (1981) J. Biol. Chem. 256, 1669-1676.
 28. Weintraub, S.T., Muhoberac, B.B., Wharton, D.C.
(1982) J. Biol. Chem. 257, 4940-4946.
 29. Scott, R.A., Cramer, S.P., Shaw, R.W., Beinert, H., Gray, H.B. (1981) Proc. Natl. Acad. Sci. U.S.A. 78, 664-667.
 30. Scott, R.A., Schwartz, J.R., Cramer, S.P. (1984) in EXAFS and Near Edge Structure III (Hodgson, K.O., Hedman, B., Penner-Hahn, J.O., Eds.) 111-116.
 31. Powers, L., Chance, B., Ching, Y., Angiolillo, P.
(1981) Biophys. J. 34, 465-498.

32. Vännngård, T. (1972) in Biological Applications of Electron Spin Resonance (Swartz, H.M., Bolton, J.R., & Borg, D.C., Eds.) pp. 411-447, Wiley-Interscience, New York.
33. Brudvig, G., Chan, S.I. (1979) FEBS Lett. 106, 139-141.
34. Casey, R.P. (1985) Meth. Enzymol. in press.
35. Hunter, D.R., Capaldi, R.A. (1974) Biochem. Biophys. Res. Comm. 56, 623-628.
36. Brunori, M., Sarti, P., Colosimo, A., Antonini, G., Malatesta, F., Jones, M.G., Wilson M.T. (1985) EMBO J. 4, 2365-2368.
37. Webb, J.L. (1966) Enzyme and Metabolic Inhibitors Vol. 2, pp. 729-985, Academic Press, New York.
38. Martin, C.T. (1985) PhD. Thesis, California Institute of Technology, Pasadena, California.
39. Stevens, T.H., Martin, C.T., Wang, H., Brudvig, G.W., Scholes, C.P., Chan, S.I. (1982) J. Biol. Chem. 257, 12106-12113.
40. Church, W.B., Guss, J.M., Potter, J.J., Freeman, H.C. (1986) J. Biol. Chem. 261, 234-236.
41. Tsudzuki, T., Orii, Y., Okunuki, K. (1967) J. Biochem. 62, 37-45.
42. Buse, G., Meinecke, L., Bruch, B. (1985) J. Inorg. Biochem 23, 149-153.
43. Stonehuerner, J., O'Brien, P., Kendrick, L., Hall, J., Millett, F. (1985) J. Biol. Chem. 260, 11456-11460.
44. Stucki, J.W. (1978) in Energy Conservation in Biological Membranes, 29. Mosbach Colloquium (Schafer, G. and Klingenberg, M., Eds.) pp. 264-287, Springer-Verlag, Berlin.
45. Blair, D.F., Gelles, J., Chan, S.I. (1986) Biophys. J. in press.
46. Wilson, D.F., Owen, C.S., Holian, A. (1977) Arch. Biochem. Biophys. 182, 749-762.
47. Forman, N.G., Wilson, D.F. (1982) J. Biol. Chem.

257, 12908-12915.

48. Wikström, M. (1981) Proc. Natl. Acad. Sci. U.S.A. 78, 4051-4054.
49. Blair, D.F., Gelles, J., Chan, S.I. (1986) manuscript in preparation.
50. Malmström, B.G. (1982) Annu. Rev. Biochem. 51, 21-59.
51. Pietrobon, D., Azzone, G.F., Walz, D. (1981) Eur. J. Biochem. 117, 389-394.